Calhoun: The NPS Institutional Archive

DSpace Repository

Theses and Dissertations | 1. Thesis and Dissertation Collection, all items

1985-12

The effects of digital control on longitudinal autopilots for bank-to-turn and skid-turn missiles.

Karaiskos, Ioannis C.

http://hdl.handle.net/10945/21298

Copyright is reserved by the copyright owner

Downloaded from NPS Archive: Calhoun

http://www.nps.edu/library

Calhoun is the Naval Postgraduate School's public access digital repository for research materials and institutional publications created by the NPS community. Calhoun is named for Professor of Mathematics Guy K. Calhoun, NPS's first appointed -- and published -- scholarly author.

Dudley Knox Library / Naval Postgraduate School
411 Dyer Road / 1 University Circle
Monterey, California USA 93943

NAVAL POSTGRADUATE SCHOOL
Monterey, California

THESIS

THE EFFECTS OF DIGITAL CONTROL ON LONGITUDINAL AUTOPILOTS FOR BANK-TO-TURN AND SKID-TURN MISSILES

by

Ioannis C. Karaiskos

December 1985

Thesis Advisor: Daniel J. Collins

Approved for public release; distribution unlimited

T226738

REPORT DOCUMENTATION PAGE

ORT SECURITY CLASSIFICATION: UNCLASSIFIED	1b. RESTRICTIVE MARKINGS
URITY CLASSIFICATION AUTHORITY	3. DISTRIBUTION / AVAILABILITY OF REPORT: Approved for public release; distribution unlimited
CLASSIFICATION / DOWNGRADING SCHEDULE	
ORMING ORGANIZATION REPORT NUMBER(S)	5. MONITORING ORGANIZATION REPORT NUMBER(S)
ME OF PERFORMING ORGANIZATION: val Postgraduate School; 6b. OFFICE SYMBOL (If applicable): 67	7a. NAME OF MONITORING ORGANIZATION: Naval Postgraduate School
DRESS (City, State, and ZIP Code): nterey, California 93943-5100	7b. ADDRESS (City, State, and ZIP Code): Monterey, California 93943-5100
ME OF FUNDING / SPONSORING GANIZATION; 8b. OFFICE SYMBOL (If applicable)	9. PROCUREMENT INSTRUMENT IDENTIFICATION NUMBER
DRESS (City, State, and ZIP Code)	10. SOURCE OF FUNDING NUMBERS: PROGRAM ELEMENT NO. / PROJECT NO. / TASK NO. / WORK UNIT ACCESSION NO.

LE (Include Security Classification)
E EFFECTS OF DIGITAL CONTROL ON LONGITUDINAL AUTOPILOTS FOR BANK-TO-TURN AND SKID-RN MISSILES

RSONAL AUTHOR(S): Ioannis C. Karaiskos

YPE OF REPORT	13b. TIME COVERED	14. DATE OF REPORT (Year, Month, Day)	15. PAGE COUNT
laster's Thesis	FROM _____ TO _____	1985 December	140

PPLEMENTARY NOTATION

COSATI CODES			18. SUBJECT TERMS (Continue on reverse if necessary and identify by block number)
ELD	GROUP	SUB-GROUP	BTT Autopilots, Pitch Uncoupled Autopilot, ClassicalDesign Modern Design, State Feedback, Estimator, Coupled Roll and Pitch Autopilots, Robustness

STRACT (Continue on reverse if necessary and identify by block number)

This work addresses the design and analysis of the discrete longitudinal autopilot for ication to the bank-to-turn (BTT) missiles.

In the development the classical design and analysis were reviewed using the continuous upled pitch channel autopilot for circular airframe. Then,applying analog-to-digital ersion, the corresponding discrete autopilot was designed. The performance of both inuous and discrete open loop systems was analyzed according to the desired requirements.

In the following section, utilizing modern control design techniques for the discrete pitch nel autopilot, the control law was designed, assuming availability of all the states and ng the desired poles to be at the same place as in the classical design. Therefore the discrete e-feedback autopilot was obtained and analyzed. The next step was the design of an estimator

TRIBUTION / AVAILABILITY OF ABSTRACT: NCLASSIFIED/UNLIMITED ☐ SAME AS RPT. ☐ DTIC USERS	21. ABSTRACT SECURITY CLASSIFICATION: unclassified
AME OF RESPONSIBLE INDIVIDUAL: Daniel J. Collins	22b. TELEPHONE (Include Area Code): (408) 646 2826 / 22c. OFFICE SYMBOL: 67Co

RM 1473, 84 MAR — 83 APR edition may be used until exhausted. All other editions are obsolete.

SECURITY CLASSIFICATION OF THIS PAGE: unclassified

19. (Continued)

which estimates the entire state vector, given measurements of the portion of the state. The performance of the estimator was analyzed too.
Finally coupling the discrete pitch and roll channel autopilots the overall performance of the discrete system was obtained and analyzed. The resulting design was also proved to be robust.

Approved for public release, distribution unlimited

The Effects of Digital Control on Longitudinal Autopilots for Bank-to-Turn and Skid-Turn Missiles

by

Ioannis C. Karaiskos
Lieutenant, Hellenic Navy
B.S., Hellenic Naval Academy, 1977

Submitted in partial fulfillment of the
requirements for the degree of

MASTER OF SCIENCE IN ENGINEERING SCIENCE

from the

NAVAL POSTGRADUATE SCHOOL
December 1985

ABSTRACT

This work addresses the design and analysis of the discrete longitudinal autopilot for application to the bank-to-turn (BTT) missiles.

In the development the classical design and analysis were reviewed using the continuous uncoupled pitch channel autopilot for circular airframe. Then,applying analog-to-digital conversion, the corresponding discrete autopilot was designed. The performance of both continuous and discrete open loop systems was analyzed according to the desired requirements.

In the following section, utilizing modern control design techniques for the discrete pitch channel autopilot, the control law was designed, assuming availability of all the states and taking the desired poles to be at the same place as in the classical design. Therefore the discrete state-feedback autopilot was obtained and analyzed. The next step was the design of an estimator which estimates the entire state vector, given measurements of the portion of the state. The performance of the estimator was analyzed too.

Finally coupling the discrete pitch and roll channel autopilots the overall performance of the discrete system was obtained and analyzed. The resulting design was also proved to be robust.

TABLE OF CONTENTS

I. INTRODUCTION 19

II. CLASSICAL LINEAR DESIGN AND ANALYSIS OF LONGITUDINAL UNCOUPLED CHANNEL AUTOPILOT FOR CIRCULAR AIRFRAME 23

A. GENERAL 23

B. AIRFRAME CONFIGURATION 24

C. UNCOUPLED LINEAR PITCH CHANNEL AUTOPILOT 26

1. Aerodynamic Model 26

2. Pitch Control Law 28

3. Transfer Functions of Aerodynamic Model 33

4. Design Approach and Analysis of the Continuous Open Loop System 34

5. Design Approach and Analysis of the Discrete Open Loop System 56

6. Comparison of Continuous and Discrete Systems 65

III. MODERN CONTROL DESIGN AND ANALYSIS OF LONGITUDINAL UNCOUPLED CHANNEL AUTOPILOT 66

A. GENERAL 66

B. STATE FEEDBACK DESIGNED AUTOPILOT 68

1. Design Approach and Analysis of Control Law 68

2. Performance of System 70

3. Simplified State Feedback Designed Autopilot....78
C. ESTIMATOR DESIGNED AUTOPILOT....79
1. Design Approach and Analysis of Discrete Closed Loop Estimator....79
2. Performance of System....88
3. Simplified Estimator Designed Autopilot....97
IV. DISCRETE COUPLED PITCH AND ROLL CHANNEL AUTOPILOTS....105
A. GENERAL....105
B. DESIGN APPROACH AND ANALYSIS OF THE DISCRETE STATE FEEDBACK AUTOPILOT....106
C. PERFORMANCE OF SYSTEM....106
D. ROBUSTNESS OF SYSTEM....114
V. CONCLUSIONS AND RECOMMENDATIONS....122
APPENDIX A: GEOMETRIC AND MASS PROPERTIES OF MISSILE CONFIGURATION....123
APPENDIX B: ANALOG TO DIGITAL CONVERSION OF UNCOUPLED PITCH CHANNEL AUTOPILOT....124
APPENDIX C: PROGRAM LOGIC FOR COMPUTING CONTROL LAW **K** VIA ACKERMANN'S FORMULA....125
APPENDIX D: COMPUTER PROGRAM FOR APPLICATION OF ACKERMANN'S FORMULA....127
APPENDIX E: ANALOG TO DIGITAL CONVERSION OF COUPLED PITCH AND ROLL CHANNEL

AUTOPILOTS.....129
APPENDIX F: ROBUSTNESS DATA FILE FOR THE DISCRETE STATE FEEDBACK DESIGNED AUTOPILOT.....131
APPENDIX G: ROBUSTNESS DATA FILE FOR THE DISCRETE ESTIMATOR DESIGNED AUTOPILOT.....134
LIST OF REFERENCES 137
INITIAL DISTRIBUTION LIST 138

LIST OF TABLES

I. Linearized Aerodynamic Derivatives (M=3.95).....35

II. Stability Margins of Uncoupled Pitch Channel.....51

LIST OF FIGURES

2.1 Bank-to-Turn Autopilot.....25

2.2 Model of Circular Configuration-1/6 Scale.....27

2.3 Aerodynamic Sign Convention.....29

2.4 Linear Pitch Channel Dynamic Model.....30

2.5 Pitch Control Law.....31

2.6 Uncoupled Pitch Channel Autopilot.....32

2.7 Pitch Normal Acceleration vs Time; Uncoupled Pitch Channel; Continuous Open Loop System.....42

2.8 Pitch Angular Rate vs Time; Uncoupled Pitch Channel; Continuous Open Loop System.....43

2.9 Pitch Tail Incidence vs Time; Ucoupled Pitch Channel; Continuous Open Loop System.....44

2.10 Pitch Normal Acceleration; Uncoupled Pitch Channel; Continuous Open Loop System; Gain vs Frequency.....45

2.11 Pitch Normal Acceleration; Uncoupled Pitch Channel; Continuous Open Loop System; Phase vs Frequency.....46

2.12 Pitch Angular Rate; Uncoupled Pitch Channel; Continuous Open Loop System; Gain vs Frequency.....47

2.13 Pitch Angular Rate; Uncoupled Pitch Channel; Continuous Open Loop System; Phase vs Frequency.....48

2.14 Pitch Tail Incidence; Uncoupled Pitch Channel; Continuous Open Loop System; Gain vs Frequency.....49

2.15 Pitch Tail Incidence; Uncoupled Pitch Channel;

Continuous Open Loop System; Phase vs Frequency.....50
2.16 Pitch Normal Acceleration; Uncoupled Pitch Channel;
Continuous Open Loop System; Pole-Zero Map.....52
2.17 Pitch Angular Rate; Uncoupled Pitch Channel;
Continuous Open Loop System; Pole-Zero Map.....53
2.18 Pitch Tail Incidence; Uncoupled Pitch Channel;
Continuous Open Loop System; Pole-Zero Map.....54
2.19 Pitch Normal Acceleration vs Time; Uncoupled Pitch
Channel; Discrete Open Loop System.....57
2.20 Pitch Angular Rate vs Time; Uncoupled Pitch Channel;
Discrete Open Loop System.....59
2.21 Pitch Tail Incidence vs Time; Ucoupled Pitch Channel;
Discrete Open Loop System.....60
2.22 Pitch Normal Acceleration; Uncoupled Pitch Channel;
Discrete Open Loop System; Pole-Zero Map.....61
2.23 Pitch Angular Rate; Uncoupled Pitch Channel;
Discrete Open Loop System; Pole-Zero Map.....62
2.24 Pitch Tail Incidence; Uncoupled Pitch Channel;
Discrete Open Loop System; Pole-Zero Map.....63
3.1 Pitch Normal Acceleration vs Time; Uncoupled Pitch
Channel; Discrete State-Feedback Autopilot.....72
3.2 Pitch Angular Rate vs Time; Uncoupled Pitch Channel;
Discrete State-Feedback Autopilot.....73
3.3 Pitch Tail Incidence vs Time; Uncoupled Pitch Channel;
Discrete State-Feedback Autopilot.....74

3.4 Pitch Normal Acceleration ; Uncoupled Pitch Channel; Discrete State-Feedback Autopilot; Pole-Zero Map.....75
3.5 Pitch Angular Rate; Uncoupled Pitch Channel; Discrete State-Feedback Autopilot; Pole-Zero Map.....76
3.6 Pitch Tail Incidence; Uncoupled Pitch Channel; Discrete State-Feedback Autopilot; Pole-Zero Map.....77
3.7 Pitch Normal Acceleration vs Time; Uncoupled Pitch Channel; Discrete Simplified State-Feedback Autopilot.....80
3.8 Pitch Angular Rate vs Time; Uncoupled Pitch Channel; Discrete Simplified State-Feedback Autopilot.....81
3.9 Pitch Tail Incidence vs Time; Uncoupled Pitch Channel; Discrete Simplified State-Feedback Autopilot.....82
3.10 Pitch Normal Acceleration ; Uncoupled Pitch Channel; Discrete Simplified State-Feedback Autopilot; Pole-Zero Map.....83
3.11 Pitch Angular Rate; Uncoupled Pitch Channel; Discrete Simplified State-Feedback Autopilot; Pole-Zero Map.....84
3.12 Pitch Tail Incidence; Uncoupled Pitch Channel; Discrete Simplified State-Feedback Autopilot; Pole-Zero Map.....85
3.13 Open Loop Estimator.....87
3.14 Closed Loop Estimator.....87
3.15 Pitch Normal Acceleration vs Time; Uncoupled Pitch Channel; Discrete Estimator Autopilot.....90
3.16 Pitch Angular Rate vs Time; Uncoupled Pitch Channel; Discrete Estimator Autopilot.....91

3.17 Pitch Tail Incidence vs Time; Uncoupled Pitch Channel; Discrete Estimator Autopilot....92
3.18 Pitch Normal Acceleration ; Uncoupled Pitch Channel; Discrete State Feedback and Estimator Autopilots; Pole-Zero Map....93
3.19 Pitch Angular Rate; Uncoupled Pitch Channel; Discrete State Feedback and Estimator Autopilots; Pole-Zero Map....94
3.20 Pitch Tail Incidence; Uncoupled Pitch Channel; Discrete State Feedback and Estimator Autopilots; Pole-Zero Map....95
3.21 Pitch Normal Acceleration vs Time; Uncoupled Pitch Channel; Discrete Simplified Estimator Autopilot....99
3.22 Pitch Angular Rate vs Time; Uncoupled Pitch Channel; Discrete Simplified Estimator Autopilot....100
3.23 Pitch Tail Incidence vs Time; Uncoupled Pitch Channel; Discrete Simplified Estimator Autopilot....101
3.24 Pitch Normal Acceleration ; Uncoupled Pitch Channel; Discrete Simplified Estimator Autopilot; Pole-Zero Map....102
3.25 Pitch Angular Rate; Uncoupled Pitch Channel; Discrete Simplified Estimator Autopilot; Pole-Zero Map:....103
3.26 Pitch Tail Incidence; Uncoupled Pitch Channel; Discrete Simplified Estimator Autopilot; Pole-Zero Map....104
4.1 Pitch Normal Acceleration vs Time; Coupled Pitch and

Roll Channels; Discrete State-Feedback Autopilot.....108

4.2 Pitch Angular Rate vs Time; Coupled Pitch and Roll Channels; Discrete State-Feedback Autopilot.....109

4.3 Pitch Tail Incidence vs Time; Coupled Pitch and Roll Channels;Discrete State-Feedback Autopilot.....110

4.4 Pitch Normal Acceleration ; Coupled Pitch and Roll Channels; Discrete State-Feedback Autopilot; Pole-Zero Map.....111

4.5 Pitch Angular Rate; Coupled Pitch and Roll Channels; Discrete State-Feedback Autopilot; Pole-Zero Map.....112

4.6 Pitch Tail Incidence; Coupled Pitch and Roll Channels; Discrete State-Feedback Autopilot; Pole-Zero Map.....113

4.7 SVADMO vs Frequency; Coupled Pitch and Roll Channels; Discrete State-Feedback Autopilot.....116

4.8 SVADMO vs Frequency; Coupled Pitch and Roll Channels; Discrete Estimator Autopilot.....117

4.9 MIN.ADD.IN.SV vs Frequency; Coupled Pitch and Roll Channels; Discrete State-Feedback Autopilot.....118

4.10 MIN.ADD.IN.SV vs Frequency; Coupled Pitch and Roll Channels; Discrete Estimator Autopilot.....119

BTT	Bank-to-Turn
CBTT	Coordinated Bank-to-Turn, minimum sideslip, positive a, $\varphi_e \leq 180$ deg.
C_l	rolling moment coefficient
C_m	pitching moment coefficient
C_{ma}	slope of curve of pitching moment coefficient C_m vs a
$C_{m\delta p}$	change in C_m per degree pitch control incidence, δ_p
C_N	normal force coefficient
C_{Na}	slope of curve of normal force coefficient C_N vs a
$C_{N\delta p}$	change in C_N per degree pitch control incidence, δ_p
C_Y	side force coefficient
d	reference length for coefficients (= 2 ft)
I_{yy}	moment of inertia about $\overline{y}_B$ axis
I_{zz}	moment of inertia about $\overline{z}_B$ axis
I_{xx}	moment of inertia about $\overline{x}_B$ axis
K_A	autopilot pitch acceleration error gain
K_{YP}	CBTT autopilot coordination branch gain
p	roll rate about $\overline{x}_B$
$\dot{p}$	roll acceleration about $\overline{x}_B$
POC	preferred orientation control
$\overline{q}$	dynamic pressure
q	pitch rate about $\overline{y}_B$
$\dot{q}$	pitch angular accelaration about $\overline{y}_B$

Q_e	constant or equilibrium pitch angular rate
r	yaw angular rate about $\bar{z}_B$
$\dot{r}$	yaw angular acceleration about $\bar{z}_B$
S	reference area for coefficients ($=\pi$ ft^2)
STT	Skid-to-Turn, roll attitude stabilized
u	velocity component in $\bar{x}_B$ direction
v	velocity component in $\bar{y}_B$ direction, assumed to constant
V	constant missile flight path velocity
$\bar{V}$	missile velocity vector
w	velocity component in $\bar{z}_B$ direction
$\bar{x}_B$	body-fixed roll axis, along axis of symmetry, positive forward
$\bar{y}_B$	body-fixed pitch axis, positive starboard
$\bar{z}_B$	body-fixed yaw axis, forms right handed orthogonal system with $\bar{x}_B$ and $\bar{y}_B$
$\bar{z}_v$	vehicle axis in downward direction along local gravity vector, approximated as inertial axis
n_z	achieved normal acceleration in $\bar{z}_B$ direction
n_{zc}	commanded normal acceleration in $\bar{z}_B$ direction
n_y	achieved normal acceleration in $\bar{y}_B$ direction
n_Z	achieved normal acceleration in $\bar{z}_v$ direction
n_Y	achieved normal acceleration in $\bar{y}_v$ direction
n_c	normal acceleration command from guidance computer in $\bar{z}_v$ direction plus anti-gravity bias command
n_{Zc}	normal acceleration guidance command in $\bar{z}_v$ direction
n_{Yc}	normal acceleration guidance command in $\bar{y}_v$ direction

φ_c	roll attitude command from guidance computer, zero degrees in $-\bar{z}_v$ direction and 90 degrees in $\bar{y}_v$ direction
φ	roll attitude, zero degrees in $-\bar{z}_v$ direction and 90 degrees in $\bar{y}_v$ direction
φ_e	roll attitude error, $\varphi_c-\varphi$
θ	Elevation Euler Angle, second rotation, $\int(q\cos\varphi-r\sin\varphi)dt$
ψ	Azimuth Euler Angle, first rotation about $\bar{y}_v$, $\int(q\cos\varphi+r\sin\varphi)dt$
δ_p	pitch control incidence (positive tail incidence produces negative pitching moment)
δ_{pc}	commanded pitch control incidence, δ_p
δ_Y	yaw control incidence (positive tail incidence produces negative yawing moment)
δ_{Yc}	commanded yaw control incidence, δ_Y
δ_R	roll control incidence (positive tail incidence produces positive rolling moment)
δ_{Rc}	commanded roll control incidence , δ_R
a_e	constant or equilibrium angle-of-attack
a	angle-of-attack
$\dot{a}$	angle-of-attack rate
β	angle of sideslip
$\dot{\beta}$	sideslip angular rate
OPTSYS	Optimal Systems Control Program
ORACLS	Optimal Regulator Algorithms for the Control of Linear Systems
X	plant state = $N_s \times 1$ or $n \times 1$

N_s	number of states
U	control = $N_c \times 1$ or $m \times 1$
N_c	number of controls
F	continuous plant system matrix
A	discrete plant system matrix
G	continuous plant control input matrix
B	dicrete plant control input matrix
y	output measurements
H	plant output matrix
J	plant direct transmission matrix
K	control gain (law)
L	estimator gain
T	sampling period

ACKNOWLEDGEMENT

I would like to express my gratitude to Professor D.J. Collins, for his valuable guidance and assistance that helped me finish this work.

I would also like to dedicate this thesis to my wife Stavroula, and my parents Christos and Ioanna for their love and understanding.

I. INTRODUCTION

Missile systems designed to meet the threats of the future will require capabilities far beyond of those currently available. Future requirements dictate the need for dramatic increases in Short Range Air-to-Air Missile (SRAAM) maneuverability and guidance accuracy. Many current missile designs, which are characterized by cruciform airframes and skid-to-turn (STT) steering, cannot be extended to meet these requirements due to low aerodynamic efficiency. Bank-to-turn steering provides the capability to design asymmetric missile airframes which optimize aerodynamic performance in one plane and thus obtain the SRAAM maneuverability and accuracy requirements. Furthermore the ramjet engine chin inlet configuration is believed to provide a greater range capability than other inlet configurations, and BBT control is required to satisfy the sideslip constraints imposed by chin inlets.

In addition, to its potential advantages, BBT steering introduces some technical concerns which must be carefully evaluated. For example, the methodology for designing a bank-to-turn autopilot is not well developed. Such a design must take into account the aerodynamic and kinematic coupling terms as well as allow for operation a low signal levels (i.e, small angle of attack) when the preferred roll orientation is poorly defined. In addition, the coupling of body motion into the guidance signals is another major concern for BBT systems. Recent analyses have indicated that some skid-to-turn (STT) systems can tolerate a limited amount of radome-

induced instabilities without severe performance degradation [Ref.1]. In a BBT system a coupling loop is closed through roll rate as well as pitch and yaw rates [Ref.2]. It is not known whether BBT systems can tolerate coupling induced instabilities. Another concern is the interaction of BBT control with missile functions such as detection (seeker), guidance signal processing ,control surface effectiveness, etc.

All the above concerns must be investigated before BBT steering can be considered a viable method to control high performance tactical missiles.

Many missile programs were initiated during the past decade to improve the capability of steering a tactical missile via BTT control. The results have greatly advanced the understanding of the various missile subsystems.

In the autopilot area, specifically, many types of autopilots have been found which force the missile to roll or bank so that the steering maneuver occurs with the missile airframe oriented in a specific or preferred direction with respect to the incoming airsteam. This entire class of autopilots referred to as Preferred Orientation Control (POC) autopilots.

The main criterion for the selection of one particular type of autopilot is based upon the guidance, airframe, and propulsion system requirements. Generally missiles with either one or two planes of symmetry use a POC autopilot which forces the missile to bank in order to turn (BTT) like an aircraft, and if this motion is coordinated it is usually referred to as CBTT.

In order to take full advantage of CBTT control, planar airframes have been designed to increase lifting capability in one direction without the weight and drag penalty associated with orthogonal lifting surfaces [Ref.1].

These airframe have aerodynamic properties which have the potential to enhance CBTT control.

The present work addresses the design and analysis of the discrete pitch channel autopilot for application to the bank-to-turn (BTT) missiles, with circular airframe configuration. The circular airframe is chosen because it is stable for all angles of attack.

In the development the classical design and analysis of the uncoupled pitch channel autopilot as were developed in reference [Ref.3], are reviewed. Using state-space representation a tenth order system is formulated and the Step Response, Bode and Pole-Zero Map plots are obtained and analyzed according to the desired requirements. Then the continuous system is converted into the corresponding discrete system using Analog to Digital conversion from ORACLS, and analyzed according to the Step-Response,and Pole-Zero Map plots obtained. A comparison of the plots of both the continuous and discrete systems shows no significant differences.

Next, utilizing modern control design techniques and assuming that we have all the states at our disposal for feedback purposes, the control law is designed using the Ackermann's formula [Ref. 6] and taking the desired poles to be at the same place as in the classical case. Using the control law gains the discrete state-feedback autopilot is designed and the Step Response,and Pole-Zero Map plots are obtained and analyzed. Then, since we usually know only a portion of the state variables, an estimator is introduced in order to estimate the entire state vector given measurements of that portion. The poles of the estimator are moved to the left of the original poles of the system in order to get faster response. Plots as above are obtained and an

analysis is made. Next the designed discrete pitch channel autopilot is coupled with the discrete roll channel autopilot and the whole discrete system is analysed and proved to be robust. Finally conclusions and recommendations for future study are stated.

The analysis in all the above cases was performed using the existing at NPS Optimal Systems Control Program (OPTSYS) for the continuous system, Optimal Regulator Algorithms for the Control of Linear Systems (ORACLS) for the discrete system, and Pole Placement and Robustness Design Program (POPLAR) for the robustness of the discrete system.

II. CLASSICAL LINEAR DESIGN AND ANALYSIS OF LONGITUDINAL UNCOUPLED CHANNEL AUTOPILOT FOR CIRCULAR AIRFRAME

A. GENERAL

The initial phase in the design of the CBTT autopilot involved the design of individual, uncoupled channels, pitch, yaw, and roll, with prescribed relationships between speeds of response which would meet the CBTT requirements when coupled.

The design technique for the uncoupled pitch channel was classical, using a combination of Frequency Response and Root Locus techniques [Ref. 2], to achieve practical bandwidths and in turn provide the range of required missile body angular rates and control motions. In addition, the resulting design is found to be robust.

The whole design was done for a flight condition at M=3.95 and Altitude=60 KFT.

The requirements for the classical design technique, as stated in [Ref. 2] are:

1. High Frequency Attenuation in Actuator Command Branch

   ≥ 15 dB at 100 rad/sec and zero angle-of-attack. This requirement limits autopilot speeds of response.

2. Relative Stability:

   Gain margins ≥ 6 dB, Phase margins ≥ 30 degrees with a goal of 12 dB and 50 degrees.

3. Acceleration Time Response

a. 63 percent time constant of 0.5 seconds for a step command of acceleration at the flight condition of interest (M=3.95, Altitude=60 KFT) and small angle of attack. This response is representative of a tactical missile of this size.

b. Overshoot ≤ 10 percent.

c. Zero steady state error in acceleration to reduce variations of guidance navigation gain.

In this chapter the airframe configuration, the aerodynamic model and control law for the pitch channel are reviewed. The transfer functions for circular airframe which is stable for all angles of attack [Ref. 2], are derived. An analysis for the uncoupled pitch channel, as regards the acceleration response, the body angular rate and control surface deflection, in terms of time resposnes and pole-zero map plots for both the continuous and discrete system and frequency responses for the continuous system, is made, using the existing at NPS Optimal Systems Control Program (OPTSYS) for the continuous system, and Optimal Regulator Algorithms for the Control of Linear Systems (ORACLS) for the discrete system. Finally a comparison of the continuous and discrete system by analyzing the above results is made.

A general block diagram of the BTT autopilot is shown in Figure 2.1.

B. AIRFRAME CONFIGURATION

An investigation has been conducted by NASA [Ref.4] to compare the experimental aerodynamic characteristics of a low-drag missile concept with a body of circular cross section to one with a body of 3:1 elliptical

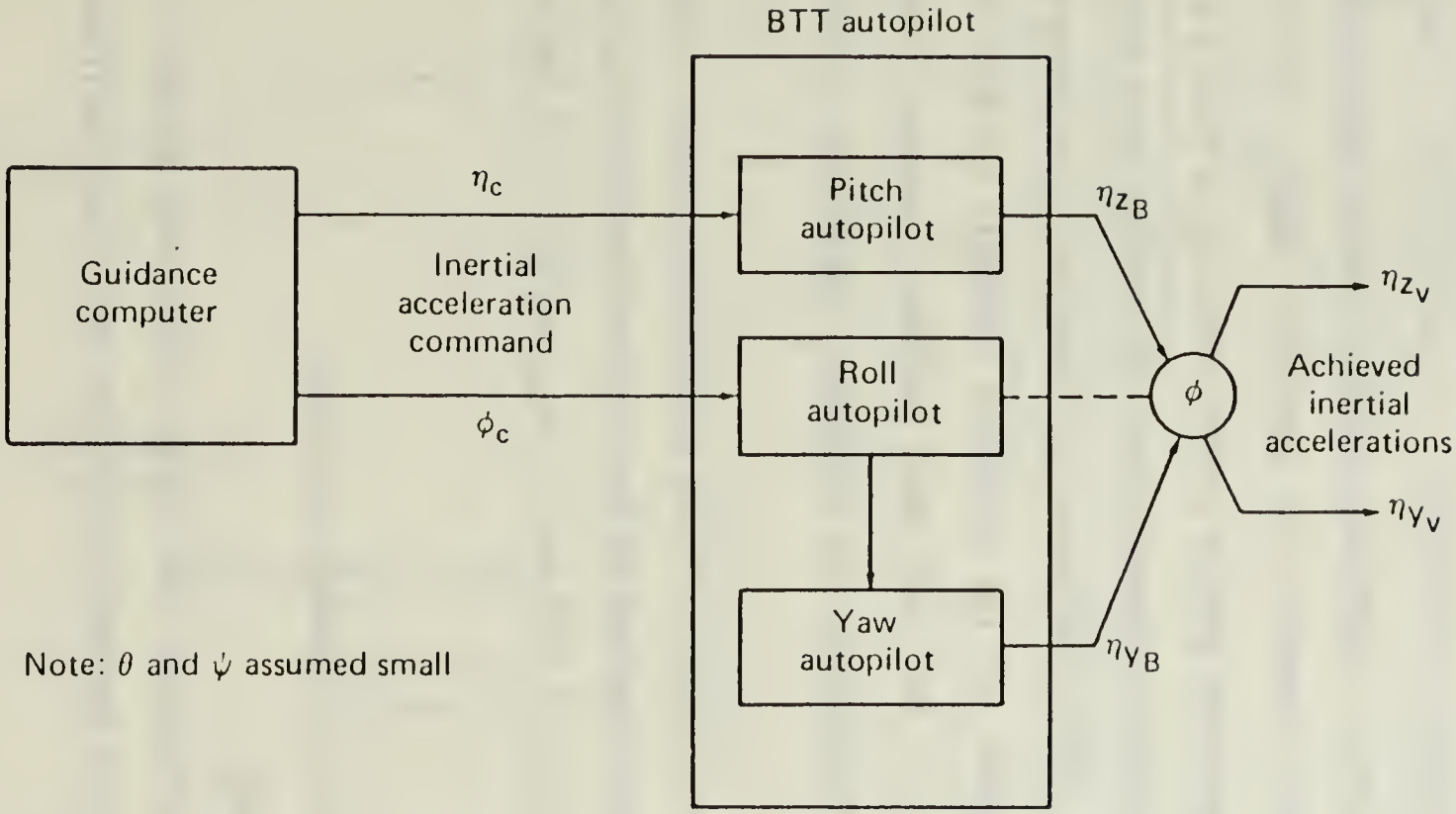

Figure 2.1 Bank-to-Turn Autopilot.

cross section, the bodies having identical cross section area distributions. The concepts were of mono-wing design with constant wing span. Tail surfaces were located flush at the body base with ±30 degrees dihedral. Wind-tunnel tests were performed at Mach numbers from 0.5 to 4.63 and at angles of attack from about -5^0 to $+28^0$.

The comparison shows no significant subsonic normal force differences at low angles of attack; however, at supersonic speeds, the elliptical concept increasingly provides greater normal force up to Mach 2.5 to 3.0, beyond which an incremental increase of about 25 percent holds through the angle of attack range. More pronounced nonlinearities in pitching moment occur at subsonic speed for the elliptical concept, as well as less longitudinal stability at all test Mach numbers. However, levels of directional and lateral stability are increased, especially at the higher angles of attack.

This work uses the circular airframe configuration which is shown in Figure 2.2 and it is taken from [Ref. 4]. The circular cross sectional body has a closure ratio A_{base}/A_{max} of 0.69 and the A_{max} occurs at 68 percent body length.

C. UNCOUPLED LINEAR PITCH CHANNEL AUTOPILOT

1. Aerodynamic Model

The following addresses the linear design and analysis of the continuous uncoupled pitch channel autopilot for the circular airframe.

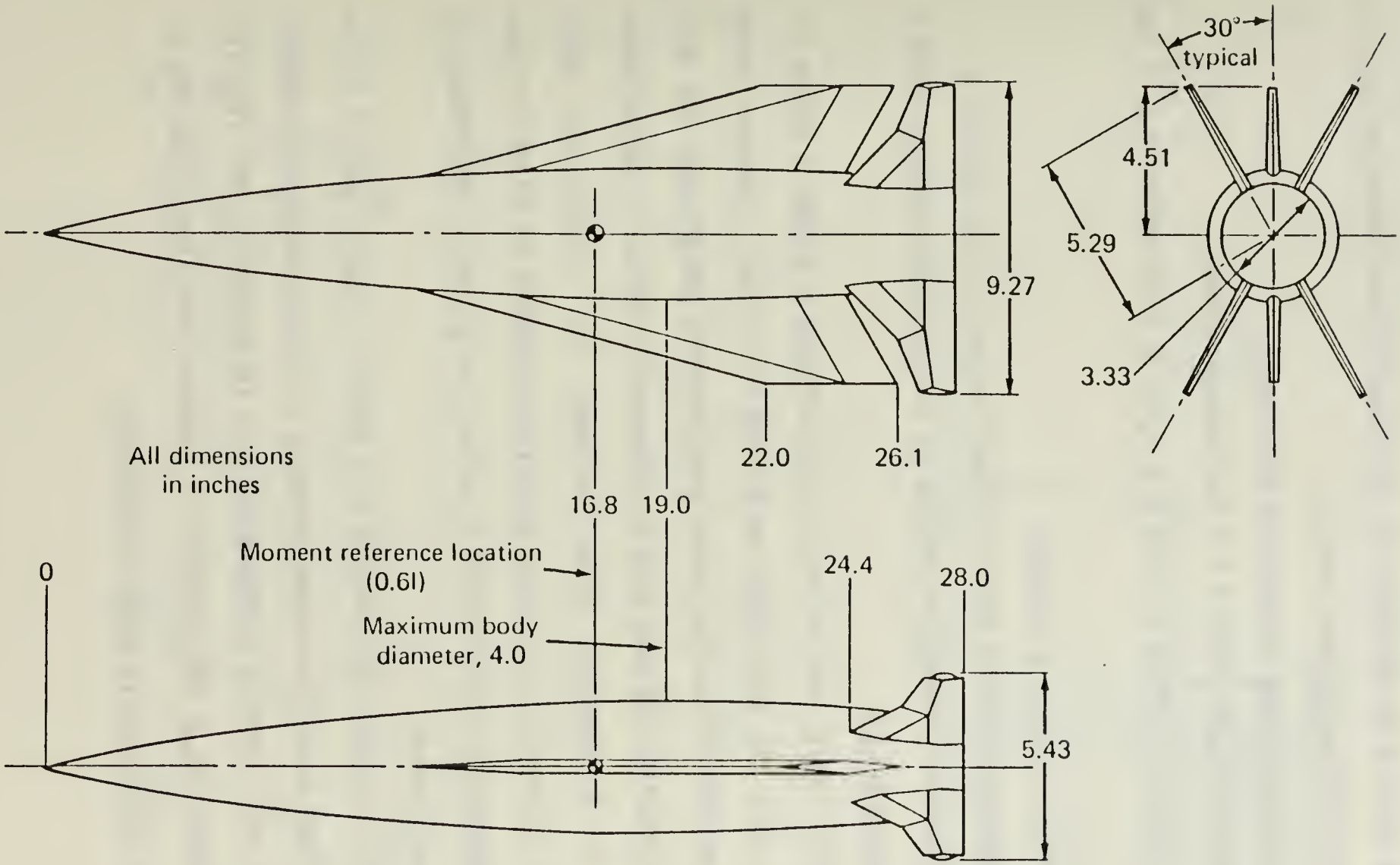

Figure 2.2 Model of Circular Configuration-1/6 Scale.

A linearized aerodynamic model was developed for stability studies. The method used is an extension of the linearization technique used for skid-to-turn (STT) aerodynamic models.

The following three assumptions were made:

a. Plane $\overline{X}_B$-$\overline{Z}_B$ of Figure 2.3 is the maneuver plane.

b. Missile is trimmed in pitch (i.e, M_y=0, at fixed values of a, q, and δ_p).

c. Missile roll rate is constant.

The resulting model is shown in block diagram form in Figure 2.4.

Aerodynamic stability derivatives for M=3.95 are provided in Table I.

2. Pitch Control Law

The pitch control law for the circular airframe is shown in Figure 2.5 as given in [Ref. 2]. Lag-leads were used to prevent guidance noise saturation problems. The rate error compensation determines the high frequency attenuation and was used to minimize the effect of aerodynamic variations on acceleration time response. The acceleration error compensation determines the acceleration time response. An integrator was used in the acceleration error branch to satisfy the guidance requirement of zero steady-state error.

A normal acceleration command (n_{zc}) equal to 1 gee is applied to the pitch control law which uses measurements of missile body pitch angular rate (q) and pitch normal acceleration (n_z) to determine the required actuator command (δ_{pc}). The actuator is modeled as a first order lag at 188.4 rad/sec (30 HZ) and is shown in Figure 2.6.

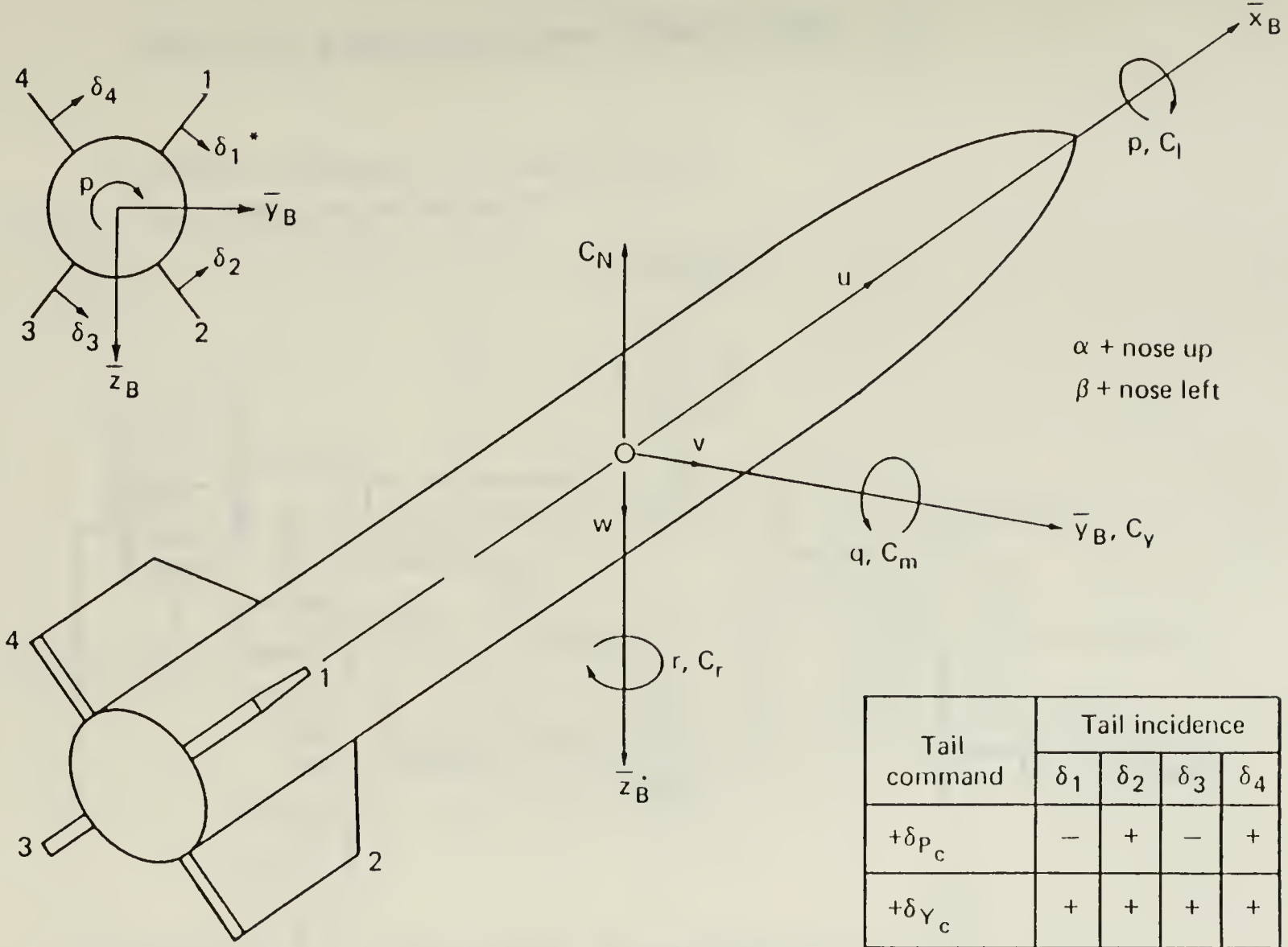

*Arrow indicates direction of positive leading edge deflection

Tail command	Tail incidence			
	δ_1	δ_2	δ_3	δ_4
$+\delta_{P_c}$	−	+	−	+
$+\delta_{Y_c}$	+	+	+	+
$+\delta_{R_c}$	+	−	−	+

Figure 2.3 Aerodynamic Sign Convention.

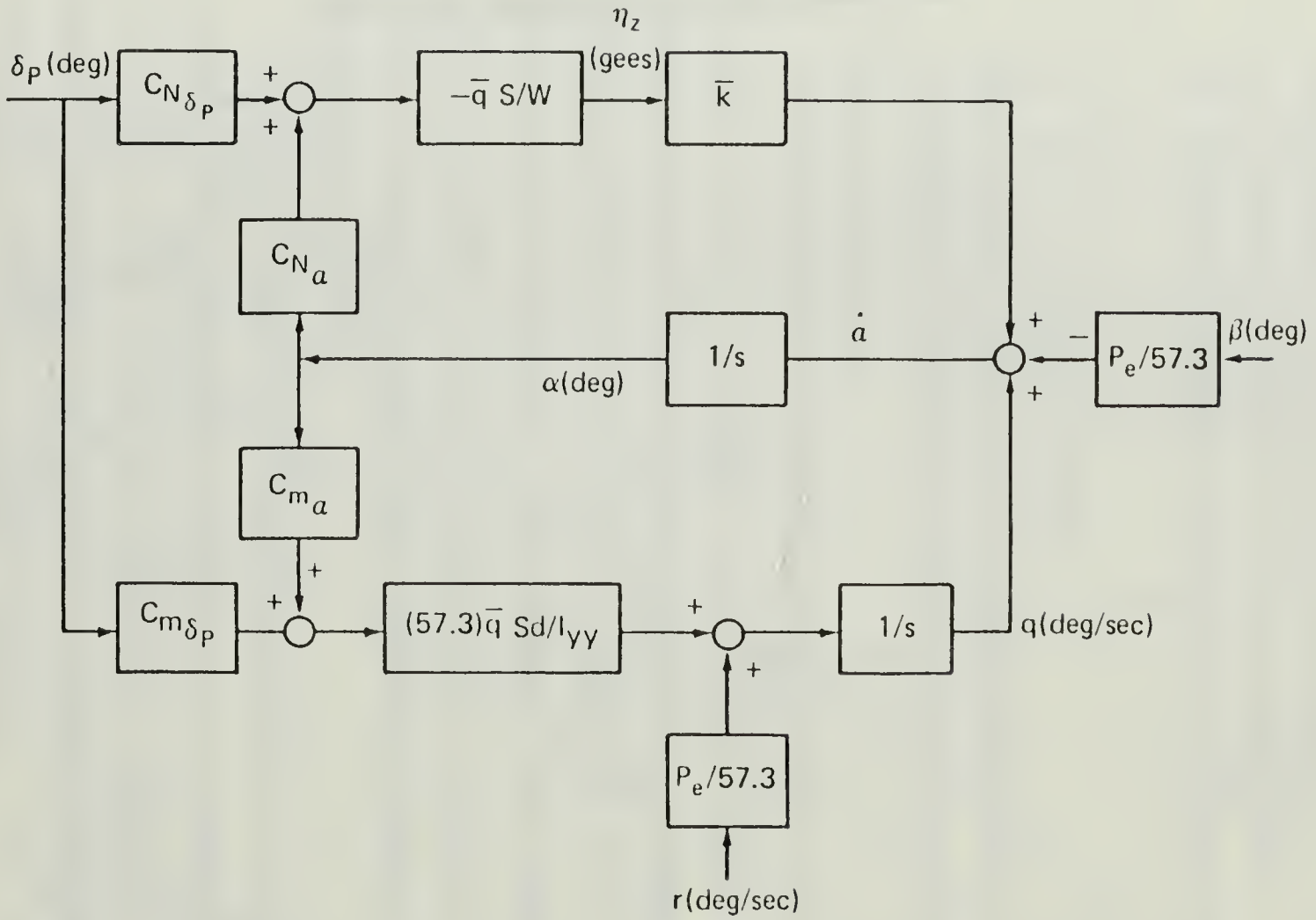

Note: 1. P_e = constant roll rate (deg/sec).

2. η_z,α,β,q, r are perturbation of missile from trim.

Figure 2.4 Linear Pitch Channel Dynamic Model.

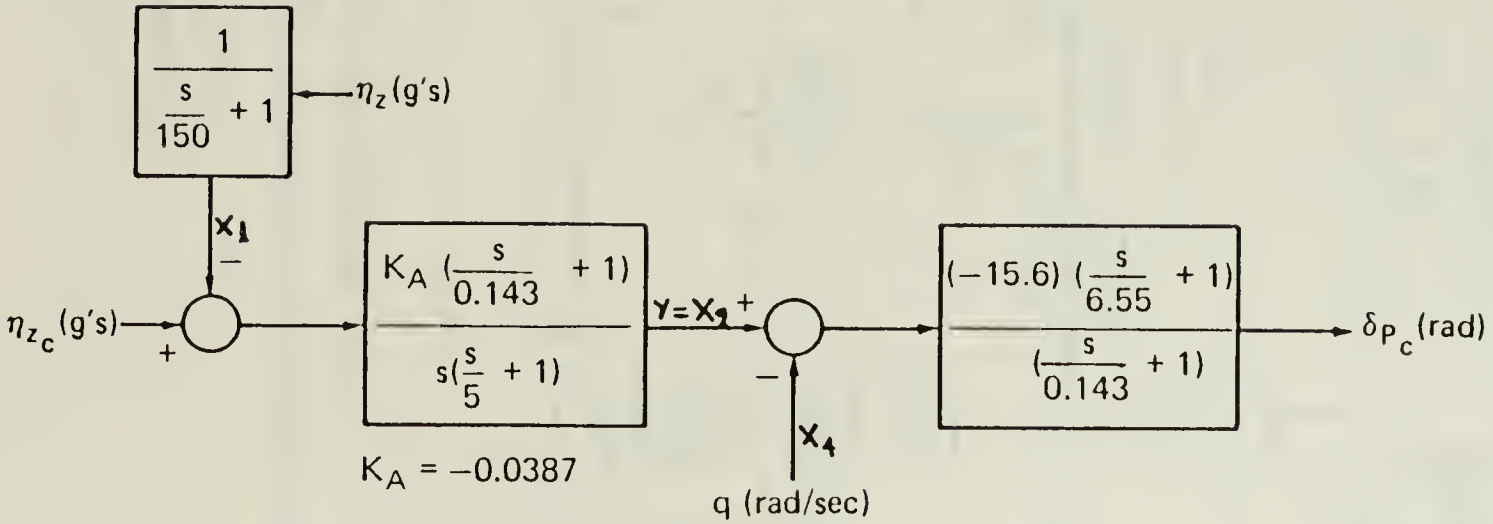

Figure 2.5 Pitch Control Law.

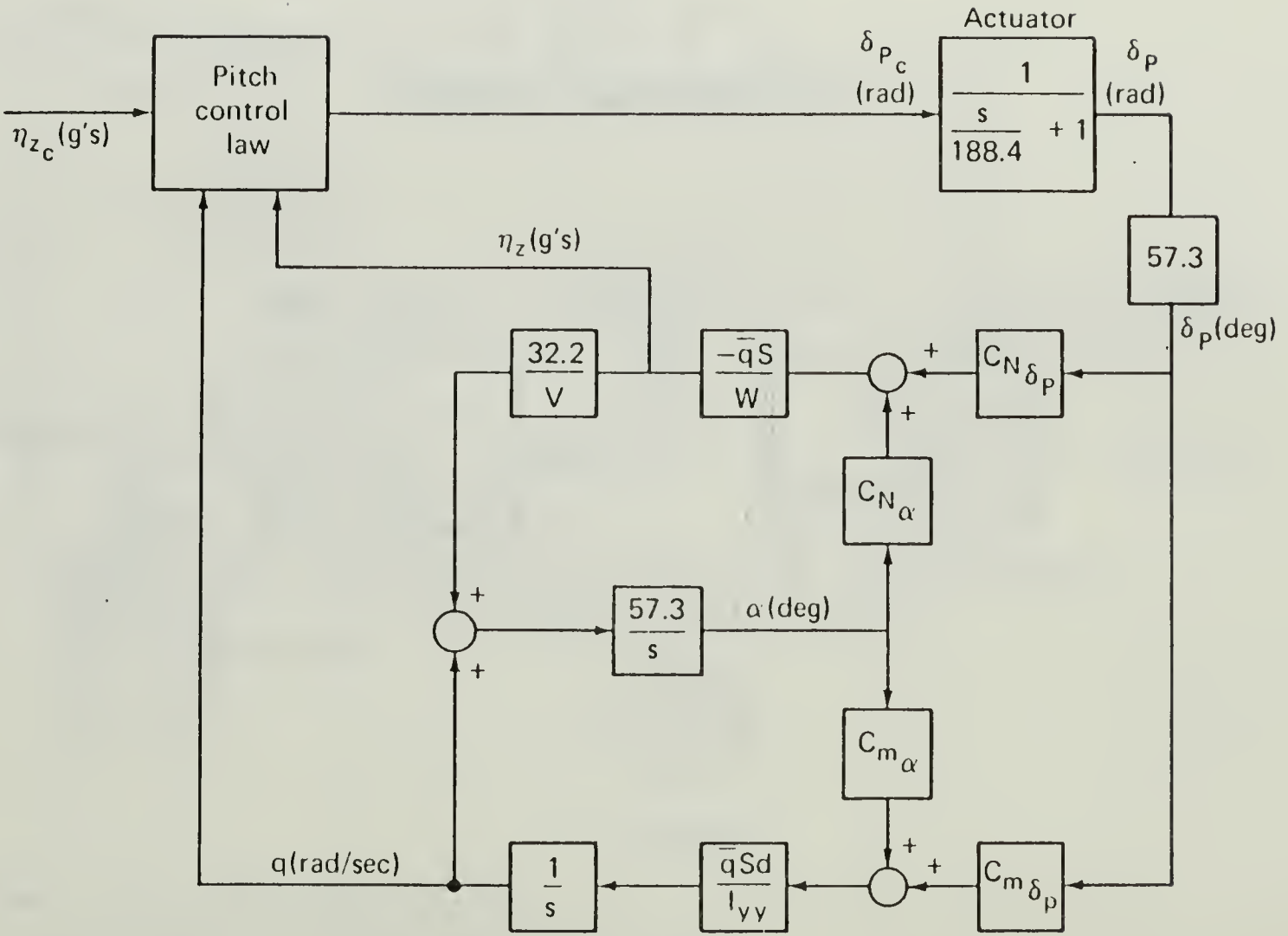

Figure 2.6 Uncoupled Pitch Channel Autopilot.

3. Transfer Functions of Aerodynamic Model

Uncoupled pitch aerodynamic transfer functions are

$$\frac{q}{\delta_p} = \frac{k(AE-BC)}{-C} \cdot \frac{\frac{E}{k(AE-BC)}s + 1}{\frac{1}{-C}s^2 + \frac{Ak}{-C}s + 1}, \quad \text{deg/sec/deg} \quad \text{(II.C.3-1)}$$

$$\frac{n_z}{\delta_p} = \frac{AE-BC}{-C} \cdot \frac{\frac{B}{AE-BC}s^2 + 1}{\frac{1}{-C}s^2 + \frac{Ak}{-C}s + 1}, \quad \text{g's/deg} \quad \text{(II.C.3-2)}$$

$$A = \frac{\bar{q}S}{W} C_{Na}, \quad B = \frac{\bar{q}S}{W} C_{N\delta p}, \quad C = \frac{(57.3)\ \bar{q}Sd}{I_{yy}} C_{ma}$$

$$E = \frac{(57.3)\ \bar{q}Sd}{I_{yy}} C_{m\delta p}, \quad k = \frac{1845}{V}$$

Where:

V=Ma=3.95 x 968.47= 3825.46 ft/sec
S= π ft^2
d= 2 ft
q= 1650 lb/ft^2
I_{xx}= 804 slug-ft^2
W= 2525 lbs
C_{ma} = -0.06
$C_{m\delta p}$= -0.08
C_{Na} = 0.15
$C_{N\delta p}$ = 0.04

As referred to in Appendix A and Table I.

Then
A =0.30793
B =0.08211
C = -44.33162
E = -59.10883
k = 0.48229

And substituting the aforementioned values into equations (II.C.3-1) and (II.C.3-2) they become:

$$\frac{q}{\delta_p} = \frac{-1.3361\,s - 0.159}{22.545 \times 10^{-3}\,s^2 + 3.3634 \times 10^{-3}\,s + 1} \quad (1/sec) \qquad (II.C.3\text{-}3)$$

$$\frac{n_z}{\delta_p} = \frac{106.074 \times 10^{-3}\,s^2 - 18.82}{22.545 \times 10^{-3}\,s^2 + 3.3634 \times 10^{-3}\,s + 1} \quad (g's/rad) \qquad (II.C.3\text{-}4)$$

Equations (II.C.3-3) and (II.C.3-4) are the pitch aerodynamic transfer functions for the pitch angular rate (q) about the Y_B and the achieved maneuver acceleration n_z in the Z_B direction.

4. Design Approach and Analysis of the Continuous Open Loop System

A fixed flight condition at 60 KFT altitude and M=3.95 was selected for these preliminary performance studies of circular airframe. This flight condition provides a sufficiently low dynamic pressure, so that missile maneuvers will result in large enough angles-of-attack, to exercise side slip control. The above fixed condition was selected, in order to reduce the complexities of CBTT autopilots.

TABLE I

Linearized Aerodynamic Derivatives (M=3.95)

Circular Airframe

	$\alpha=0^\circ$	$\alpha=10^\circ$	$\alpha=20^\circ$
$C_{Y\beta}$	-0.065	-0.082	-0.111
$C_{n\beta}$	-0.025	-0.019	-0.003
$C_{l\beta}$	0	-0.009	-0.020
$C_{Y\delta Y}$	0.021	0.022	0.028
$C_{n\delta Y}$	-0.050	-0.053	-0.062
$C_{l\delta Y}$	0	-0.016	-0.038
$C_{Y\delta R}$	0	-0.009	-0.022
$C_{n\delta R}$	0	0.018	0.044
$C_{l\delta R}$	0.031	0.035	0.044
$C_{N\alpha}$	0.15	0.17	0.22
$C_{N\delta P}$	0.04	0.04	0.05
$C_{m\alpha}$	-0.060	-0.065	-0.118
$C_{m\delta P}$	-0.080	-0.095	-0.115

Reference Center of Gravity (C.G) at 0.6 l

The analysis of the uncoupled pitch channel autopilot is based, on the time responses, and Bode plots of maneuver plane acceleration, body angular rates and tail incidence angles, obtained by OPTSYS control program of NPS. For that reason the differential equations of the uncoupled pitch channel autopilot must be put in state-space form $\dot{X}=FX+GU$, which is obtained as follows:

a. Equations of Control Law

(1) Acceleration Filter Equation

$$X_1 = \frac{1}{\frac{s}{150} + 1} n_z \qquad \text{(II.C.4-1)}$$

or

$$X_1 S + 150 X_1 = 150 n_z \qquad \text{(II.C.4-2)}$$

and utilizing inverse Laplace Transformation it becomes:

$$\dot{X}_1 = -150 X_1 + 150 n_z \qquad \text{(II.C.4-3)}$$

(2) Acceleration Compensator Equation

$$\frac{Y}{(n_{zc}-X_1)} = \frac{(-0.0387)\,\frac{s + 0.143}{0.143}}{\frac{s\,(s + 5)}{5}} \qquad \text{(II.C.4-4)}$$

or by minor manipulation

$$\frac{Y}{(n_{zc}-X_1)} = \frac{-0.27063\,s - 0.0387}{0.2\,s^2 + s} \qquad \text{(II.C.4-5)}$$

and utilizing inverse Laplace Transformation it becomes:

$$\ddot{Y}+5\dot{Y}=-1.3531(\dot{n}_{zc}-\dot{X}_1)-0.1935(n_{zc}-X_1) \qquad \text{(II.C.4-6)}$$

Using state-space representation of a system, in which the forcing function involves derivatives terms [Ref. 5: pp 675-678] one yields:

$$\dot{X}_2= X_3-1.3531(n_{zc}-X_1) \qquad \text{(II.C.4-7)}$$

$$\dot{X}_3= -5X_3+6.572(n_{zc}-X_1) \qquad \text{(II.C.4-8)}$$

$$Y = X_2 \qquad \text{(II.C.4-9)}$$

(3) Rate Compensator Equation

$$\delta_{pc} = \frac{(-15.6)\dfrac{s+6.55}{6.55}}{\dfrac{s+0.143}{0.143}}(X_2 - X_4) \qquad \text{(II.C.4-10)}$$

or

$$\delta_{pc} = \frac{-2.3816\,s - 15.6}{6.993\,s + 1}(X_2 - X_4) \qquad \text{(II.C.4-11)}$$

and using inverse Laplace Transformation it yields:

$$\dot{\delta}_{pc}=-0.143\delta_{pc}-340.58 \times 10^{-3}(\dot{X}_2-\dot{X}_4)-2.2308(X_2-X_4) \qquad \text{(II.C.4-12)}$$

b. Actuator Equation

$$\delta_p = \frac{1}{\dfrac{s+188.4}{188.4}}\delta_{pc} \qquad \text{(II.C.4-13)}$$

and using inverse Laplace Transformation it yields:

$$\dot{\delta}_p = -188.4\,\delta_p+188.4\,\delta_{pc} \qquad \text{(II.C.4-14)}$$

c. Equations of Aerodynamic Model

From aerodynamic transfer function, Eq. (II.C.3-3)

$$\frac{q}{\delta_p} = \frac{-1.3361\, s - 0.159}{22.545 \times 10^{-3} s^2 + 3.3634 \times 10^{-3} s + 1}, \text{ or}$$

$$22.545 \times 10^{-3} q s^2 + 3.3634 \times 10^{-3} q s + q = -1.3361\, \delta_p s - 0.159\, \delta_p \quad \text{(II.C.4-15)}$$

and using inverse Laplace Transformation it yields:

$$\ddot{q} + 149.18610^{-3}\, \dot{q} + 44.3557\, q = -59.2637\, \dot{\delta}_p - 7.0526\, \delta_p \quad \text{(II.C.4-16)}$$

Using state-space representation of a system, in which the forcing function involves derivatives terms [Ref. 5: pp 675-678] one obtain:

$$\dot{X}_4 = X_5 - 59.2637\, \delta_p \quad \text{(II.C.4-17)}$$

$$\dot{X}_5 = -149.186 \times 10^{-3} X_5 - 44.3557\, X_4 + 1.7887\, \delta_p \quad \text{(II.C.4-18)}$$

$$X_4 = q \quad \text{(II.C.4-19)}$$

From aerodynamic transfer function Eq.(II.C.3-4)

$$\frac{n_z}{\delta_p} = \frac{106.074 \times 10^{-3} s^2 - 18.82}{22.545 \times 10^{-3} s^2 + 3.3634 \times 10^{-3} s + 1}, \text{ or}$$

$$22.545 \times 10^{-3} s^2 n_z + 3.3634 \times 10^{-3} s\, n_z + n_z = 106.074 \times 10^{-3} s^2\, \delta_p - 18.82 \delta_p \quad \text{(II.C.4-20)}$$

$$\text{or} \qquad \ddot{n}_z + 149.186 \times 10^{-3}\, \dot{n}_z + 44.3557\, n_z = 4.705\, \ddot{\delta}_p - 834.775\, \delta_p \quad \text{(II.C.4-21)}$$

and proceeding as above it yields:

$$\dot{X}_6 = X_7 - 701.92 \times 10^{-3} \delta_p \quad \text{(II.C.4-22)}$$

$$\dot{X}_7 = -149.186 \times 10^{-3} X_7 - 44.3557 X_6 - 1043.36\delta_p \qquad \text{(II.C.4-23)}$$

$$n_z = X_6 + 4.705\delta_p \qquad \text{(II.C.4-24)}$$

Utilizing state-space representation, all the aforementioned equations can be modeled in a tenth order system as follows:

$$\dot{X}_1 = -150 X_1 + 150 X_6 + 705.75 \delta_p \qquad \text{(II.C.4-25)}$$

$$\dot{X}_2 = X_3 - 1.3531 n_{zc} + 1.3531 X_1 \qquad \text{(II.C.4-26)}$$

$$\dot{X}_3 = -5 X_3 + 6.572 n_{zc} - 6.572 X_1 \qquad \text{(II.C.4-27)}$$

$$\dot{X}_4 = X_5 - 59.2637 \delta_p \qquad \text{(II.C.4-28)}$$

$$\dot{X}_5 = -149.186 \times 10^{-3} X_5 - 44.3557 X_4 + 1.7887 \delta_p \qquad \text{(II.C.4-29)}$$

$$\dot{X}_6 = X_7 - 701.92 \times 10^{-3} \delta_p \qquad \text{(II.C.4-30)}$$

$$\dot{X}_7 = -149.186 \times 10^{-3} X_7 - 44.3557 X_6 - 1043.36 \delta_p \qquad \text{(II.C.4-31)}$$

$$\dot{\delta}_p = -188.4 \delta_p + 188.4 \delta_{pc} \qquad \text{(II.C.4-32)}$$

$$\dot{\delta}_{pc} = -0.143 \delta_{pc} - 2.2308 X_2 + 2.2308 X_4 - 340.58 \times 10^{-3} X_3 + 460.839 \times 10^{-3} n_{zc} - 460.839 \times 10^{-3} X_1 + 340.58 \times 10^{-3} X_5 - 20.184 \delta_p \qquad \text{(II.C.4-33)}$$

$$\dot{n}_z = -(X_7 - 887.124 \delta_p + 886.422 \delta_{pc}) \qquad \text{(II.C.4-34)}$$

A continuous, linear, constant coefficient system of differential equations, as above, can always be expressed as a set of first-order matrix differential equations $\dot{\mathbf{X}} = \mathbf{FX+GU}$ where **U** is the control input to the system. The output can be expressed as a linear combination of the state, **X**, and the input as $\mathbf{y= HX+JU}$.

The state method of representing a dynamic system is very useful because it standardizes the information required into three matrices, **F**, **G**, and **H**, no matter how complicated the system is.

In our case the matrices are:

$$\dot{X}=\begin{bmatrix}\dot{X}_1\\ \dot{X}_2\\ \dot{X}_3\\ \dot{X}_4\\ \dot{X}_5\\ \dot{X}_6\\ \dot{X}_7\\ \dot{\delta}_p\\ \dot{\delta}_{pc}\\ \dot{n}_z\end{bmatrix} \qquad X=\begin{bmatrix}X_1\\ X_2\\ X_3\\ X_4\\ X_5\\ X_6\\ X_7\\ \delta_p\\ \delta_{pc}\\ n_z\end{bmatrix} \qquad G=\begin{bmatrix}0\\ -1.3531\\ 6.572\\ 0\\ 0\\ 0\\ 0\\ 0\\ 0.4608\\ 0\end{bmatrix}$$

$$U = n_{zc}$$

$$F=\begin{bmatrix}
-150 & 0 & 0 & 0 & 0 & 0 & 0 & 0 & 0 & 150\\
1.353 & 0 & 1 & 0 & 0 & 0 & 0 & 0 & 0 & 0\\
-6.572 & 0 & -5 & 0 & 0 & 0 & 0 & 0 & 0 & 0\\
0 & 0 & 0 & 0 & 1 & 0 & 0 & -59.26 & 0 & 0\\
0 & 0 & 0 & -44.36 & -0.1492 & 0 & 0 & 1.789 & 0 & 0\\
0 & 0 & 0 & 0 & 0 & 0 & 1 & -0.7019 & 0 & 0\\
0 & 0 & 0 & 0 & 0 & -44.36 & -0.1492 & -1043 & 0 & 0\\
0 & 0 & 0 & 0 & 0 & 0 & 0 & -188.4 & 188.4 & 0\\
-0.4608 & -2.231 & -0.3406 & 2.231 & 0.3406 & 0 & 0 & -20.18 & -0.143 & 0\\
0 & 0 & 0 & 0 & 0 & 0 & -1 & 887.1 & -886.4 & 0
\end{bmatrix}$$

The state-variables of interest are:

$X_4 = q$: pitch angular rate

n_z : pitch normal acceleration

δ_p : pitch tail incidence

Utilizing OPTSYS the tenth order system was analyzed in terms of time and frequency responses, using an input step function representing the "1 gee command" and trim angle-of-attack a_e=0, and the corresponding plots were obtained.

Figure 2.7 shows the pitch normal acceleration (n_z) response which has a 0.5 seconds time constant, steady-state error 0.005 and 2.0 % overshoot, and therefore is according to the requirements mentioned in section II.A.

Figures 2.8 and 2.9 show the required body angular rate (q) and control surface deflection (δ_p), to achieve the acceleration response. These responses matched those presented in [Ref. 3].

Figures 2.10 through 2.15 show the frequency responses of normal acceleration (n_z), angular rate (q), and tail incidence (δ_p). The relative stability margins are shown in Table II. Since the gain and phase margins, as shown in Table II are positive, it ensures that the closed loop (controlled) system will be stable.

Figures 2.16 through 2.18 show the Pole-Zero Maps of n_z, q and δ_p. The poles locations are found to be at:

$s_1 = -159.7 + j\ 18.99$	(Acceleration Filter)	(II.C.4-35)
$s_2 = -159.7 - j\ 18.99$	(Acceleration Compensator)	(II.C.4-36)
$s_3 = -8.290 + j\ 8.059$		(II.C.4-37)
$s_4 = -8.290 - j\ 8.059$	(Angular Rate)	(II.C.4-38)
$s_5 = -3.759 + j\ 2.515$		(II.C.4-39)
$s_6 = -3.759 - j\ 2.515$		(II.C.4-40)
$s_7 = -0.14390000$		(II.C.4-41)
$s_8 = -0.000004251$	(Actuator)	(II.C.4-42)
$s_9 = -0.07459 + j\ 6.66$	(Rate Compensator)	(II.C.4-43)
$s_{10} = -0.07459 - j\ 6.66$	(Normal Acceleration)	(II.C.4-44)

sinse all poles are in the left-half of the s-plane the system is stable.

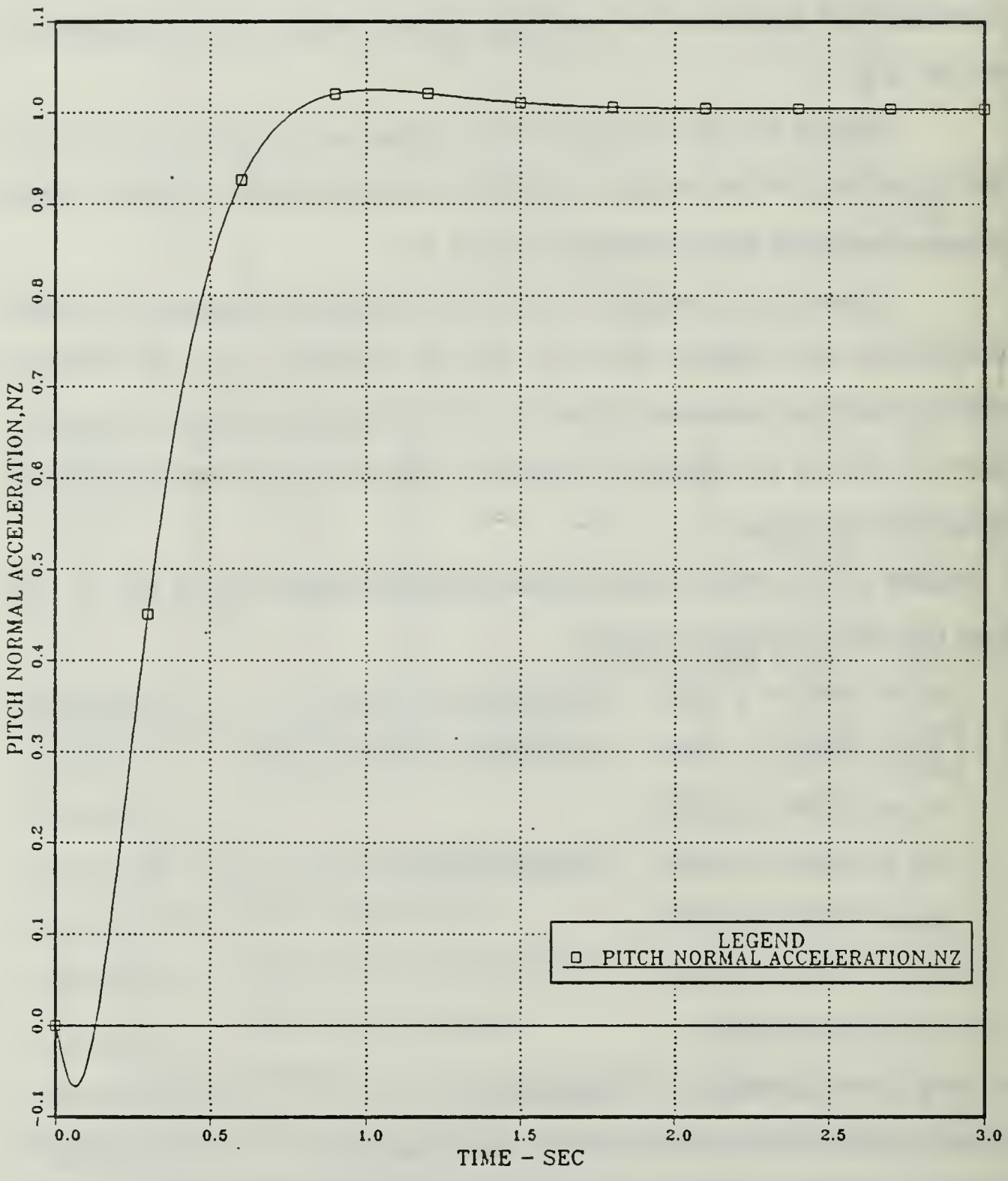

Figure 2.7 Pitch Normal Acceleration vs Time; Uncoupled Pitch Channel; Continuous Open Loop System.

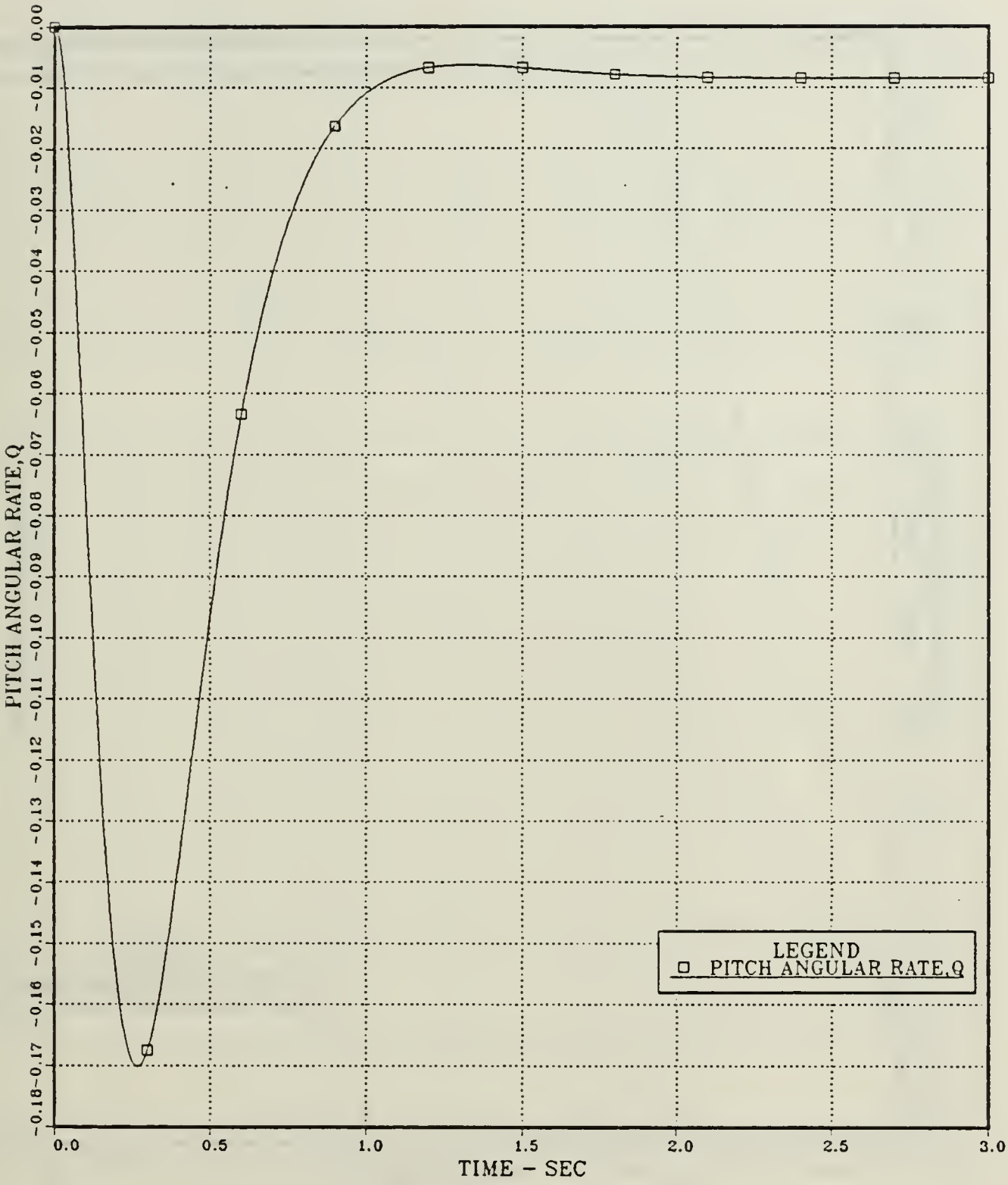

Figure 2.8 Pitch Angular Rate vs Time; Uncoupled Pitch Channel; Continuous Open Loop System.

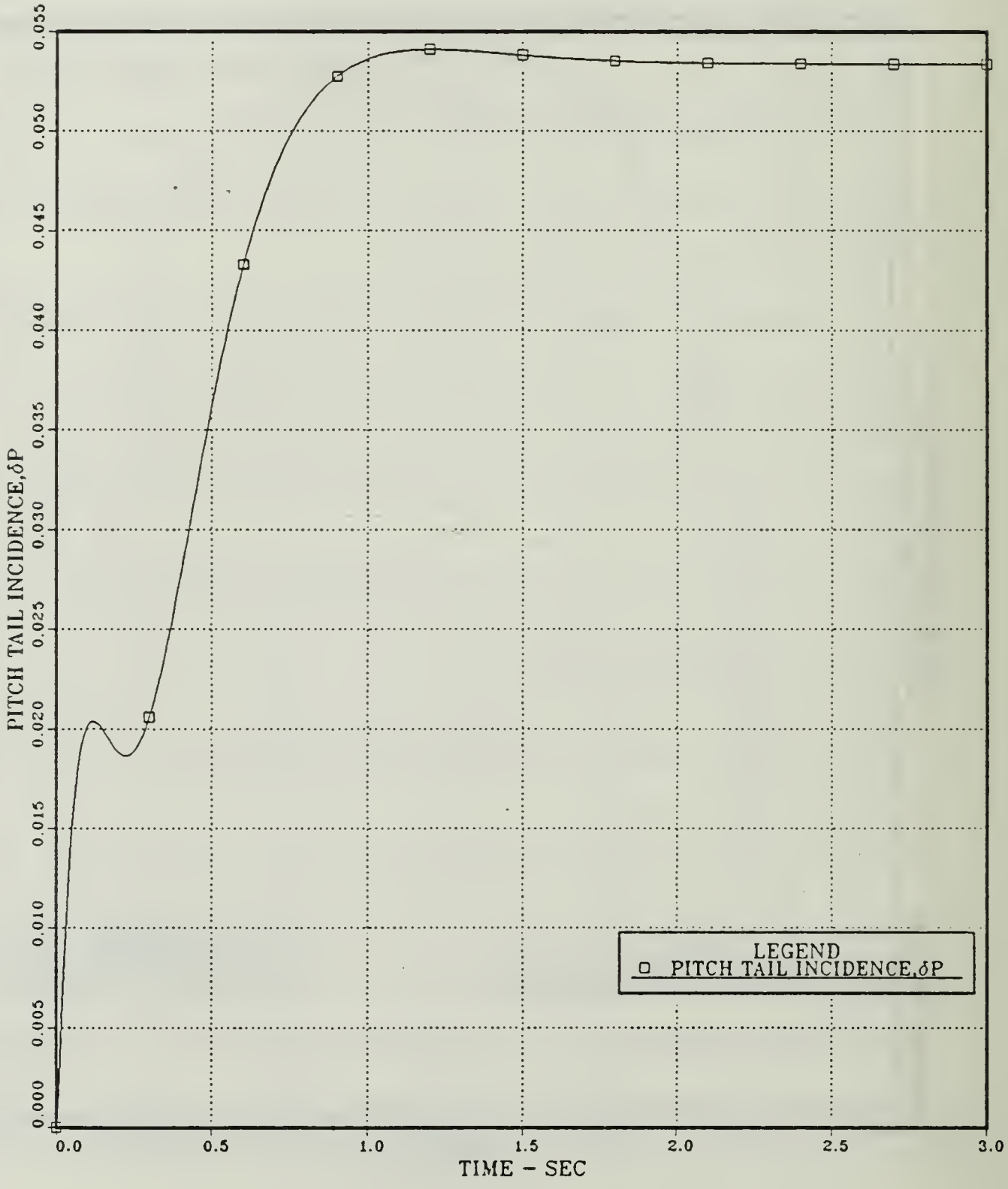

Figure 2.9 Pitch Tail Incidence vs Time; Ucoupled Pitch Channel; Continuous Open Loop System.

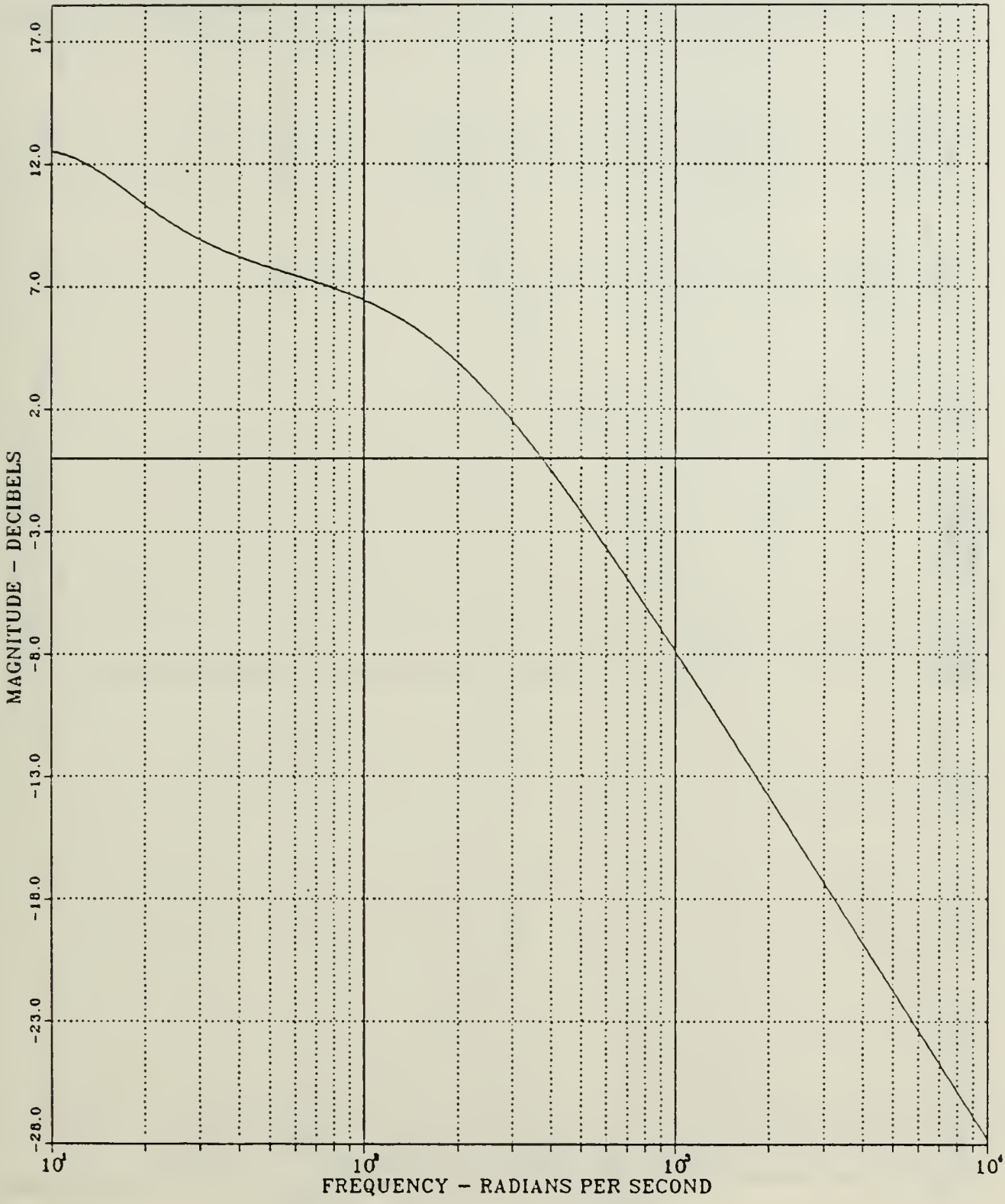

Figure 2.10 Pitch Normal Acceleration; Uncoupled Pitch Channel; Continuous Open Loop System; Gain vs Frequency.

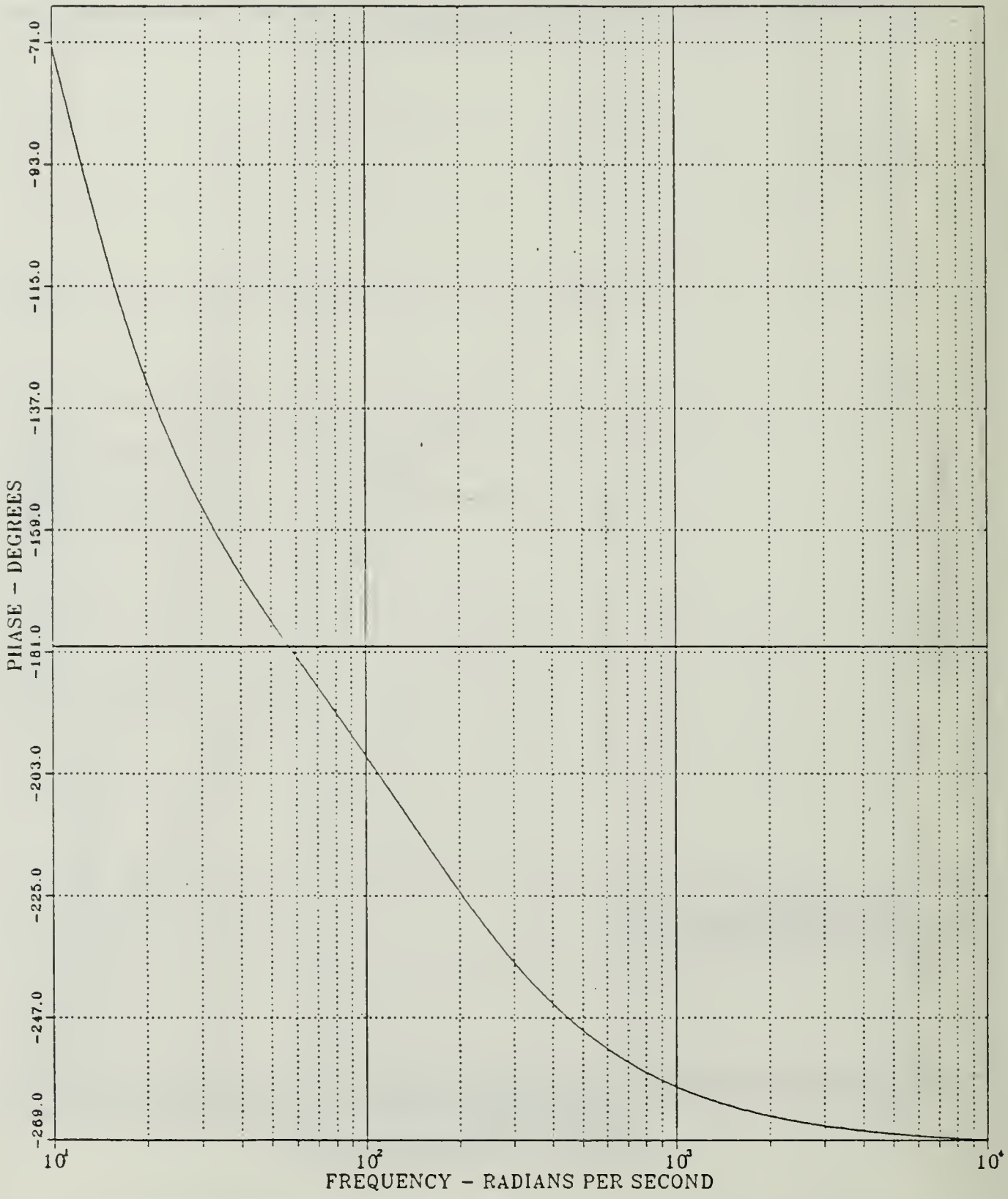

Figure 2.11 Pitch Normal Acceleration; Uncoupled Pitch Channel; Continuous Open Loop System; Phase vs Frequency.

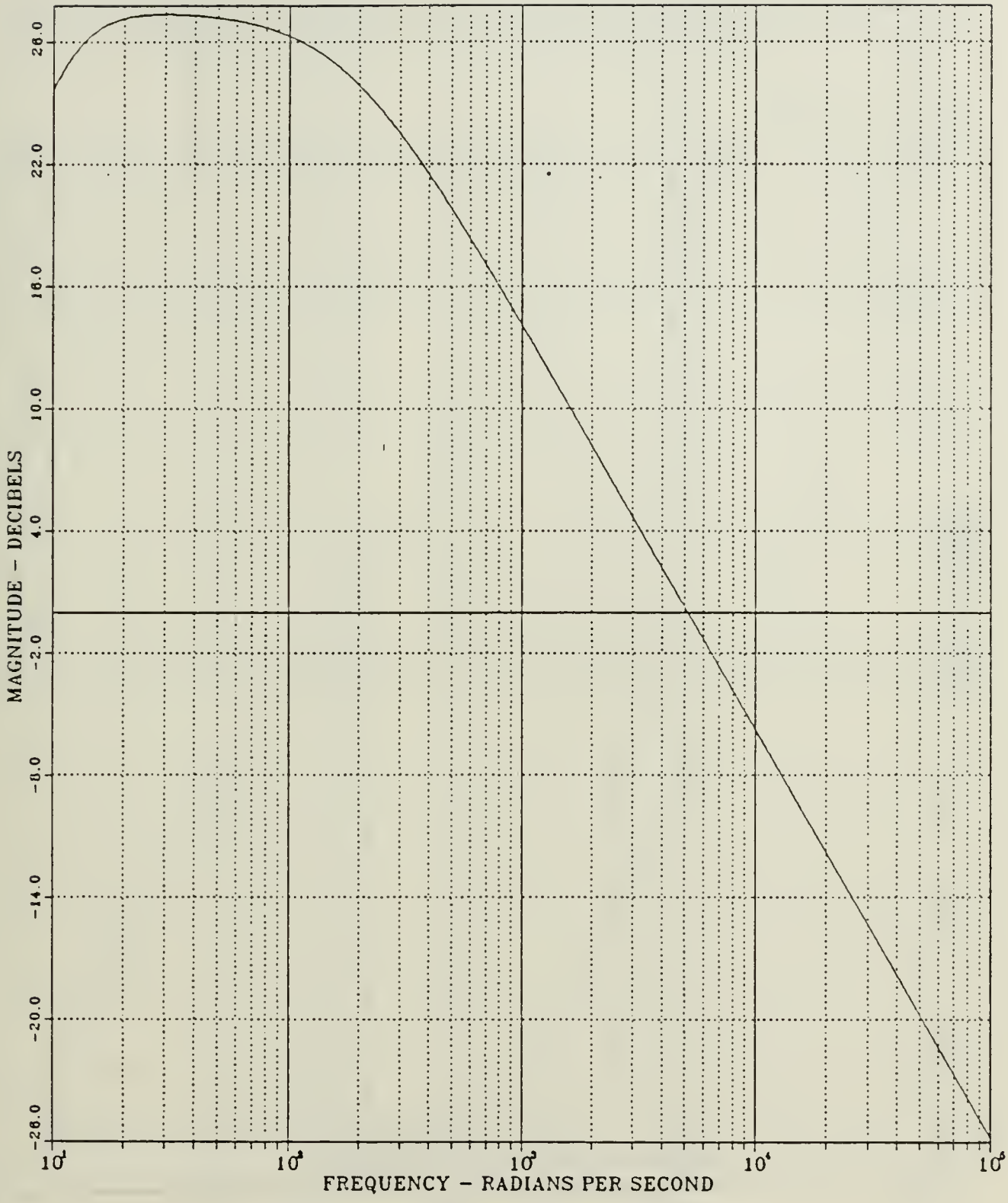

Figure 2.12 Pitch Angular Rate; Uncoupled Pitch Channel; Continuous Open Loop System; Gain vs Frequency.

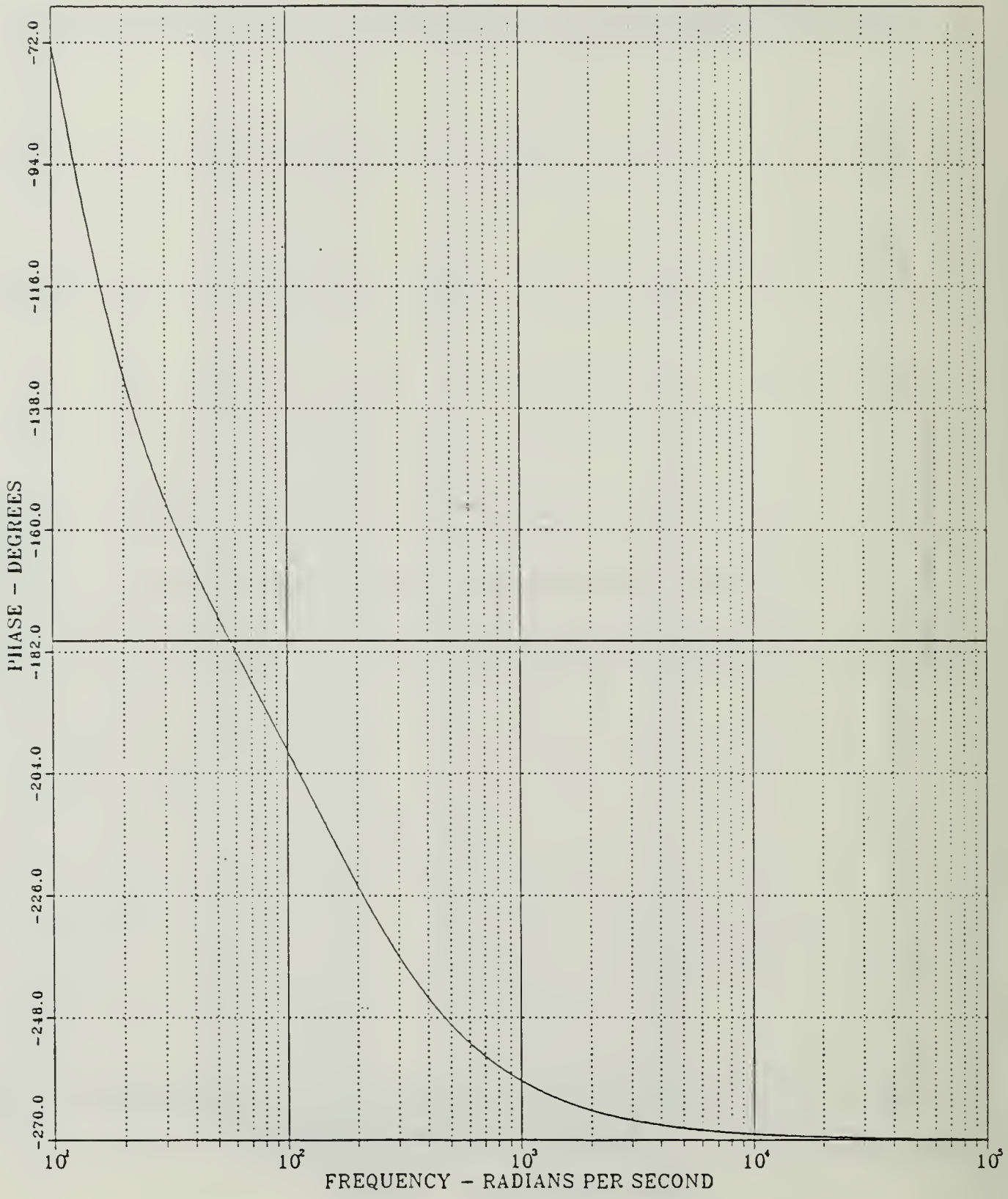

Figure 2.13 Pitch Angular Rate; Uncoupled Pitch Channel;
Continuous Open Loop System; Phase vs Frequency.

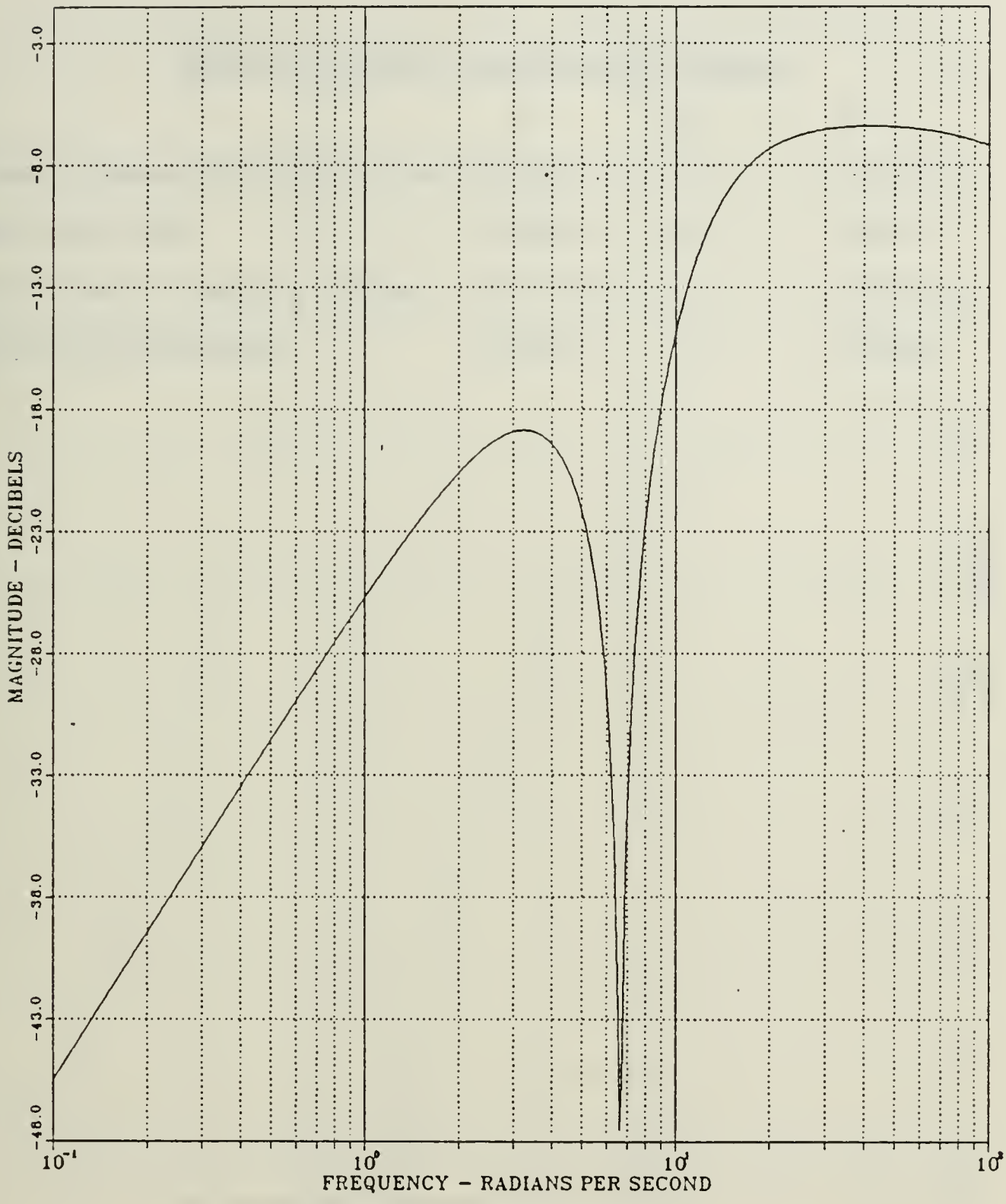

Figure 2.14 Pitch Tail Incidence; Uncoupled Pitch Channel;
Continuous Open Loop System; Gain vs Frequency.

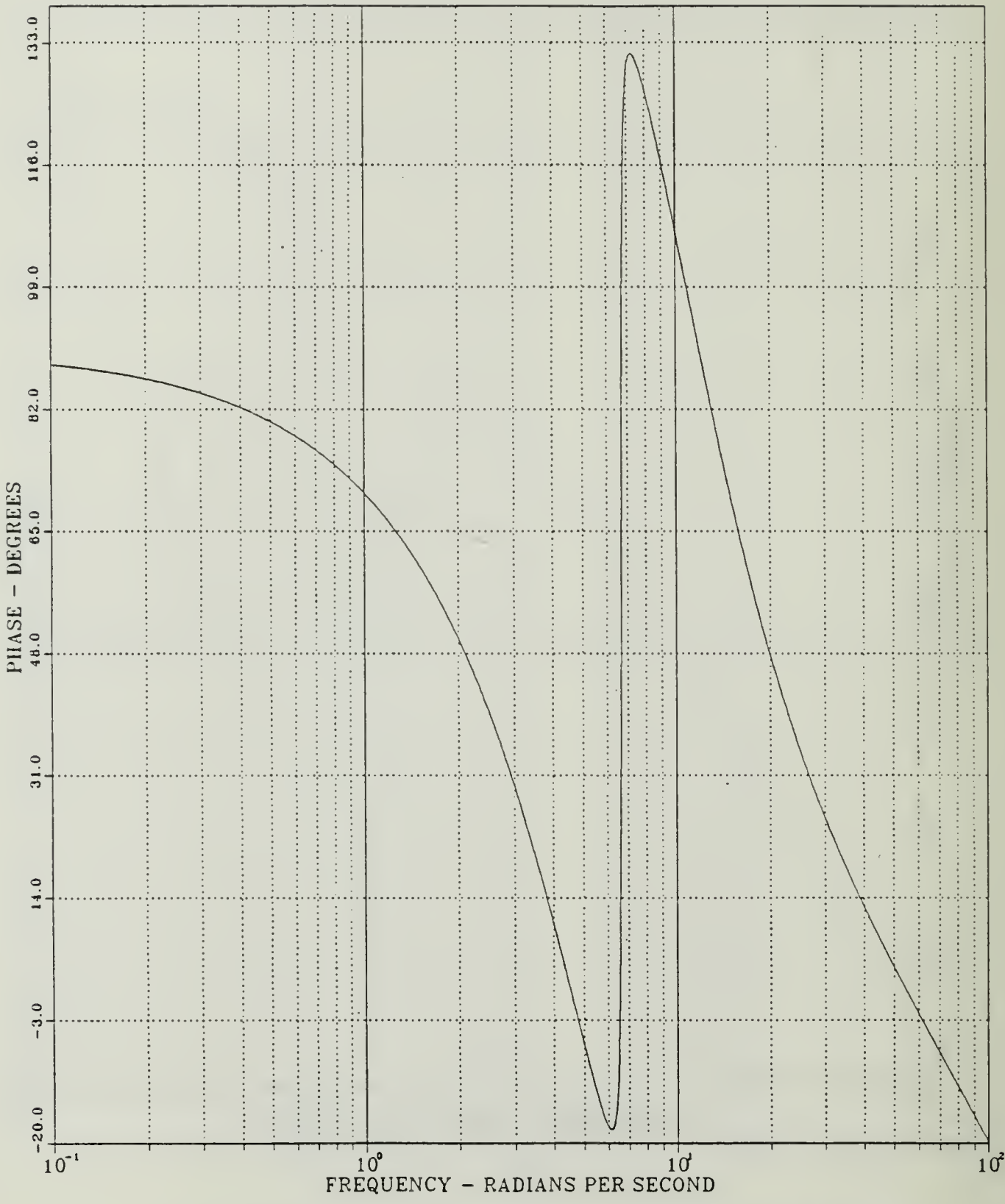

Figure 2.15 Pitch Tail Incidence; Uncoupled Pitch Channel; Continuous Open Loop System; Phase vs Frequency.

TABLE II

Stability Margins of Uncoupled Pitch Channel

	q	δ_p	nz
Phase Crossover Frequency (rad/sec):	56.6896	-----	57.2151
Gain Margin (DB):	29.0988	-----	7.5450
Gain Crossover Frequency (rad/sec):	5217.1016	-----	375.9622
Phase Margin (Degrees):	87.9482	-----	62.9508

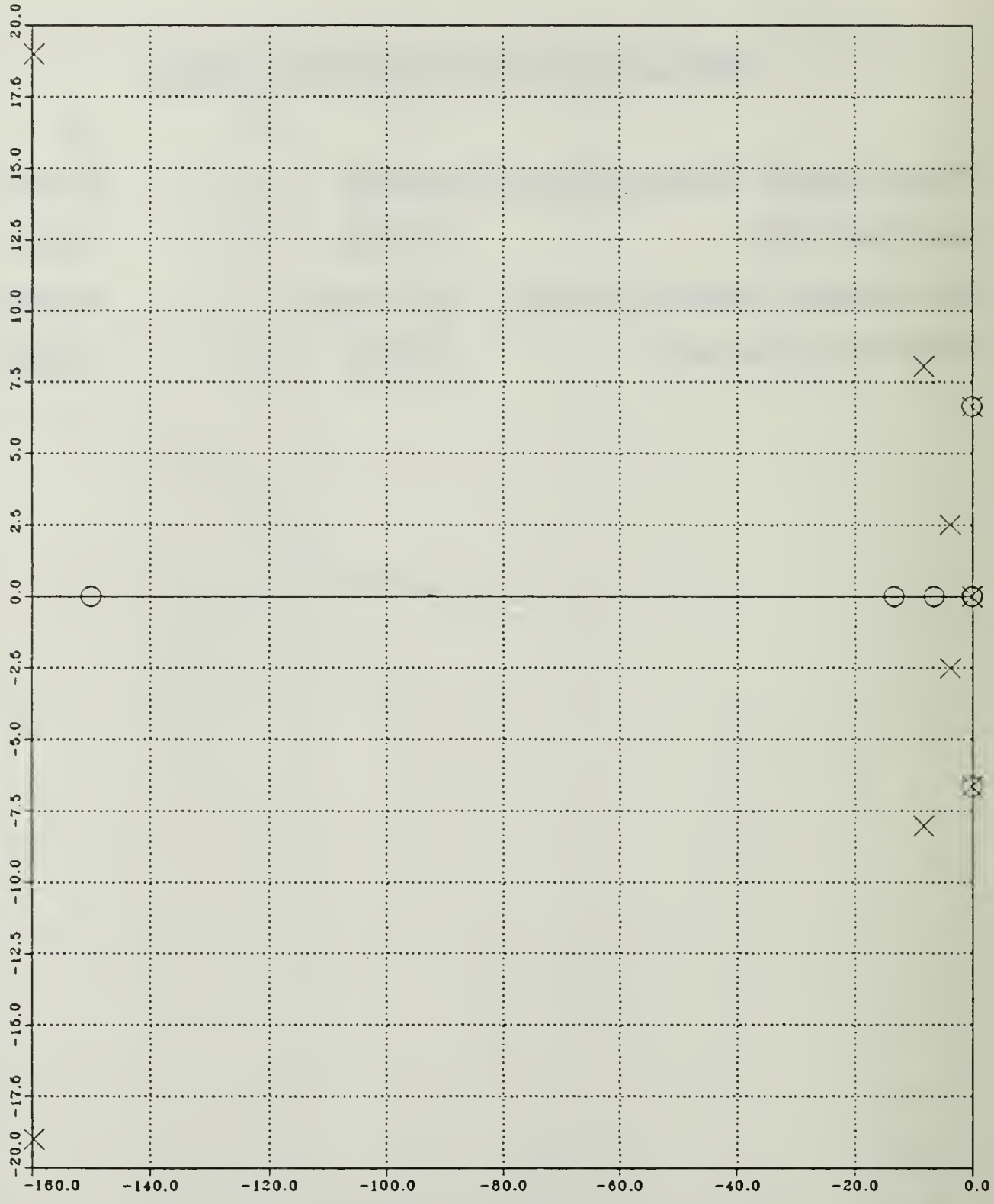

Figure 2.16 Pitch Normal Acceleration; Uncoupled Pitch Channel; Continuous Open Loop System; Pole-Zero Map.

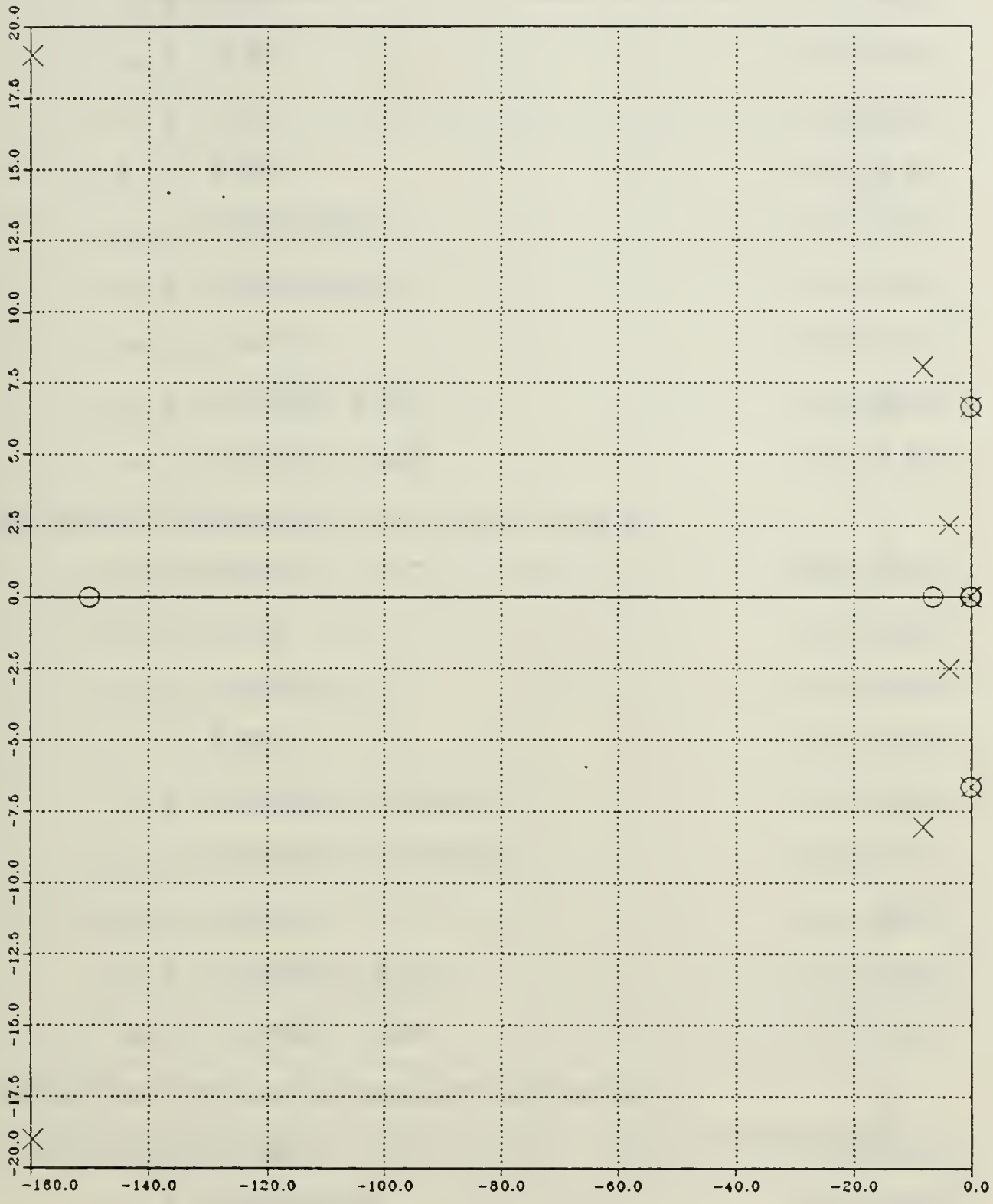

Figure 2.17 Pitch Angular Rate; Uncoupled Pitch Channel; Continuous Open Loop System; Pole-Zero Map.

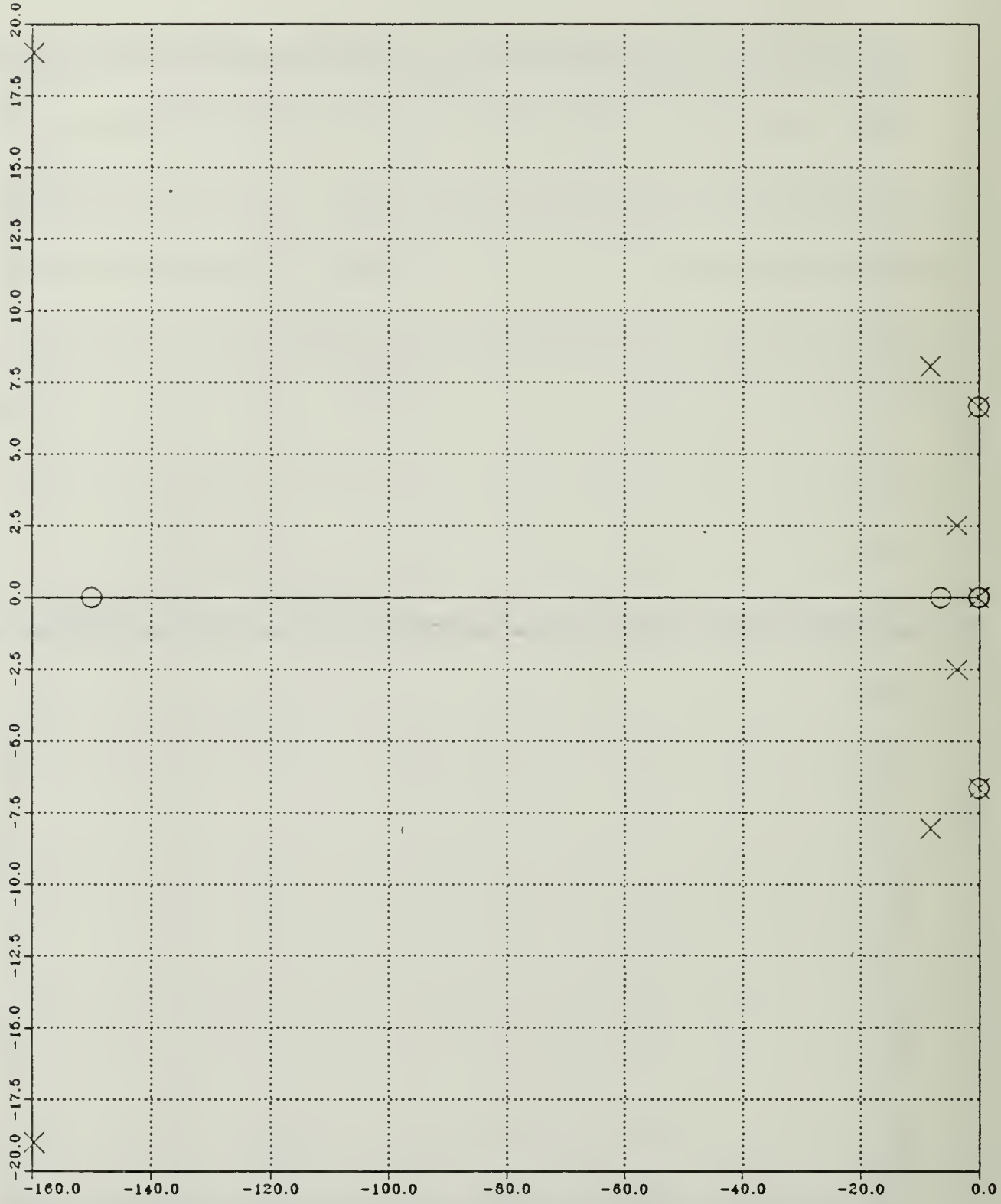

Figure 2.18 Pitch Tail Incidence; Uncoupled Pitch Channel; Continuous Open Loop System; Pole-Zero Map.

The zeros of pitch normal acceleration are found to be at:

$s_1 = -150.00$ (II.C.4-45)

$s_2 = 13.32$ (II.C.4-46)

$s_3 = -13.32$ (II.C.4-47)

$s_4 = -6.550$ (II.C.4-48)

$s_5 = -0.000008758$ (II.C.4-49)

$s_6 = 0.000004509$ (II.C.4-50)

$s_7 = -0.1430$ (II.C.4-51)

$s_8 = -0.07459 + j\,6.66$ (II.C.4-52)

$s_9 = -0.07459 - j\,6.66$ (II.C.4-53)

The zeros of pitch angular rate are found to be at:

$s_1 = -150.00$ (II.C.4-54)

$s_2 = -0.119$ (II.C.4-55)

$s_3 = 0.001734$ (II.C.4-56)

$s_4 = -6.550$ (II.C.4-57)

$s_5 = -0.000867 + j\,0.001516$ (II.C.4-58)

$s_6 = -0.000867 - j\,0.001516$ (II.C.4-59)

$s_7 = -0.1430$ (II.C.4-60)

$s_8 = -0.07459 + j\,6.66$ (II.C.4-61)

$s_9 = -0.07459 - j\,6.66$ (II.C.4-62)

The zeros of pitch tail incidence are found to be at:

$s_1 = -150.00$ (II.C.4-63)

$s_2 = -0.000001322$ (II.C.4-64)

$s_3 = -6.550$ (II.C.4-65)

$s_4 = 0.000001189$ (II.C.4-66)

$$s_5 = -0.1430 \qquad \text{(II.C.4-67)}$$

$$s_6 = -0.07459 + j\,6.66 \qquad \text{(II.C.4-68)}$$

$$s_7 = -0.07459 - j\,6.66 \qquad \text{(II.C.4-69)}$$

$$s_8 = -0.07459 + j\,6.66 \qquad \text{(II.C.4-70)}$$

$$s_9 = -0.07459 - j\,6.66 \qquad \text{(II.C.4-71)}$$

5. Design Approach and Analysis of the Discrete Open Loop System

The control of physical systems with a digital computer is becoming more and more common. Many new digital control applications are being stimulated by microprocessor technology. Among the advantages of digital logic for control are the increased flexibility of the control programs and the decision-making or logic capability of digital systems which can be shared with the control function to meet other system requirements.

In order to compute the state X(t) by use of a digital computer, the continuous-time state equation $\dot{\mathbf{X}} = \mathbf{FX+GU}$ must be converted into the discrete-time equation $\dot{\mathbf{X}} = \mathbf{AX+BU}$, assuming that the input vector **U** changes only at the equally spaced sampling instants T.

Utilizing the Analog-to-Digital conversion of ORACLS the continuous time matrices **F** and **G** were converted to the discrete time matrices **A** and **B** using sample time T=0.0125 sec (Frequency=80 cps).

The computer listing of the above conversion is shown in Appendix B.

The TRANFUNC option of ORACLS was used to analyze the dicrete open loop transfer function and time responses and pole-zero maps plots were obtained as for the continuous system.

Figures 2.19 shows the discrete time response of pitch normal acceleration (n_z) which has a 0.5 seconds time constant, steady-state error

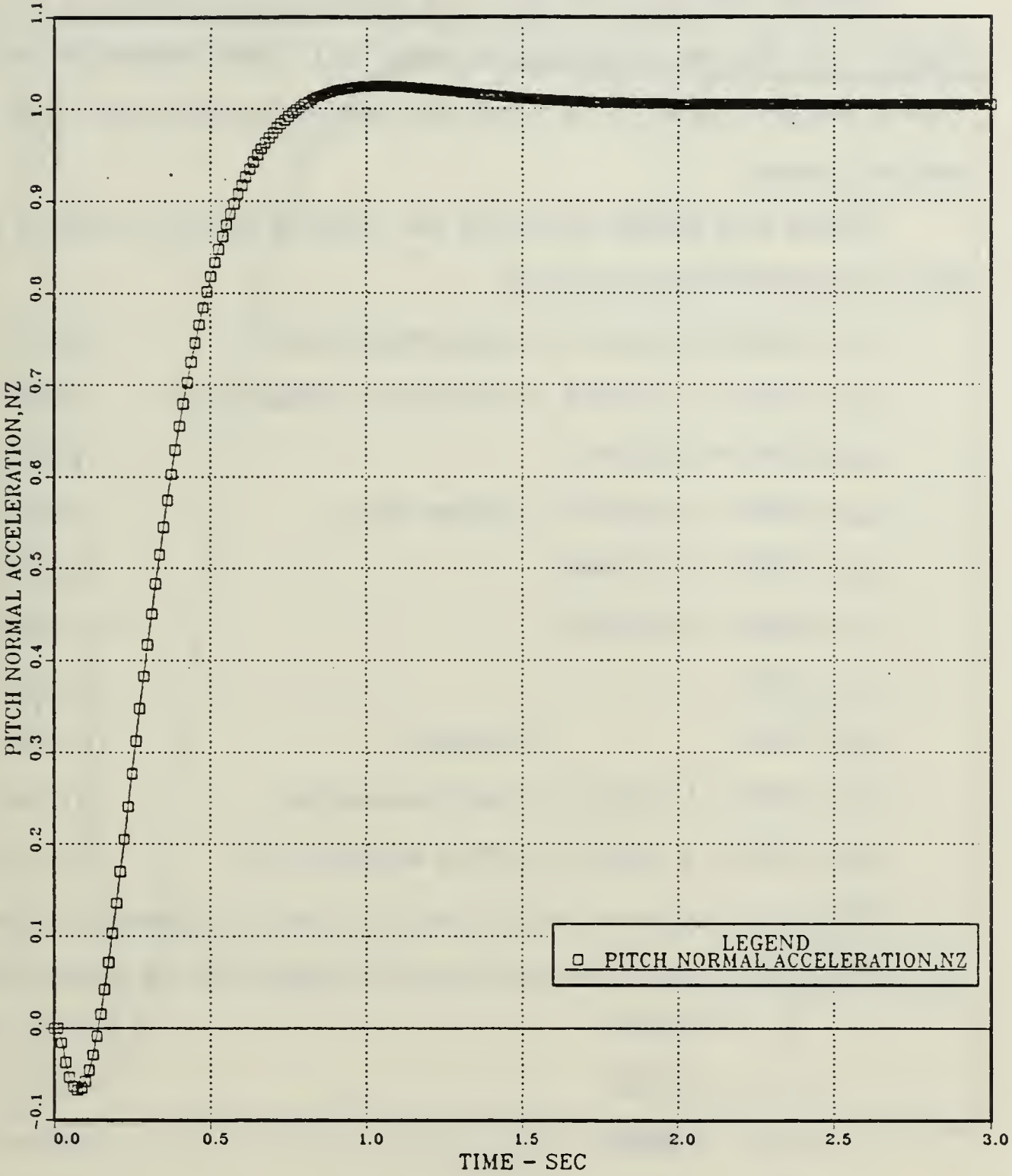

Figure 2.19 Pitch Normal Acceleration vs Time; Uncoupled Pitch Channel; Discrete Open Loop System.

about 0.005 and 2.0% overshoot, and therefore is according to the requirements mentionted in section II.A.

Figures 2.20 and 2.21 show the discrete time responses of pitch angular rate (q), and pitch tail incidence (δ_p). These responses matched those presented in [Ref. 3]. An input step function representing "1 gee" was used in all cases.

Figures 2.22 through 2.24 show the discrete Pole-Zero Maps of n_z, q, and δ_p. The poles are found to be at:

$z_1 = 0.1320 + j\ 0.03194$ (Acceleration Filter) (II.C.5-1)

$z_2 = 0.1320 - j\ 0.03194$ (Acceleration Compensator) (II.C.5-2)

$z_3 = 0.8970 + j\ 0.09067$ (II.C.5-3)

$z_4 = 0.8970 - j\ 0.09067$ (Angular Rate) (II.C.5-4)

$z_5 = 0.9536 + j\ 0.02999$ (II.C.5-5)

$z_6 = 0.9536 - j\ 0.02999$ (II.C.5-6)

$z_7 = 0.9982$ (II.C.5-7)

$z_8 = 1.0000$ (Actuator) (II.C.5-8)

$z_9 = 0.9956 + j\ 0.08307$ (Rate Compensator) (II.C.5-9)

$z_{10} = 0.9956 - j\ 0.08307$ (Normal Acceleration) (II.C.5-10)

Since all the poles are within the unit circle the system is stable.

The zeros of the discrete pitch normal acceleration are found to be at:

$z_1 = -0.4663$ (II.C.5-11)

$z_2 = 0.1532$ (II.C.5-12)

$z_3 = 0.8466$ (II.C.5-13)

$z_4 = 1.1810$ (II.C.5-14)

$z_5 = 0.9214$ (II.C.5-15)

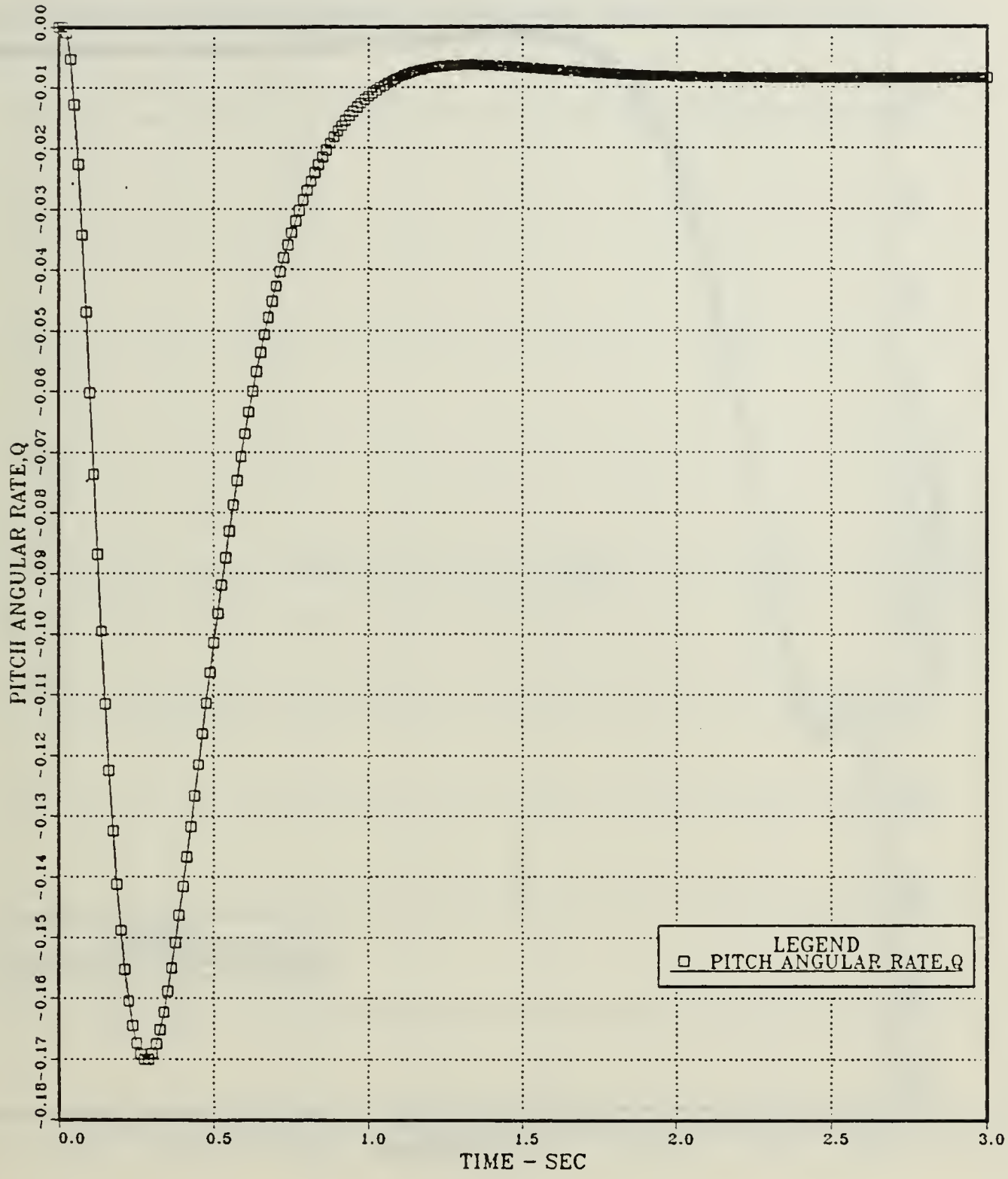

Figure 2.20 Pitch Angular Rate vs Time; Uncoupled Pitch Channel; Discrete Open Loop System.

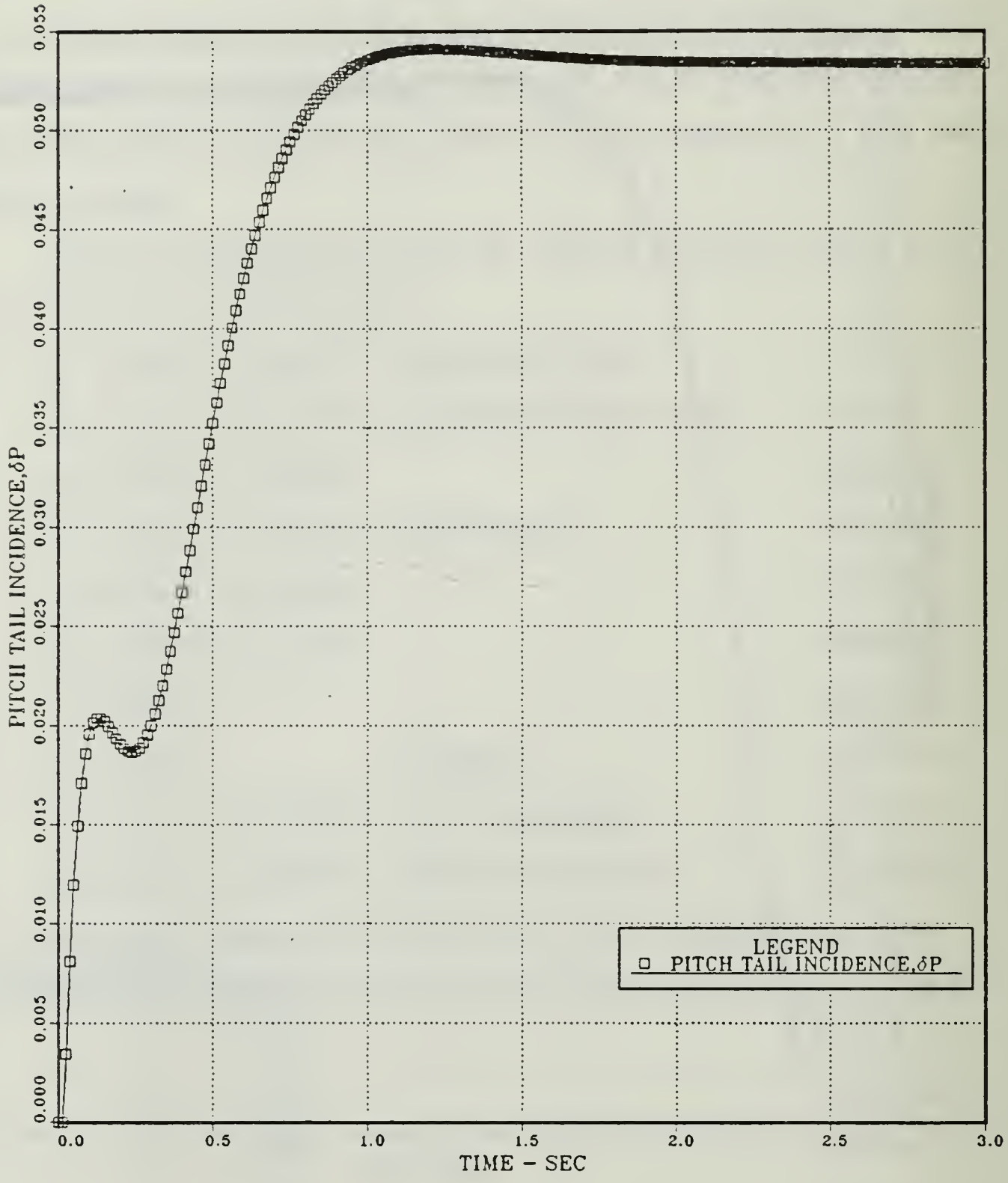

Figure 2.21 Pitch Tail Incidence vs Time; Ucoupled Pitch Channel; Discrete Open Loop System.

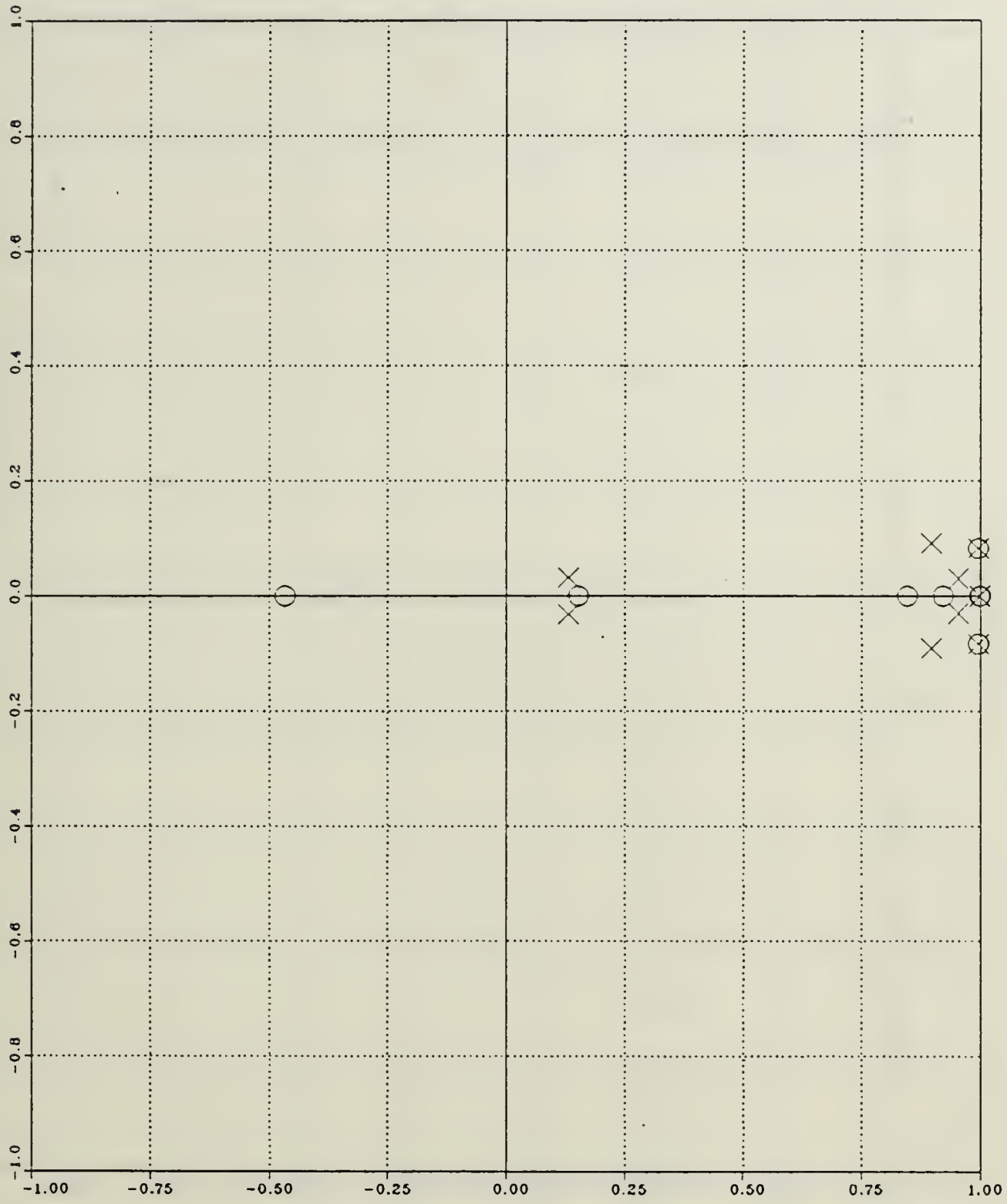

Figure 2.22 Pitch Normal Acceleration; Uncoupled Pitch Channel; Discrete Open Loop System; Pole-Zero Map.

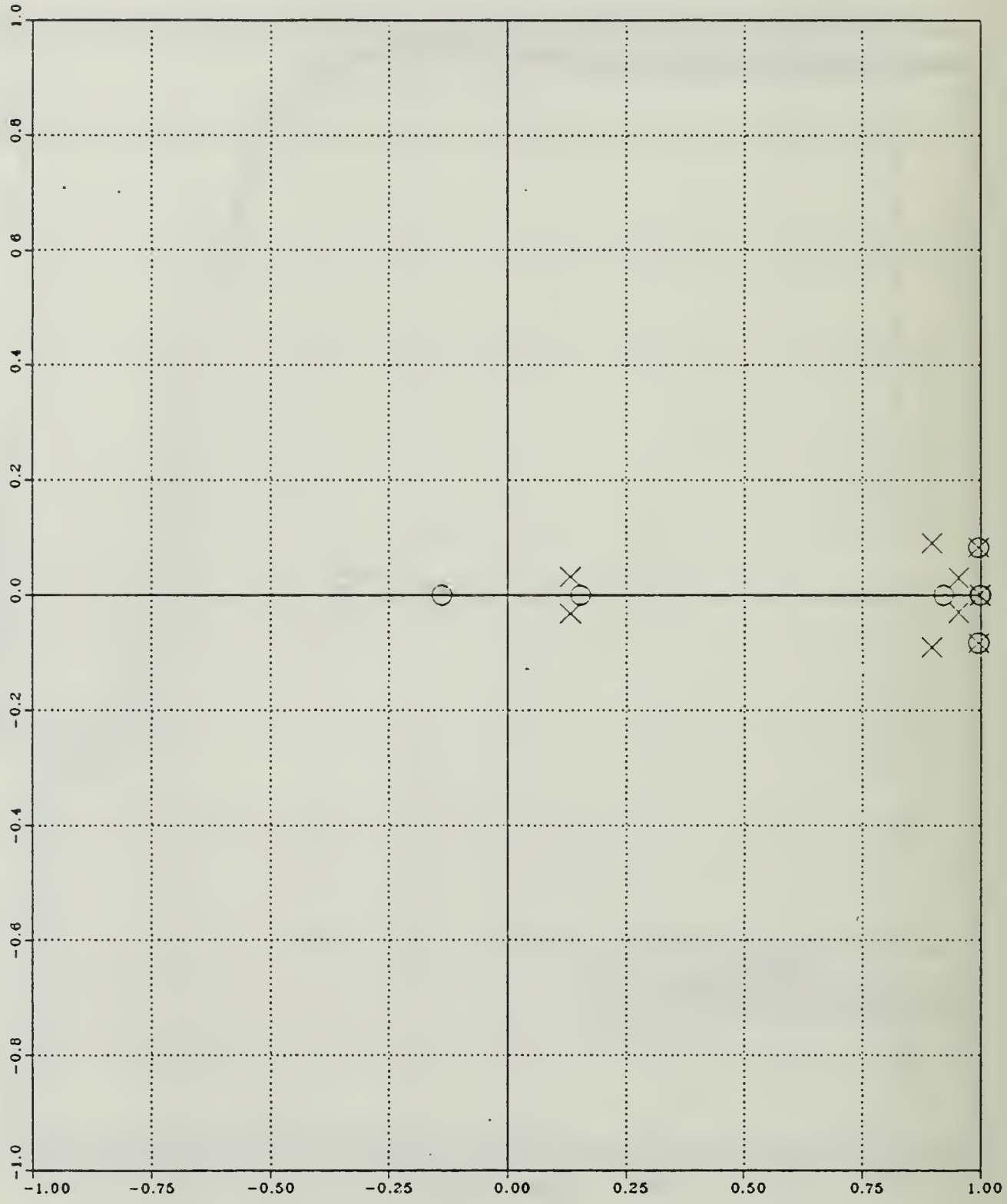

Figure 2.23 Pitch Angular Rate; Uncoupled Pitch Channel; Discrete Open Loop System; Pole-Zero Map.

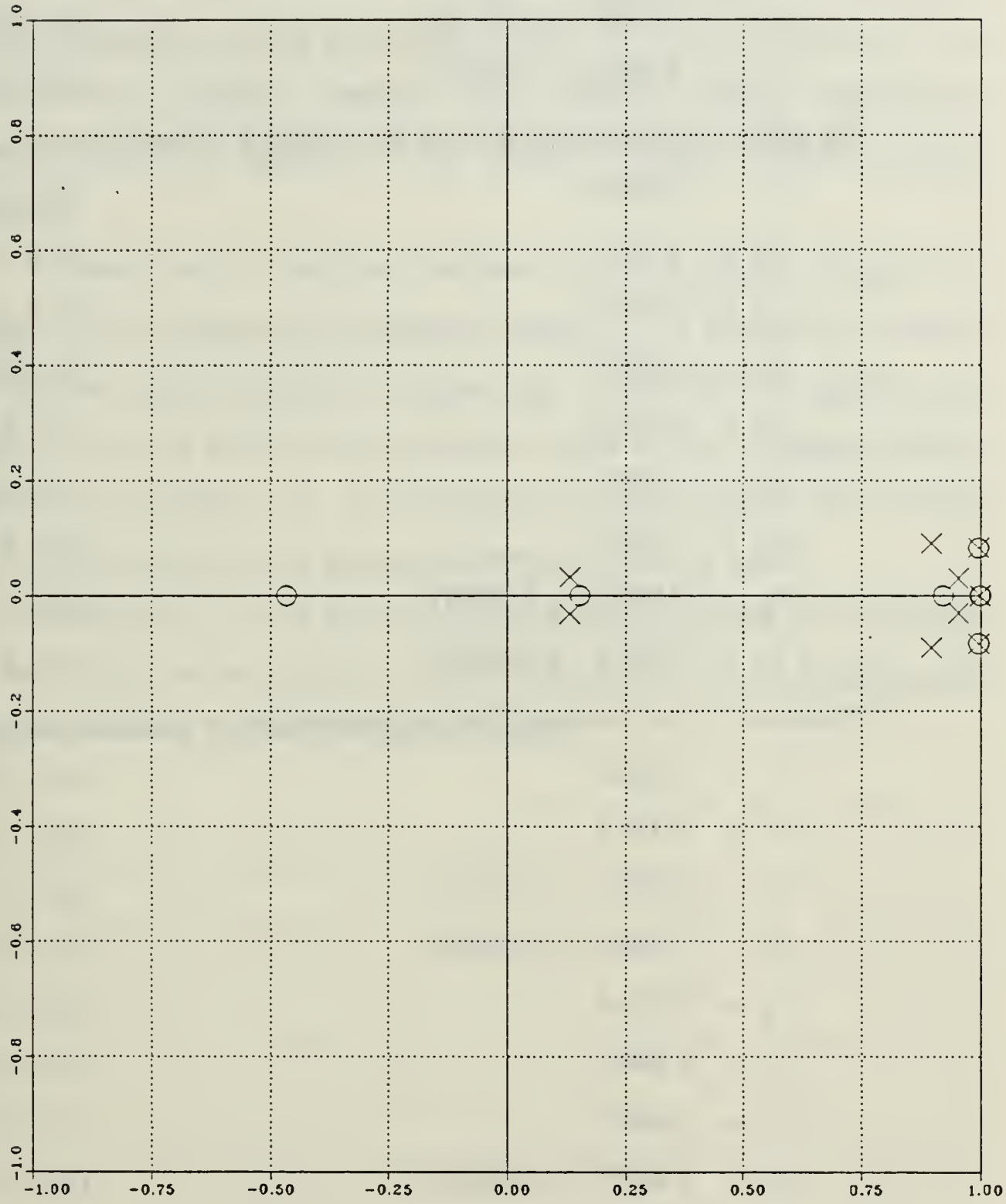

Figure 2.24 Pitch Tail Incidence; Uncoupled Pitch Channel; Discrete Open Loop System; Pole-Zero Map.

$$z_6 = 0.9982 \quad \text{(II.C.5-16)}$$

$$z_7 = 1.0000 \quad \text{(II.C.5-17)}$$

$$z_8 = 0.9956 + j\,0.08307 \quad \text{(II.C.5-18)}$$

$$z_9 = 0.9956 - j\,0.08307 \quad \text{(II.C.5-19)}$$

The zeros of the discrete pitch angular rate are found to be at:

$$z_1 = -2.2750 \quad \text{(II.C.5-20)}$$

$$z_2 = 0.1534 \quad \text{(II.C.5-21)}$$

$$z_3 = -0.1386 \quad \text{(II.C.5-22)}$$

$$z_4 = 0.9985 \quad \text{(II.C.5-23)}$$

$$z_5 = 0.9214 \quad \text{(II.C.5-24)}$$

$$z_6 = 0.9982 \quad \text{(II.C.5-25)}$$

$$z_7 = 1.0000 \quad \text{(II.C.5-26)}$$

$$z_8 = 0.9956 + j\,0.08307 \quad \text{(II.C.5-27)}$$

$$z_9 = 0.9956 - j\,0.08307 \quad \text{(II.C.5-28)}$$

The zeros of the discrete pitch tail incidence are found to be at:

$$z_1 = -0.4658 \quad \text{(II.C.5-29)}$$

$$z_2 = 0.1532 \quad \text{(II.C.5-30)}$$

$$z_3 = 0.9956 - j\,0.08307 \quad \text{(II.C.5-31)}$$

$$z_4 = 0.9956 + j\,0.08307 \quad \text{(II.C.5-32)}$$

$$z_5 = 0.9214 \quad \text{(II.C.5-33)}$$

$$z_6 = 0.9982 \quad \text{(II.C.5-34)}$$

$$z_7 = 1.0000 \quad \text{(II.C.5-35)}$$

$$z_8 = 0.9956 + j\,0.08307 \quad \text{(II.C.5-36)}$$

$$z_9 = 0.9956 - j\,0.08307 \quad \text{(II.C.5-37)}$$

6. Comparison of Continuous and Discrete Systems

In this chapter the classical design of the continuous uncoupled pitch channel autopilot, as was developed in [Ref. 3], was reviewed, and the corresponding discrete channel was obtained using state-space representation of the system and the Analog-to-Digital Conversion option of ORACLS.

A comparison of the time responses in the s-domain (Figures 2.7 through 2.9) with those in the z-domain (Figures 2.19 through 2.21) shows that the two systems behave the same way. In addition both systems are stable as it can be seen from the pole-zero maps of the continuous system (Figures 2.13 through 2.15) , and the discrete system (Figures 2.22 through 2.24) , since their poles are maping according to relation $z=e^{sT}$.

The similarity of the continuous and discrete systems allow us from now on to work on the discrete domain without any loss of accurasy, and using the computer to make things much easier.

III. MODERN CONTROL DESIGN AND ANALYSIS OF LONGITUDINAL UNCOUPLED PITCH CHANNEL AUTOPILOT

A. GENERAL

The design technique for the uncoupled pitch channel, as developed in [Ref. 3], was classical using a combination of frequency response and root-locus techniques.

In classical control theory, only the input, output, and error signals are considered important; the analysis and design of control systems are carried out using transfer functions, together with a variety of graphical techniques as root-locus plots and Nyquist plots. The unique characteristic of classical control theory is that it is based on the input-output relation of the system, or the transfer function.

The main disadvantage of classical control theory is that, generally speaking, it is applicable only to linear time-invariant systems having a single input and a single output. It is powerless for time-varying systems, non-linear systems (except simple ones), and multiple-input-multiple-output systems. Thus classical techniques (the root-locus and frequency response methods) do not apply to the design of optimal and adaptive control systems, which are mostly time-varying and/or linear.

The modern trend in engineering systems is toward greater complexity, due mainly to the requirements of complex task and good accuracy. Complex

systems may have multiple inputs and multiple outputs and may be time-varying.

Because of the necessity of meeting increasingly stringent requirements on the performance of control systems, the increase in system complexity,and easy access to large-scale computers, modern control theory, which is a new approach to the analysis and design of complex control systems, has been developed since around 1960. This new approach is based on the concept of state-space representation.

Modern control theory is contrasted with classical control theory in that the former is applicable to multiple-input-multiple-output systems, which may be linear or non-linear, time-invariant or time-varying, while the latter is applicable only to linear time-invariant single-input-single-output systems. Also, modern control theory is essentially a time-domain approach, while classical control theory is a complex frequency-domain approach.

System design in classical control theory is based on trial-and-error procedures which, in general, will not yield optimal control systems. System design in modern control theory, on the other hand, enables the engineer to design optimal control systems with respect to given performance indexes. In addition, design in modern control theory can be carried out for a class of inputs, instead of a specific input function, such as the impulse function, step function, or sinusoidal function. Also, modern control theory enables the engineer to include initial conditions in the design.

The equations of the uncoupled pitch channel autopilot have already been in state-space form $\dot{X} = AX + BU$,in the previous chapter , and therefore we proceed in the modern control design of the discrete state-feedback autopilot.

B. STATE FEEDBACK DESIGNED AUTOPILOT

1. Design Approach and Analysis of Control Law

One of the attractive features of state-space design methods is that the procedure consists of two independent steps. One step assumes that we have all the states at our disposal for feedback purposes. In general, of course, this would be unrealistic since a practical engineer would not, as a rule, find it necessary to purchase this large number of sensors, especially since he knows that he would not need them, using classical design methods. The assumption that all states are available merely allows us to proceed with the first step, namely, the control law. The remaining step is to design an "estimator" which estimates the entire state vector, given measurements of the portion of the state provided by $y = HX + JU$.

The final control algorithm will consist of the control law and the estimator combined where the control-law calculations are based on the estimated states rather than the actual states. This substitution is reasonable and the combined control law and estimator will give closed-loop dynamic characteristics which are unchanged from those assumed in designing the control law and the estimator separately. The dynamic system we obtain from the combined control law and the estimator is called the controller.The first step is to get a good control law.

The control law is simply the feedback of a linear combination of all the states, that is,

$$\mathbf{U} = -\mathbf{K}\mathbf{X} \qquad \text{(III.B.1-1)}$$

The characteristic equation of the controlled (closed loop) system is

$$\det[\, z\mathbf{I} - \mathbf{A} + \mathbf{B}\mathbf{K} \,] = 0 \qquad \text{(III.B.1-2)}$$

The control law design then consists of picking the elements of **K** so that the roots of equation III.B.1-2 are in desirable locations.

A program logic for application of Ackermann's formula to compute the control law is given in Appendix C. The program reads in the sample time T, the discrete matrices **A** , **B** and the desired pole locations in the s-plane and gives as output the control law matrix **K**.

The program used in this work was written in WATFIV computer language and is given in Appendix D.

In section III.C.5 utilizing Analog-to-Digital conversion the discrete uncoupled pitch channel matrices **A** and **B** were obtained. Also the analysis of the continuous open loop system, obtained from OPTSYS, showed the eigenvalues of the classical design to be at:

$$s_1 = -159.724 + j\ 18.9921 \qquad \text{(III.B.1-3)}$$

$$s_2 = -159.724 - j\ 18.9921 \qquad \text{(III.B.1-4)}$$

$$s_3 = -8.29048 + j\ 8.05932 \qquad \text{(III.B.1-5)}$$

$$s_4 = -8.29048 - j\ 8.05932 \qquad \text{(III.B.1-6)}$$

$$s_5 = -3.75925 + j\ 2.51463 \qquad \text{(III.B.1-7)}$$

$$s_6 = -3.75925 - j\ 2.51463 \qquad \text{(III.B.1-8)}$$

$$s_7 = -0.14393000 \qquad \text{(III.B.1-9)}$$

$$s_8 = -0.00000425 \qquad \text{(III.B.1-10)}$$

$s_9 = -0.074593 + j\ 6.65959$ (III.B.1-11)

$s_{10} = -0.074593 - j\ 6.65959$ (III.B.1-12)

Utilizing Ackermann's formula program (Appendix D) and using sample time T= 0.0125 sec (80 cps), the discrete matrices **A**,**B** (Appendix B) and desired poles locations in s-plane the continuous open loop eigenvalues (equations III.B.1-3 through III.B.1-12) the control law was found to be:

$$\mathbf{K} = [-0.0188 \quad -0.0279 \quad -0.0042 \quad 0.0290 \quad 0.0041$$
$$0.0 \quad 0.0001 \quad 1.7732 \quad -2.0162 \quad 0.0131] \quad \text{(III.B.1-13)}$$

Utilizing Transfer Function Analysis from TRANFUNC option of ORACLS, and using the discrete matrices **A**,**B** and **K** the state-feedback autopilot was designed and analysed according to step responses and Pole-Zero Maps.

2. Performance of System

A comparison of the discrete open loop eigenvalues (det[$z\mathbf{I}-\mathbf{A}$]=0), obtained using the Compensator Transfer Function Analysis from TRANFUNC option of ORACLS:

$z_1 = 0.131993 + j\ 0.0319377$ (III.B.2-1)

$z_2 = 0.131993 - j\ 0.0319377$ (III.B.2-2)

$z_3 = 0.896987 + j\ 0.0906708$ (III.B.2-3)

$z_4 = 0.896987 - j\ 0.0906708$ (III.B.2-4)

$z_5 = 0.953625 + j\ 0.0299850$ (III.B.2-5)

$z_6 = 0.953625 - j\ 0.0299850$ (III.B.2-6)

$z_7 = 0.998202$ (III.B.2-7)

$z_8 = 1.000000$ (III.B.2-8)

$z_9 = 0.995608 + j\ 0.0830713$ (III.B.2-9)

$z_{10} = 0.995608 - j\ 0.0830713$ (III.B.2-10)

with the closed loop regulator eigenvalues (det[zI-A+BK]=0) obtained using the Transfer Function Analysis from TRANFUNC option of ORACLS:

$z_1 = 0.134462 + j\ 0.0320974$ (III.B.2-11)

$z_2 = 0.134462 - j\ 0.0320974$ (III.B.2-12)

$z_3 = 0.896990 + j\ 0.0906457$ (III.B.2-13)

$z_4 = 0.896990 - j\ 0.0906457$ (III.B.2-14)

$z_5 = 0.953624 + j\ 0.0299994$ (III.B.2-15)

$z_6 = 0.953624 - j\ 0.0299994$ (III.B.2-16)

$z_7 = 0.998202$ (III.B.2-17)

$z_8 = 1.000000$ (III.B.2-18)

$z_9 = 0.995608 + j\ 0.0830713$ (III.B.2-19)

$z_{10} = 0.995608 - j\ 0.0830713$ (III.B.2-20)

shows no significant differences.

Figures 3.1 through 3.3 show the discrete closed loop time responses of pitch normal acceleration (n_z), pitch angular rate (q), and pitch tail incidence (δ_p). An input step function representing "1 gee" was used. A comparison of the responses mentioned above, with the corresponding time responses of the discrete open loop system ,Figures 2.19 through 2.21 shows that they are identical.

Figures 3.4 through 3.6 show the Pole-Zero Map plots of n_z, q, and δ_p. All the poles,given by equations III.B.2-11 through III.B.2-20, are inside the unit circle and the system is stable. There are no real zeros in the system.

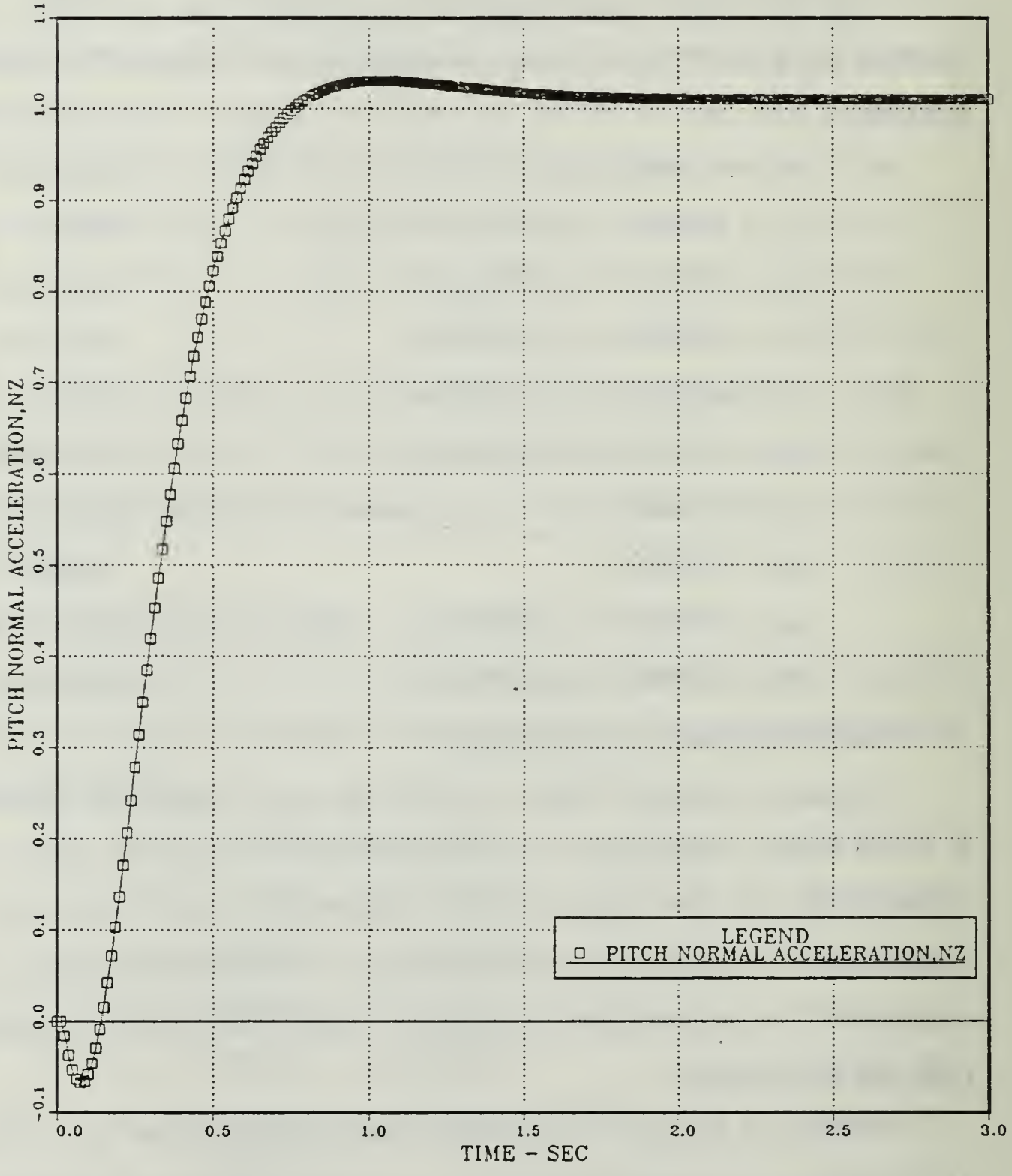

Figure 3.1 Pitch Normal Acceleration vs Time; Uncoupled Pitch Channel; Discrete State-Feedback Autopilot.

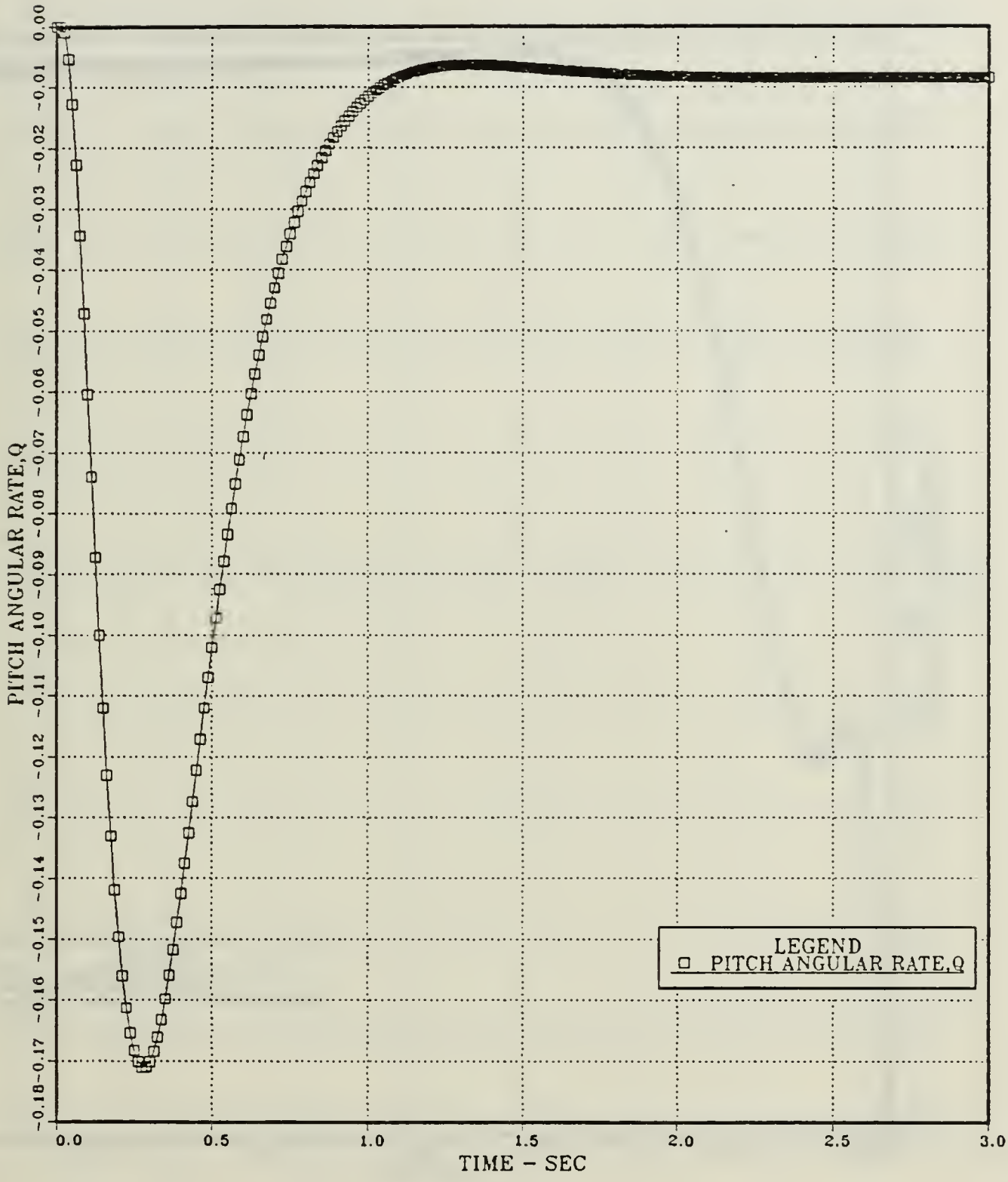

Figure 3.2 Pitch Angular Rate vs Time; Uncoupled Pitch Channel; Discrete State-Feedback Autopilot.

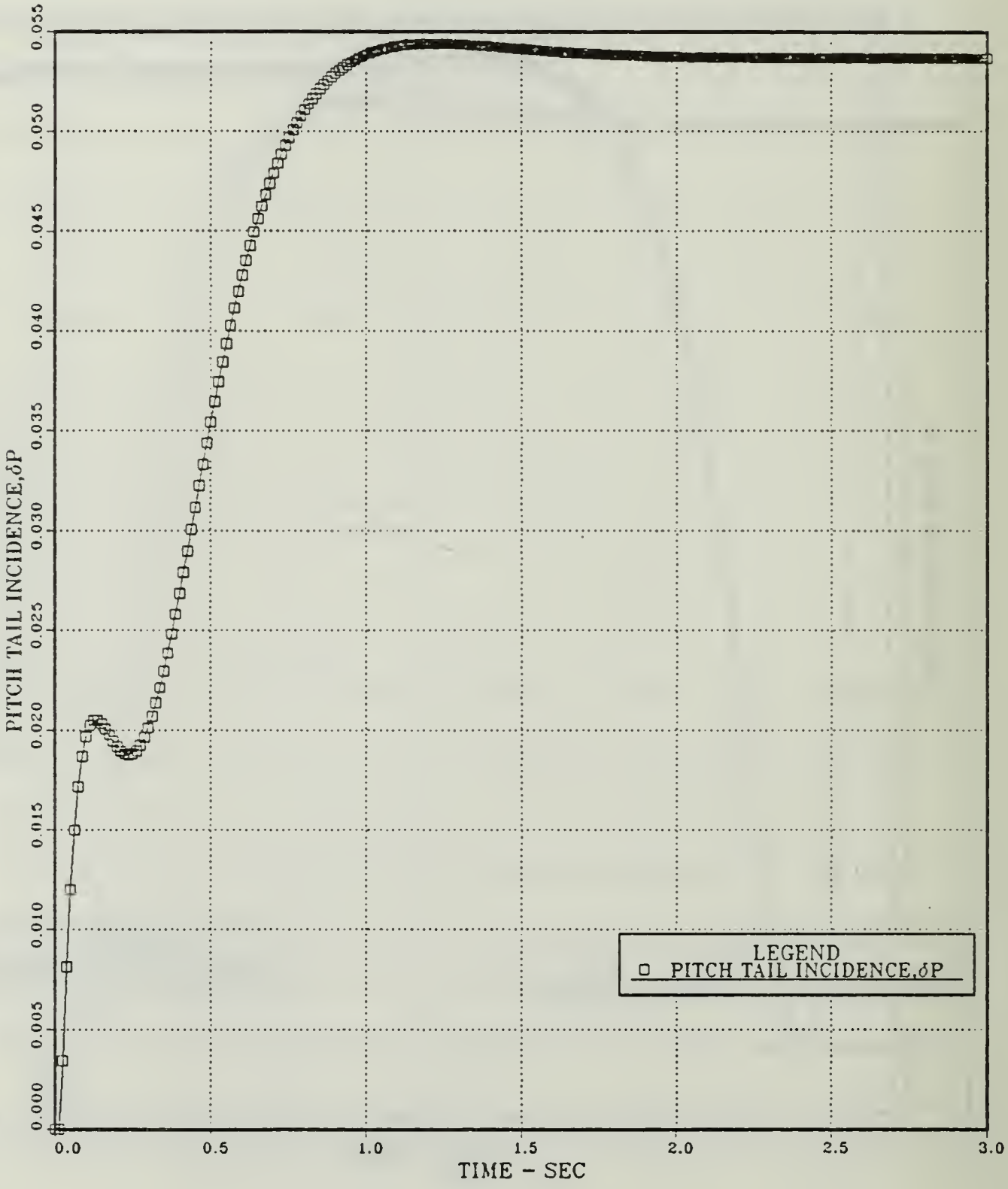

Figure 3.3 Pitch Tail Incidence vs Time; Uncoupled Pitch Channel; Discrete State-Feedback Autopilot.

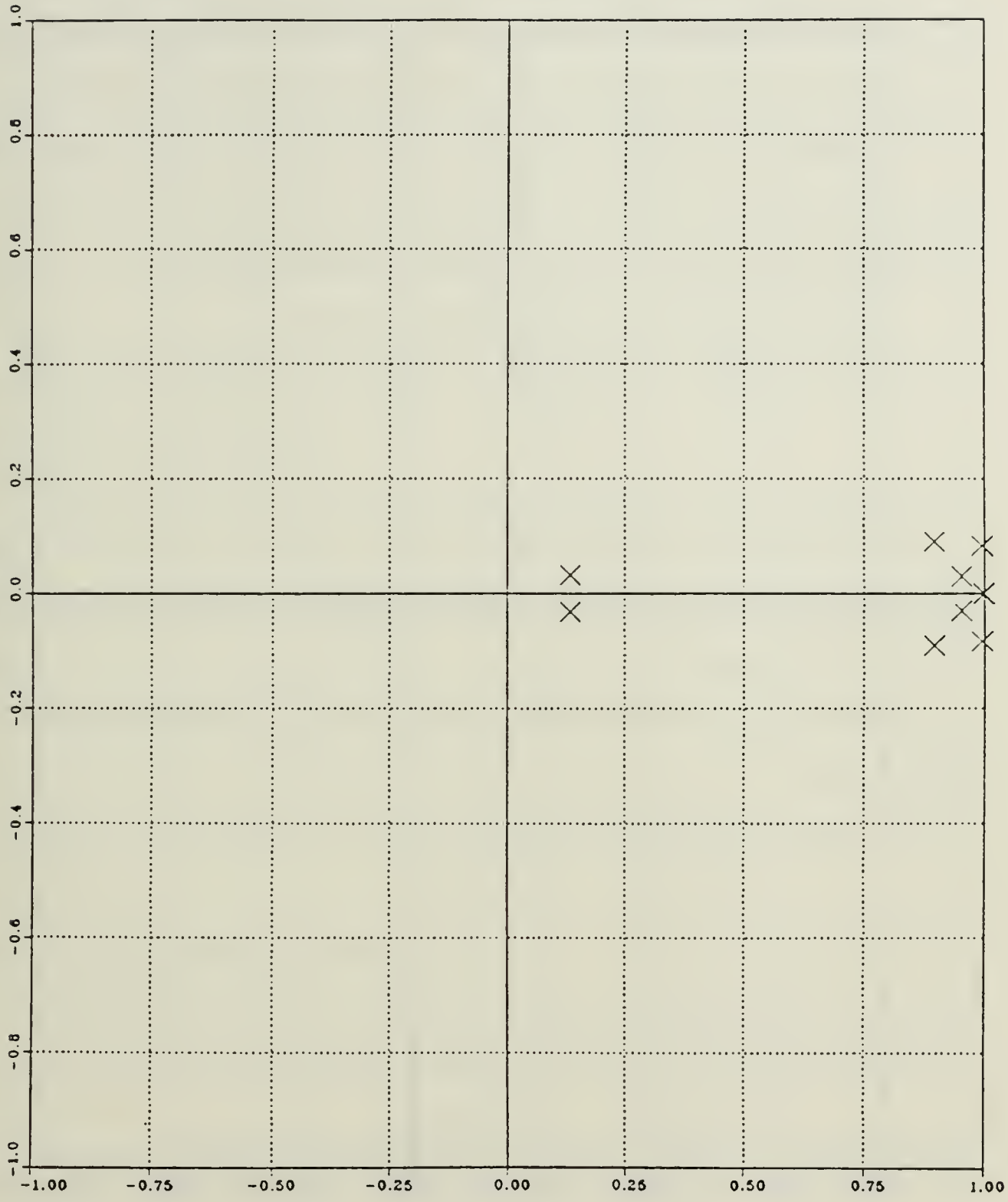

Figure 3.4 Pitch Normal Acceleration ; Uncoupled Pitch Channel; Discrete State-Feedback Autopilot; Pole-Zero Map.

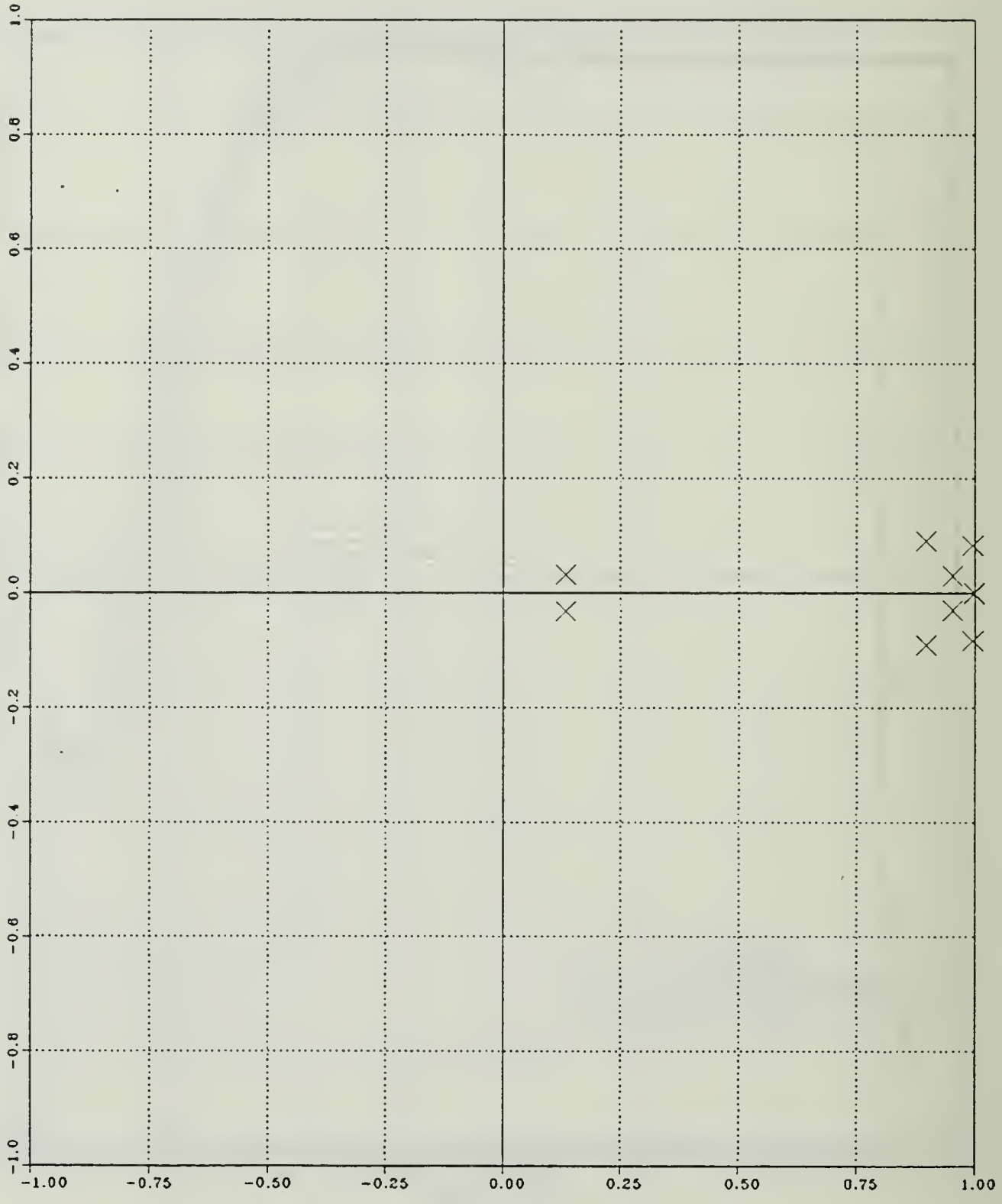

Figure 3.5 Pitch Angular Rate; Uncoupled Pitch Channel; Discrete State-Feedback Autopilot; Pole-Zero Map.

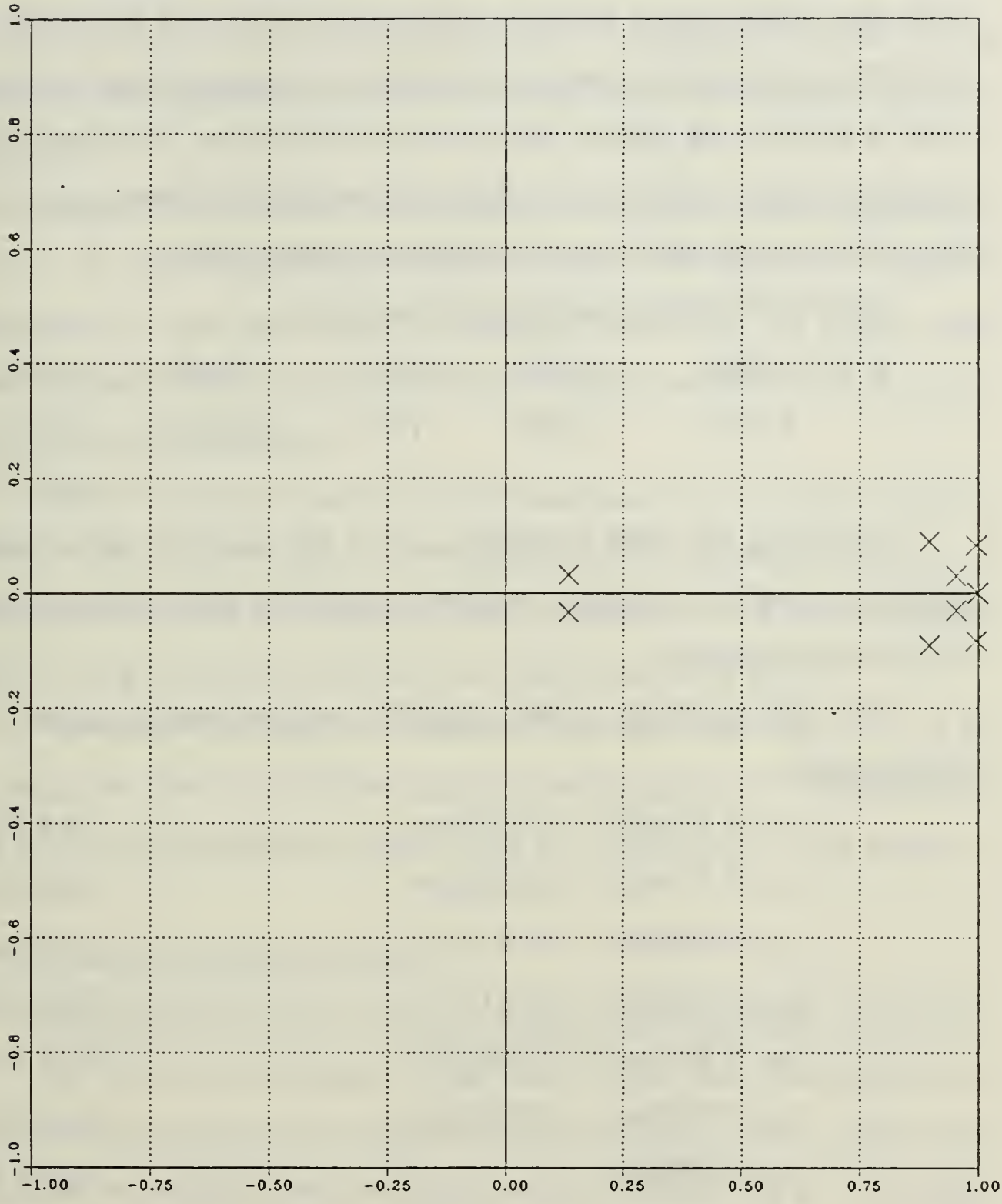

Figure 3.6 Pitch Tail Incidence; Uncoupled Pitch Channel; Discrete State-Feedback Autopilot; Pole-Zero Map.

3. Simplified State-Feedback Designed Autopilot

In the previous section the state-feedback autopilot was designed using the feedback gain vector (equation III.B.1-13), and therefore there were ten (10) returning gain loops making the system more complex. In order to simplify the system, zero gains were introdused, where those gains were very small in the state feedback gain vector,and in doing so returning gain loops were eliminated and the system became simpler.

The resulted state-feedback gain vector is:

$$\mathbf{K} = [-0.0188 \quad -0.0279 \quad 0.0000 \quad 0.0290 \quad 0.0000 \quad 0.0000 \quad 0.0000 \quad 1.7732 \quad -2.0162 \quad 0.0131] \qquad \text{(III.B.3-1)}$$

Following the same procedure, as in the case of State-Feedback Designed Autopilot, the step responses and Pole-Zero Map plots were obtained and analysed.

The pole locations of the simplified state-feedback autopilot are found to be at:

$$z_1 = 0.134458 + j\,0.0321064 \qquad \text{(III.B.3-2)}$$

$$z_2 = 0.134458 - j\,0.0321064 \qquad \text{(III.B.3-3)}$$

$$z_3 = 0.896805 + j\,0.0911170 \qquad \text{(III.B.3-4)}$$

$$z_4 = 0.896805 - j\,0.0911170 \qquad \text{(III.B.3-5)}$$

$$z_5 = 0.953644 + j\,0.0290202 \qquad \text{(III.B.3-6)}$$

$$z_6 = 0.953644 - j\,0.0290202 \qquad \text{(III.B.3-7)}$$

$$z_7 = 0.998202 \qquad \text{(III.B.3-8)}$$

$$z_8 = 1.000000 \qquad \text{(III.B.3-9)}$$

$$z_9 = 0.995608 + j\,0.0830713 \qquad \text{(III.B.3-10)}$$

$$z_{10} = 0.995608 - j\,0.0830713 \qquad \text{(III.B.3-11)}$$

A comparison of the above pole locations with those of the state-feedback designed autopilot (equations III.B.2-11 through III.B.2-20) show a very small shifting of the poles of the simplified state-feedback autopilot to the left.

Figure 3.7 shows the time response of the pitch normal acceleration (n_z) for the simplified state-feedback autopilot. An input step function representing "1 gee" was used. The response shows that the steady-state error is greater than in the case of state-feedback autopilot (Fig. 3.1), but is whithin the requirements.

Figures 3.8 and 3.9 show the time responses of pitch angular rate (q) and pitch tail incidence (δ_p) for the simplified state-feedback autopilot. A comparison with the corresponding time responses for the state-feedback autopilot (Fig. 3.2 and Fig. 3.3) shows no significant differences.

Figures 3.10 through 3.12 show the Pole-Zero Map plots of n_z, q, δ_p. All the poles, given by equations III.B.3-2 through III.B.3-11, are inside the unit circle and the system is stable. There are no real zeros in the system.

C. ESTIMATOR DESIGNED AUTOPILOT

1. Design Approach and Analysis of Discrete Closed Loop Estimator

The control law designed in the last section III.B assumed that all states were available for feedback. Since, typically, not all states are measured, an estimator must be design in order to estimate all the states, given measurements of a portion of them. If the state is $\mathbf{X}$, then the estimate is $\hat{\mathbf{X}}$ and the idea is to let $\mathbf{U} = -\mathbf{L}\hat{\mathbf{X}}$, replacing the true states by

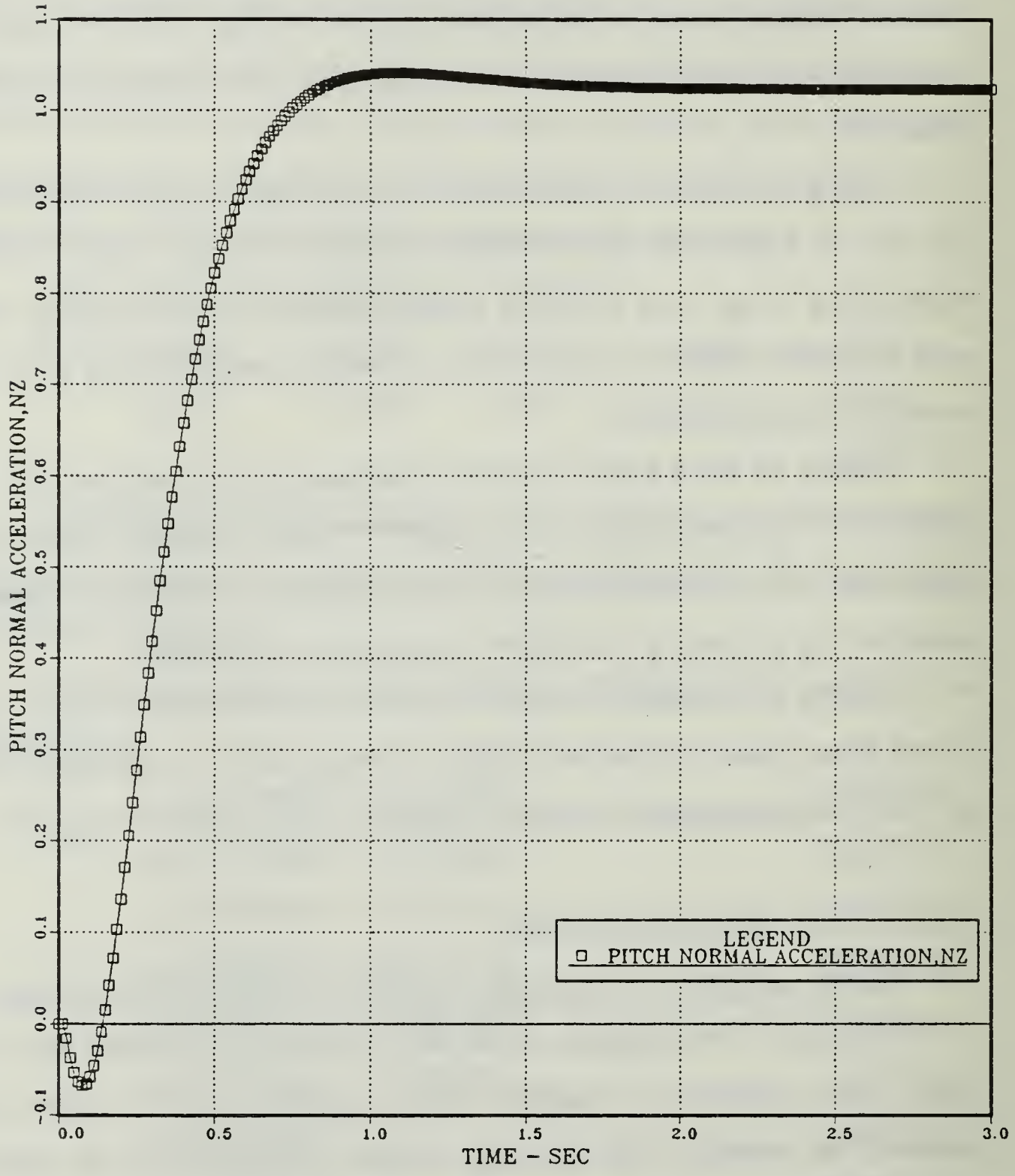

Figure 3.7 Pitch Normal Acceleration vs Time; Uncoupled Pitch Channel; Discrete Simplified State-Feedback Autopilot.

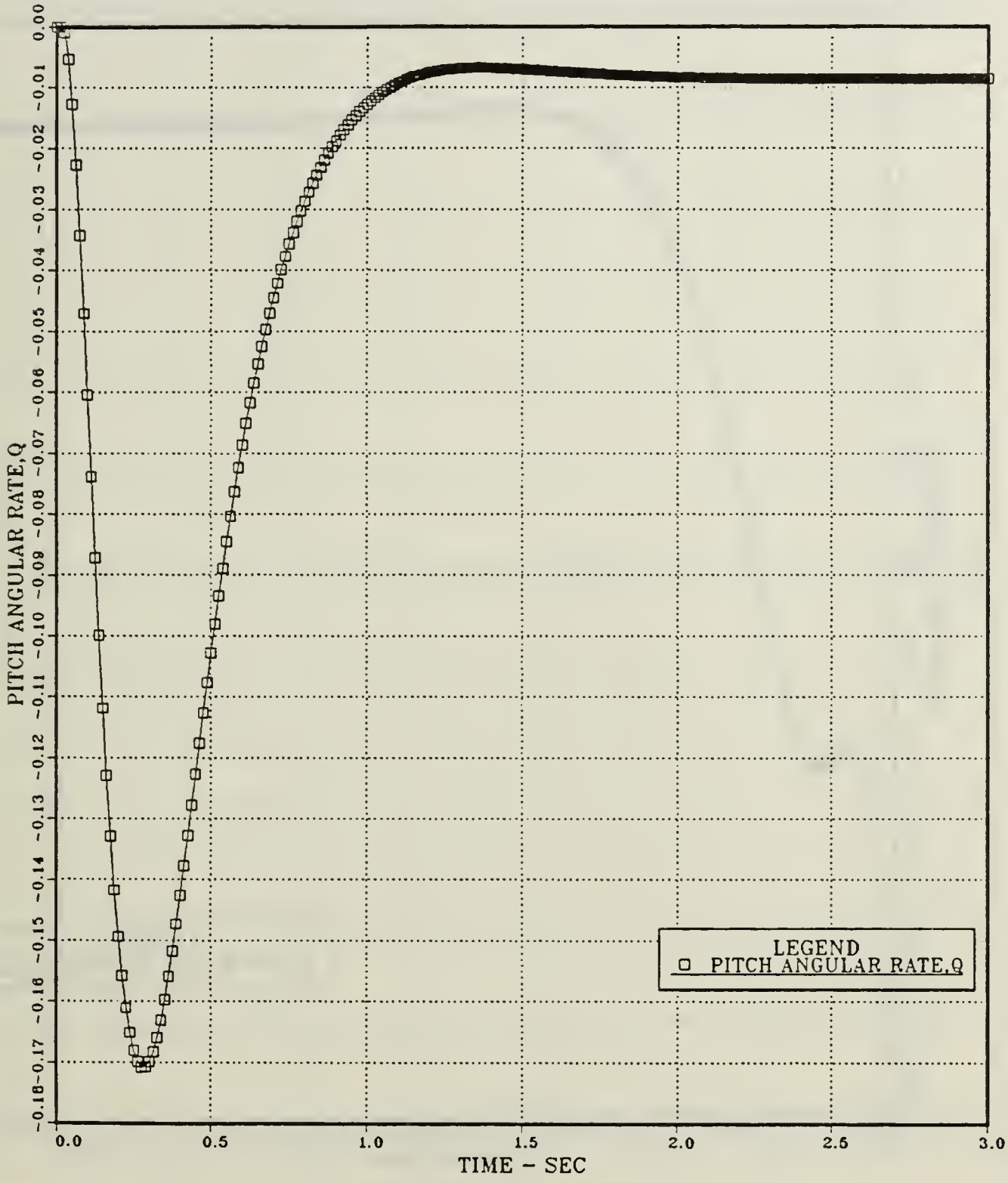

Figure 3.8 Pitch Angular Rate vs Time; Uncoupled Pitch Channel; Discrete Simplified State-Feedback Autopilot.

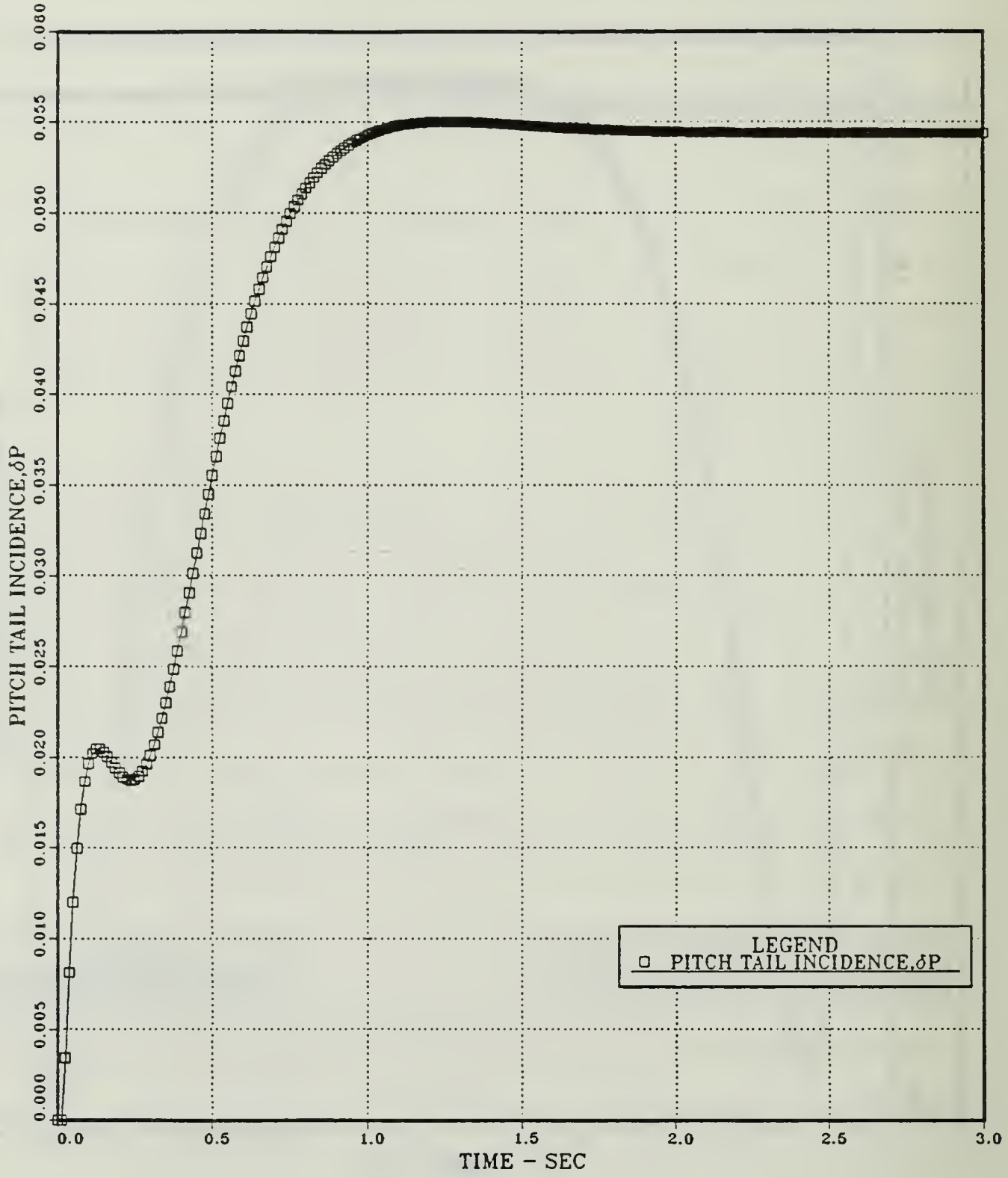

Figure 3.9 Pitch Tail Incidence vs Time; Uncoupled Pitch Channel; Discrete Simplified State-Feedback Autopilot.

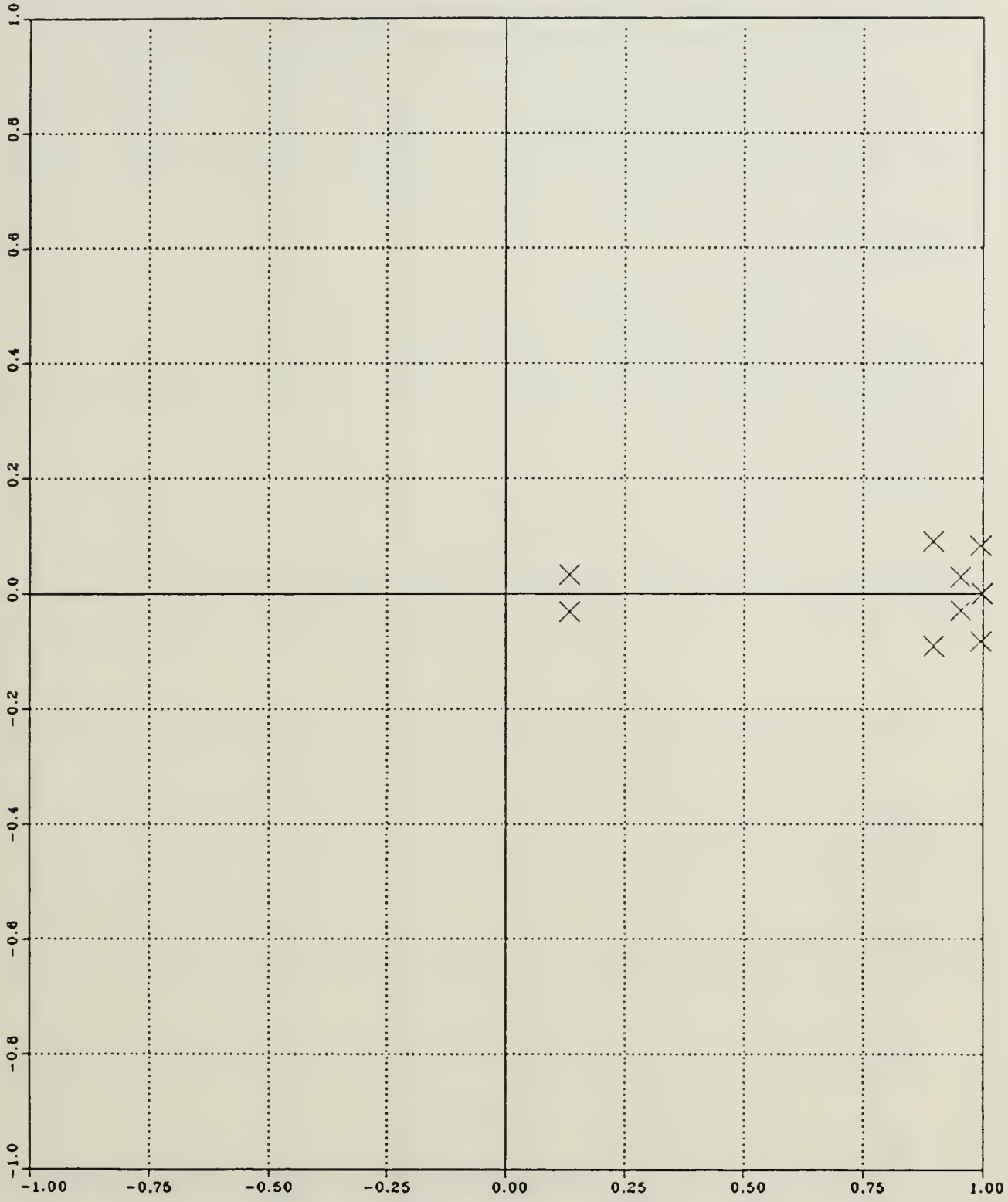

Figure 3.10 Pitch Normal Acceleration ; Uncoupled Pitch Channel;
Discrete Simplified State-Feedback Autopilot; Pole-Zero Map.

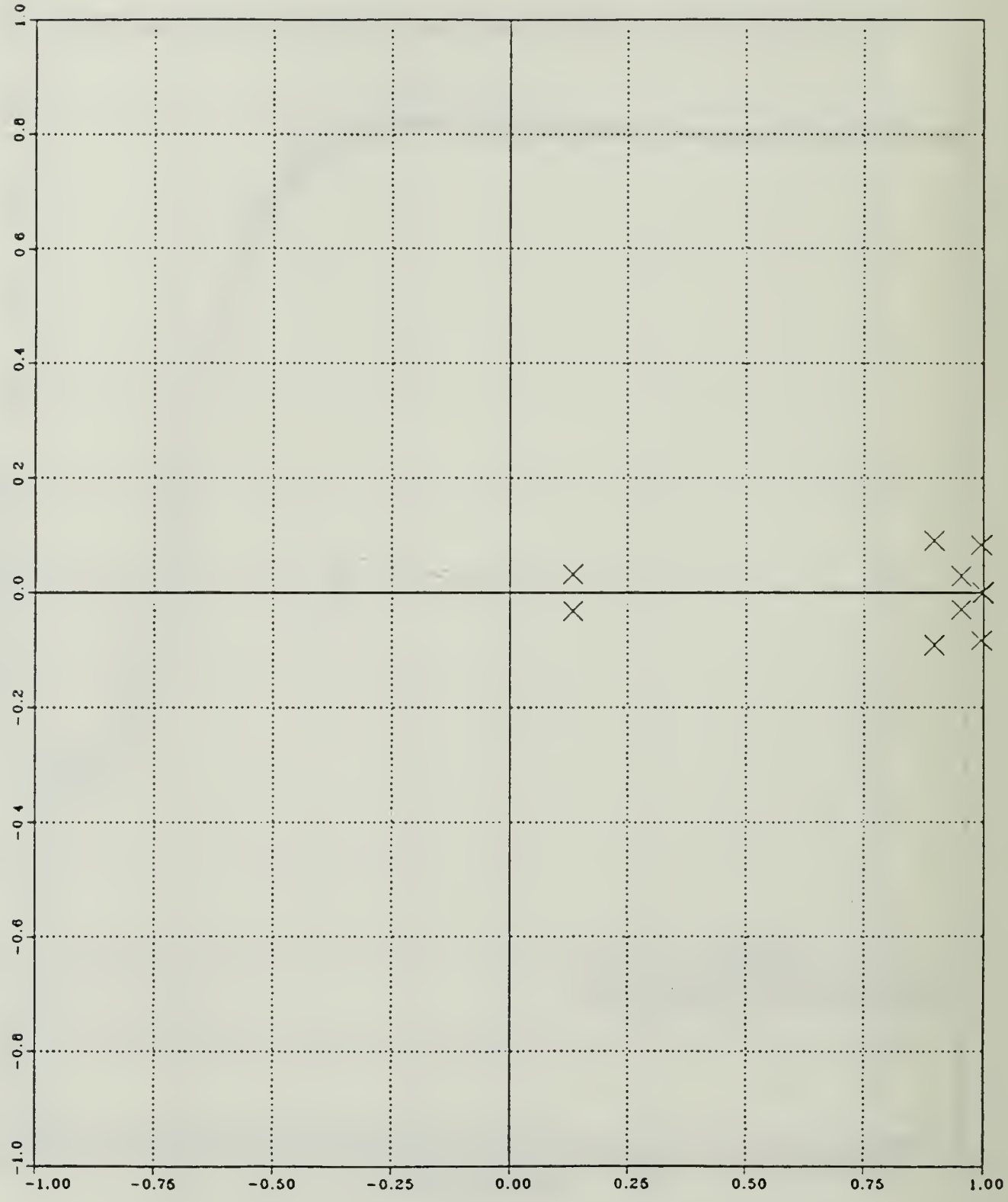

Figure 3.11 Pitch Angular Rate; Uncoupled Pitch Channel;
Discrete Simplified State-Feedback Autopilot; Pole-Zero Map.

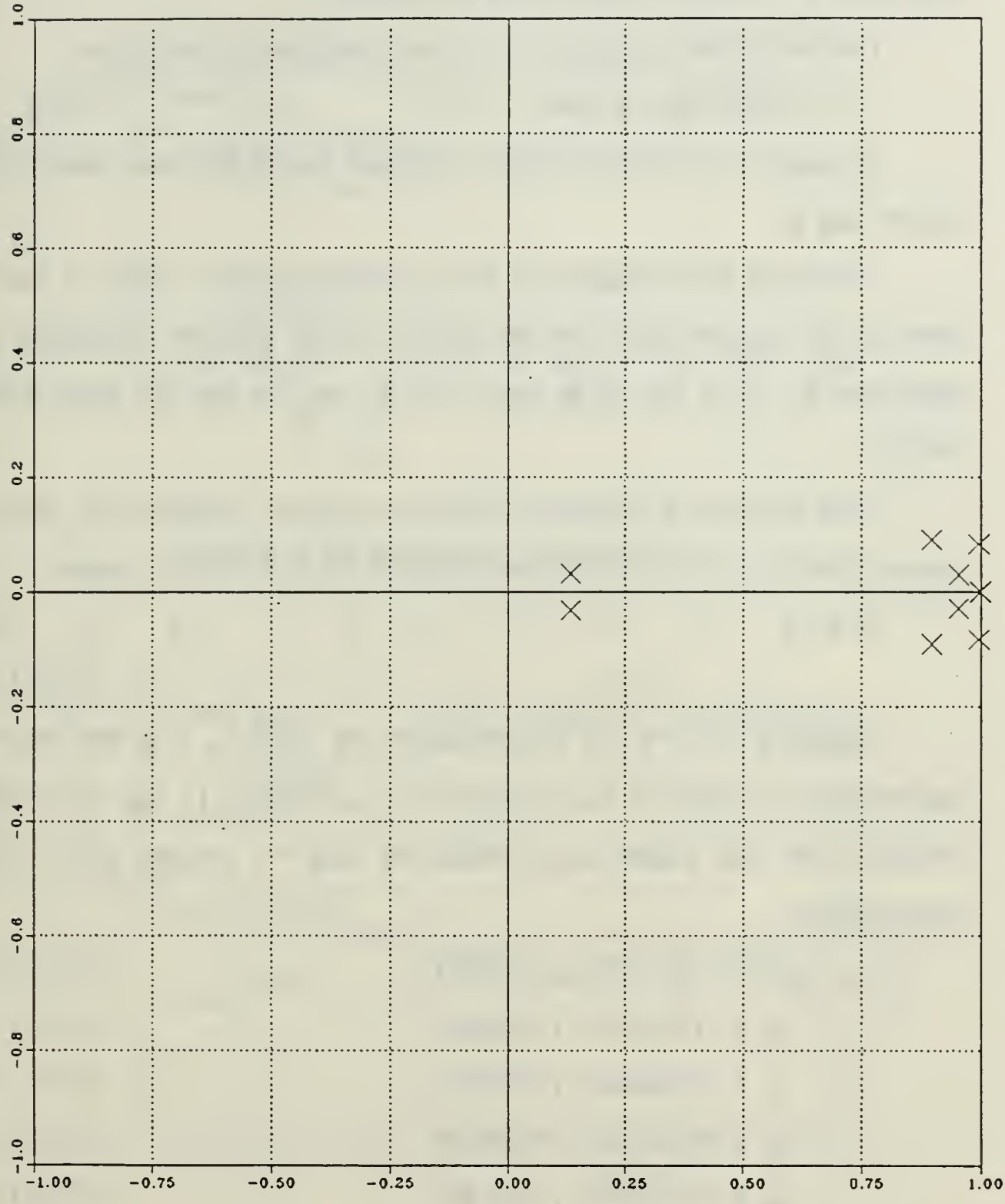

Figure 3.12 Pitch Tail Incidence; Uncoupled Pitch Channel;
Discrete Simplified State-Feedback Autopilot; Pole-Zero Map.

their estimates in the control law. Figure 3.13 shows an open loop estimator and Figure 3.14 shows a closed loop estimator.

The characteristic equation of the closed loop estimator is:

$$\det[\, zI - A + LH \,] = 0 \qquad \text{(III.C.1-1)}$$

To select **L**, we take the same approach as we did when designing the control law **K**.

If we take the transpose of **A-LH**, we get $A^T - H^T L^T$, which is the same form as the system matrix **A-BK** of the control problem. Therefore if we substitute A^T for **A**, H^T for **B**, and L^T for **K**, we can use the control design results.

Then utilizing Ackermann's formula program (Appendix D), and using sample time T= 0.0125 sec, the matrices A^T for **A**, H^T for **B**, where

$$H^T = [\, 0 \quad 0 \quad 0 \quad 1 \quad 0 \quad 0 \quad 0 \quad 0 \quad 0 \quad 0 \,] \qquad \text{(III.C.1-2)}$$

assuming that we can only measure the state $X_4 = q$, and taking the desired pole locations of the estimator to be slightly to the left from the original open loop eigenvalues (equations III.B.1-3 through III.B.1-12), as shown below:

$$s_1 = -159.729 + j\ 18.9921 \qquad \text{(III.C.1-3)}$$

$$s_2 = -159.729 - j\ 18.9921 \qquad \text{(III.C.1-4)}$$

$$s_3 = -8.29548 + j\ 8.05932 \qquad \text{(III.C.1-5)}$$

$$s_4 = -8.29548 - j\ 8.05932 \qquad \text{(III.C.1-6)}$$

$$s_5 = -3.76425 + j\ 2.51463 \qquad \text{(III.C.1-7)}$$

$$s_6 = -3.76425 - j\ 2.51463 \qquad \text{(III.C.1-8)}$$

$$s_7 = -0.148930 \qquad \text{(III.C.1-9)}$$

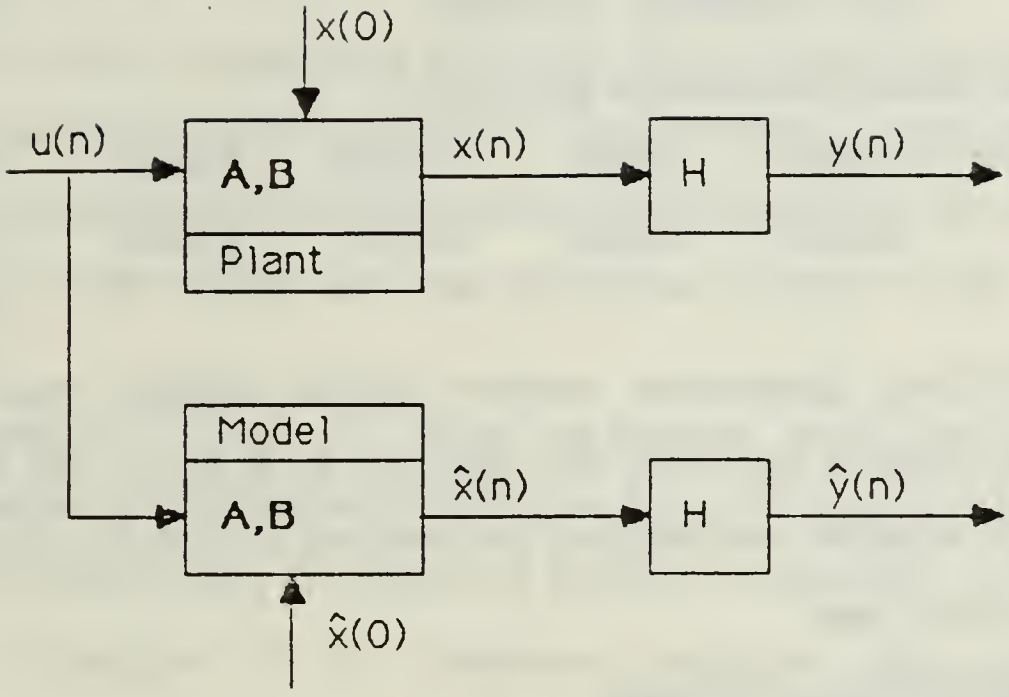

Figure 3.13 Open Loop Estimator.

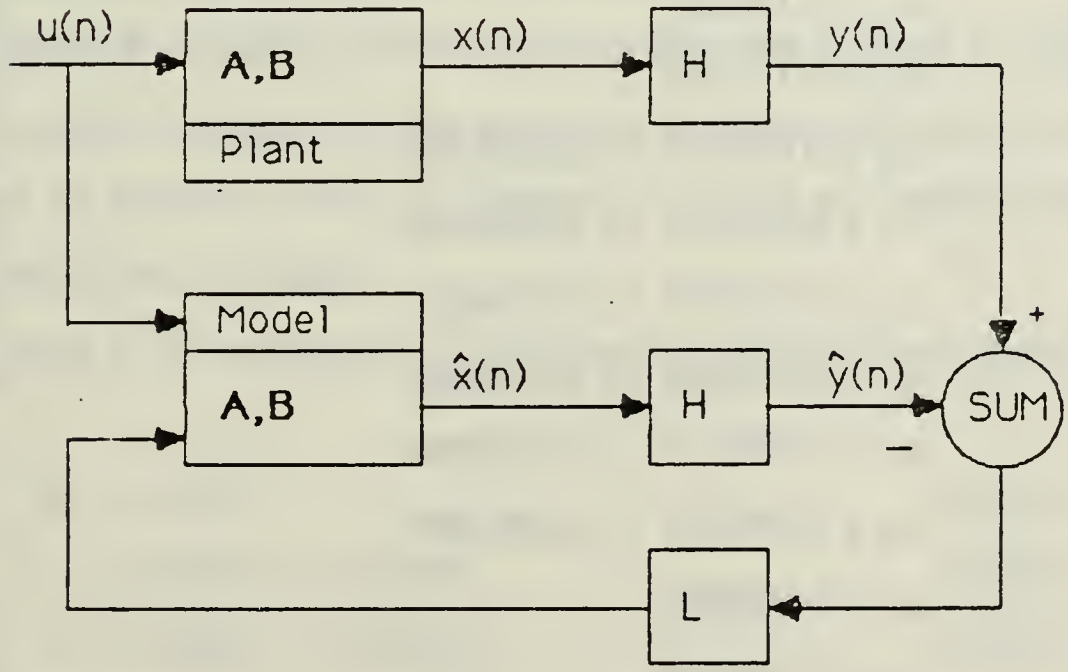

Figure 3.14 Closed Loop Estimator.

s_8 = -0.005004 (III.C.1-10)

s_9 = -0.079593 + j 6.65959 (III.C.1-11)

s_{10} = -0.079593 - j 6.65959 (III.C.1-12)

we obtain the estimator gain vector :

$$L^T = [\ -1.8784 \quad 0.0200 \quad -0.0972 \quad 0.0219 \quad 0.0041$$
$$-0.0015 \quad 0.3860 \quad 0.0720 \quad 0.0007 \quad -0.3370\ ]$$

(III.C.1-13)

Utilizing Compensator Transfer Function Analysis from TRANFUNC option of ORACLS and using the matrices **A**, **H** and **L** the closed loop estimator autopilot was designed and analyzed according to step responses and Pole-Zero Maps.

2. Performance of System

The closed loop estimator eigenvalues, det[z**I**-**A**+**LH**] = 0, obtained from Compensator Transfer Function Analysis are:

z_1 = 0.140601 (III.C.2-1)

z_2 = 0.101457 (III.C.2-2)

z_3 = 0.897018 + j 0.0908305 (III.C.2-3)

z_4 = 0.897018 - j 0.0908305 (III.C.2-4)

z_5 = 0.953599 + j 0.0299821 (III.C.2-5)

z_6 = 0.953599 - j 0.0299821 (III.C.2-6)

z_7 = 0.995619 + j 0.0830597 (III.C.2-7)

z_8 = 0.995619 - j 0.0830597 (III.C.2-8)

z_9 = 0.998203 (III.C.2-9)

z_{10} = 0.999998 (III.C.2-10)

A comparison of the above eigenvalues with those of the closed loop regulator eigenvalues det[zI-**A**+**BK**]=0, (equations III.B.2-11 through III.B.2-20), shows an acceptable difference since we estimated the entire state vector from the measurement of just one state, namely the pitch angular rate (q), and we moved the desired pole locations of the estimator to the left of the original open loop eigenvalues, in order to get a faster response.

Figures 3.15 through 3.17 show the discrete closed loop estimator time responses of pitch normal acceleration (n_z), pitch angular rate (q), and pitch tail incidence (δ_p). An input step function representing "1 gee" was used. A comparison of the responses mentioned above with the corresponding time responses of the state-feedback autopilot Figures 3.1 through 3.3 shows no differences. This is due to the fact that the same (zero) initial conditions was used for both cases.

Figures 3.18 through 3.20 show the Pole-Zero Map plots of n_z, q and δ_p for both the state-feedback and the estimator designed autopilots. All the poles, given by equations III.C.2-1 through III.C.2-10,are inside the unit circle and the system is stable.

The zeros of the estimator's pitch normal acceleration are found to be at:

$$z_1 = 0.1053 \qquad \text{(III.C.2-11)}$$

$$z_2 = 0.8970 + j\,0.09080 \qquad \text{(III.C.2-12)}$$

$$z_3 = 0.8970 - j\,0.09080 \qquad \text{(III.C.2-13)}$$

$$z_4 = 0.1413 \qquad \text{(III.C.2-14)}$$

$$z_5 = 0.9956 + j\,0.08307 \qquad \text{(III.C.2-15)}$$

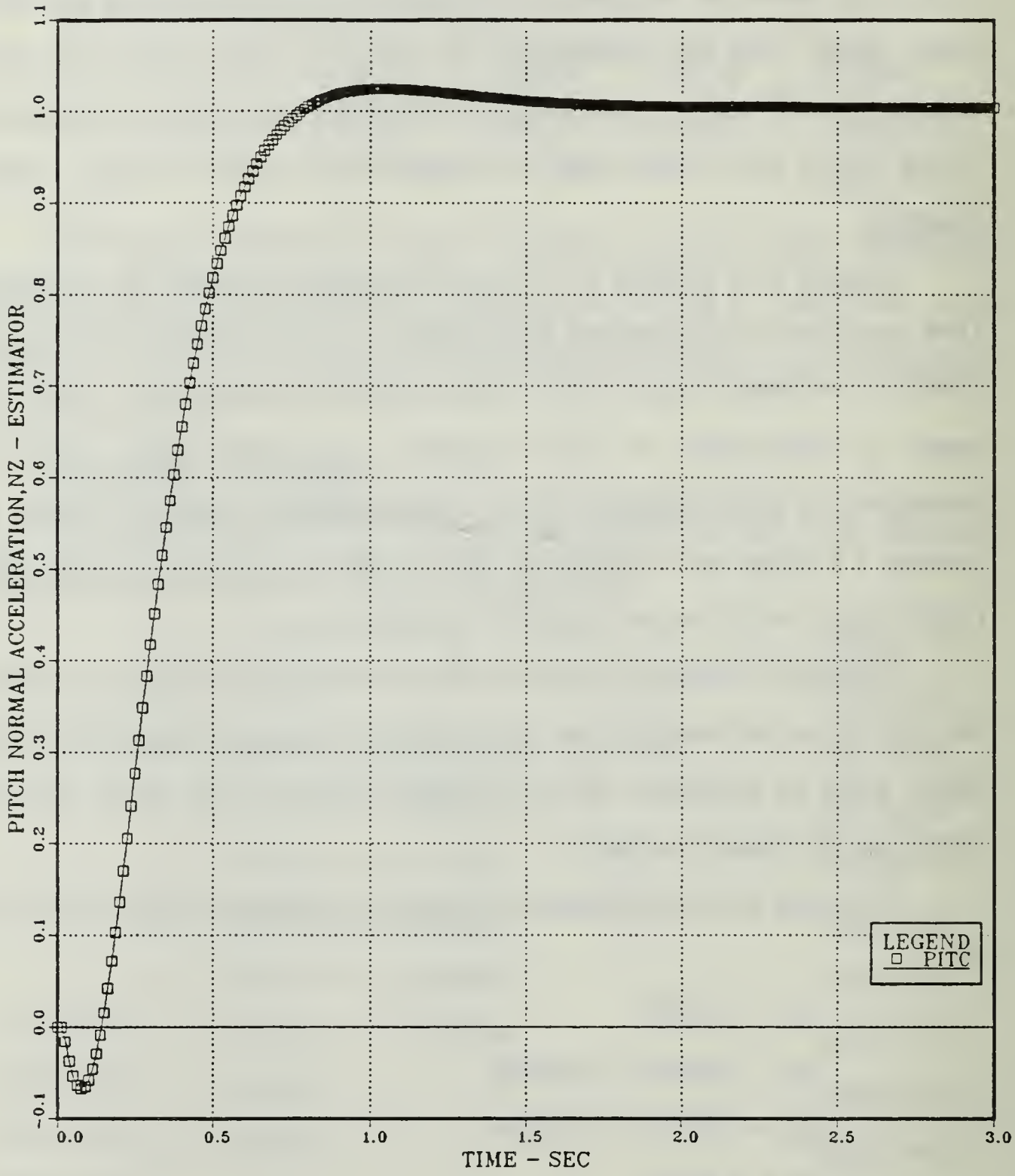

Figure 3.15 Pitch Normal Acceleration vs Time; Uncoupled Pitch Channel; Discrete Estimator Autopilot.

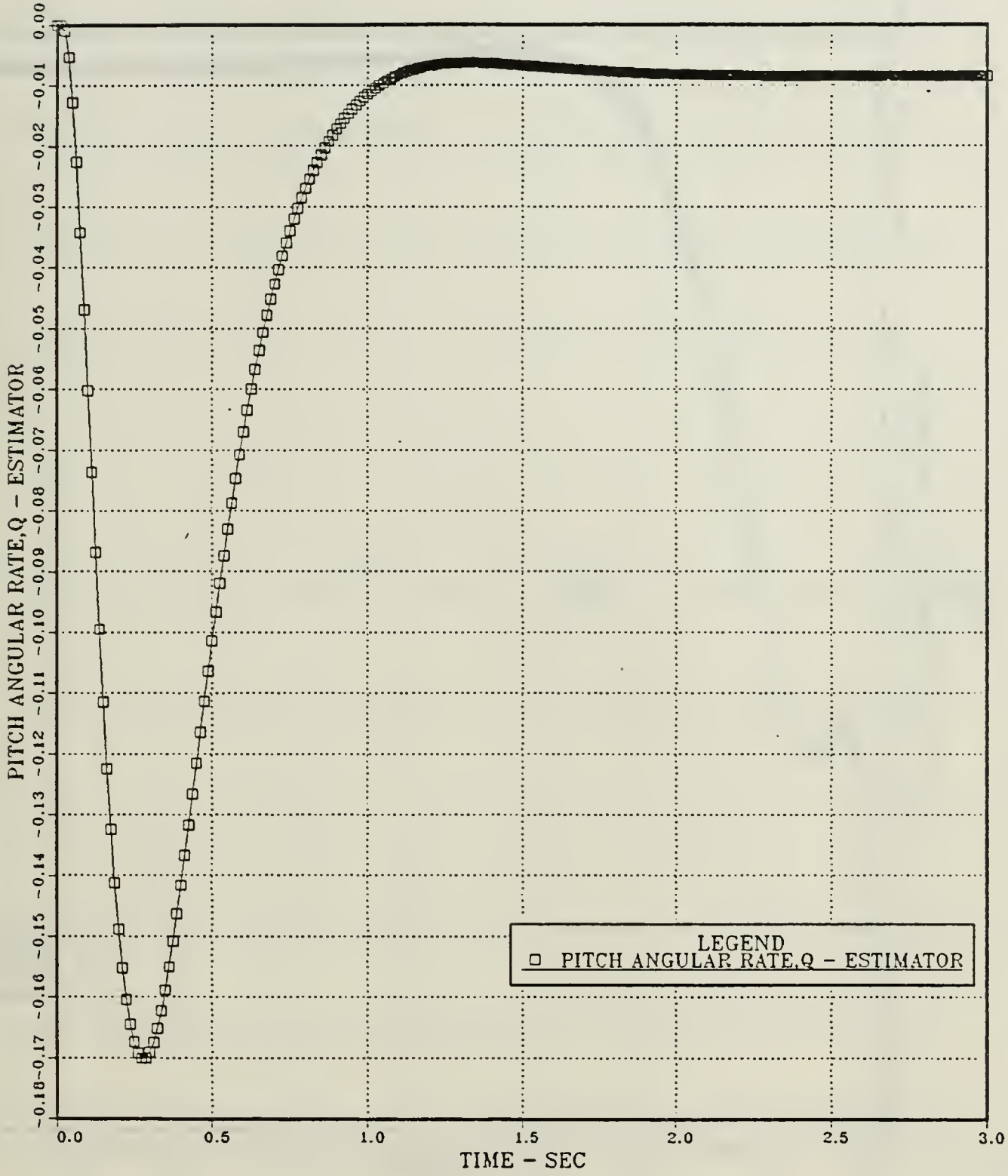

Figure 3.16 Pitch Angular Rate vs Time; Uncoupled Pitch Channel; Discrete Estimator Autopilot.

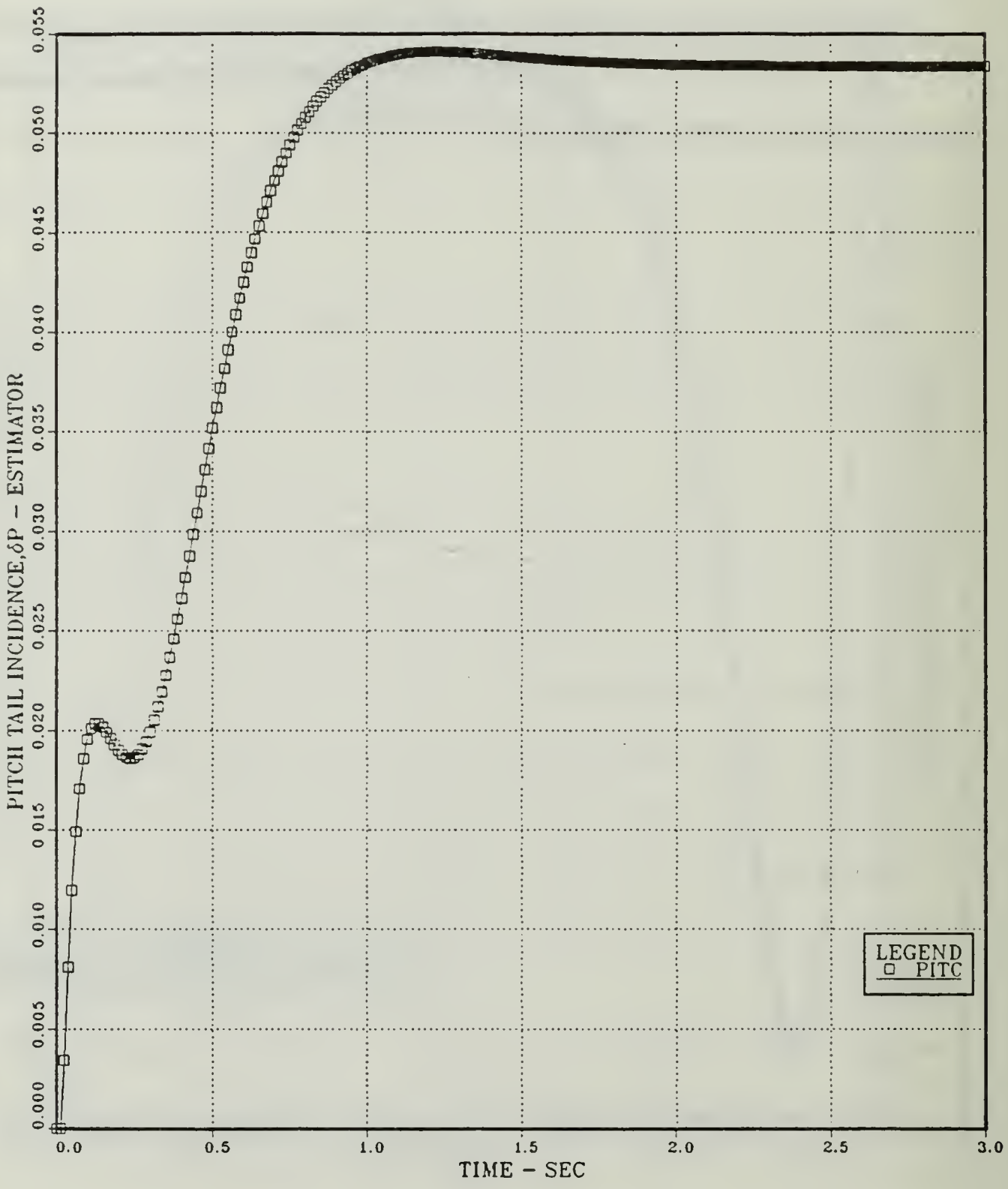

Figure 3.17 Pitch Tail Incidence vs Time; Uncoupled Pitch Channel; Discrete Estimator Autopilot.

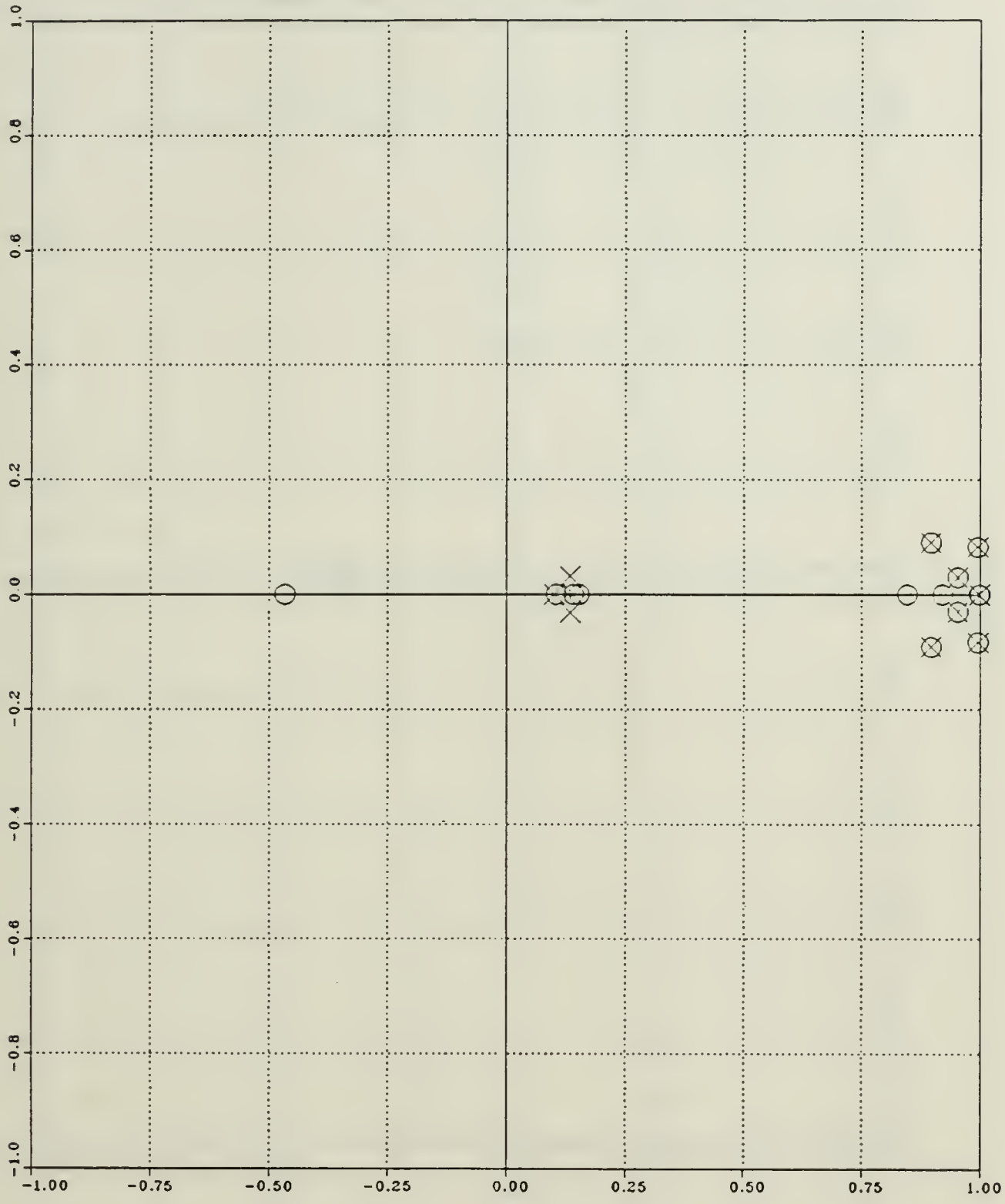

Figure 3.18 Pitch Normal Acceleration ; Uncoupled Pitch Channel; Discrete State Feedback and Estimator Autopilots; Pole-Zero Map.

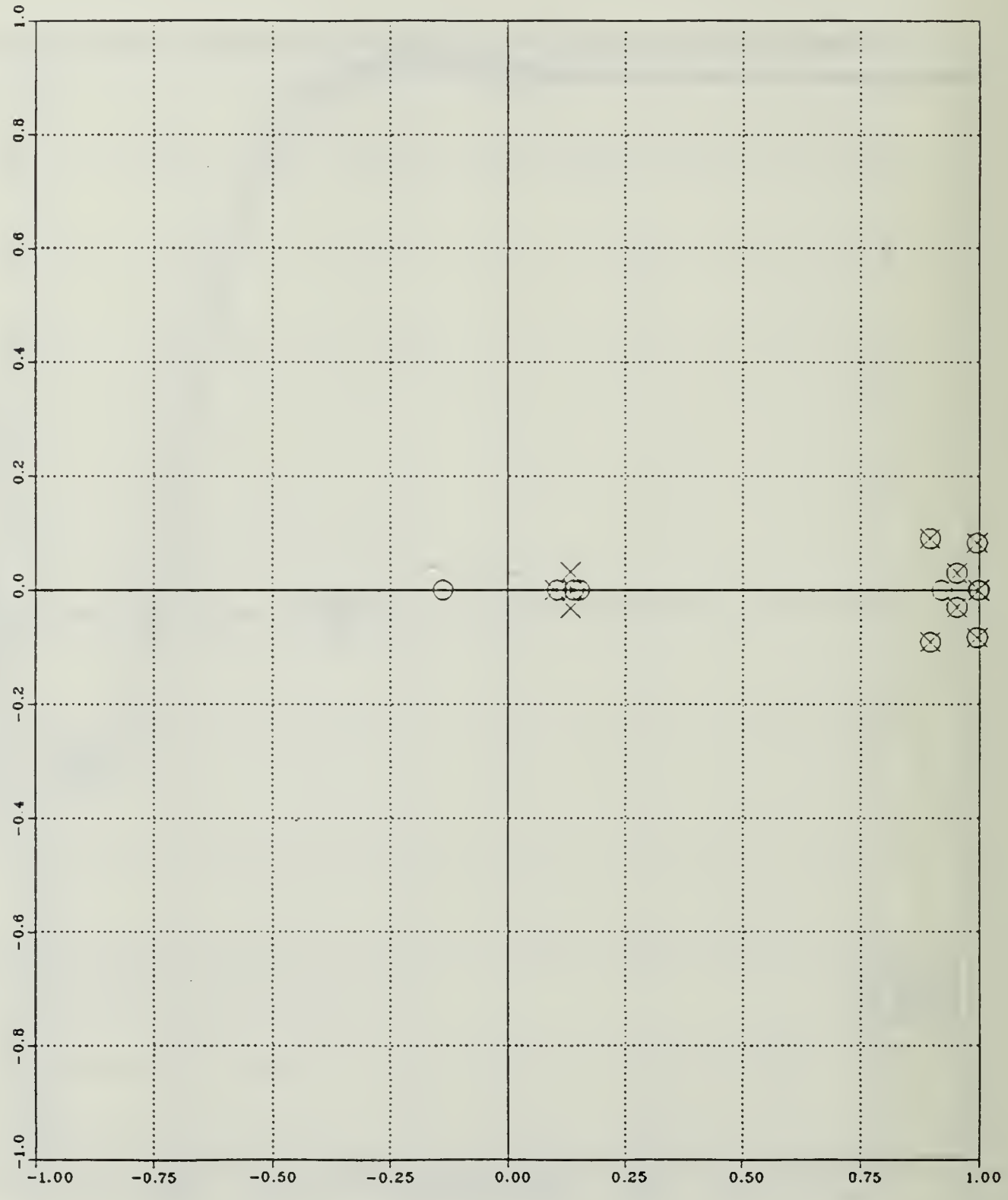

Figure 3.19 Pitch Angular Rate; Uncoupled Pitch Channel; Discrete State Feedback and Estimator Autopilots; Pole-Zero Map.

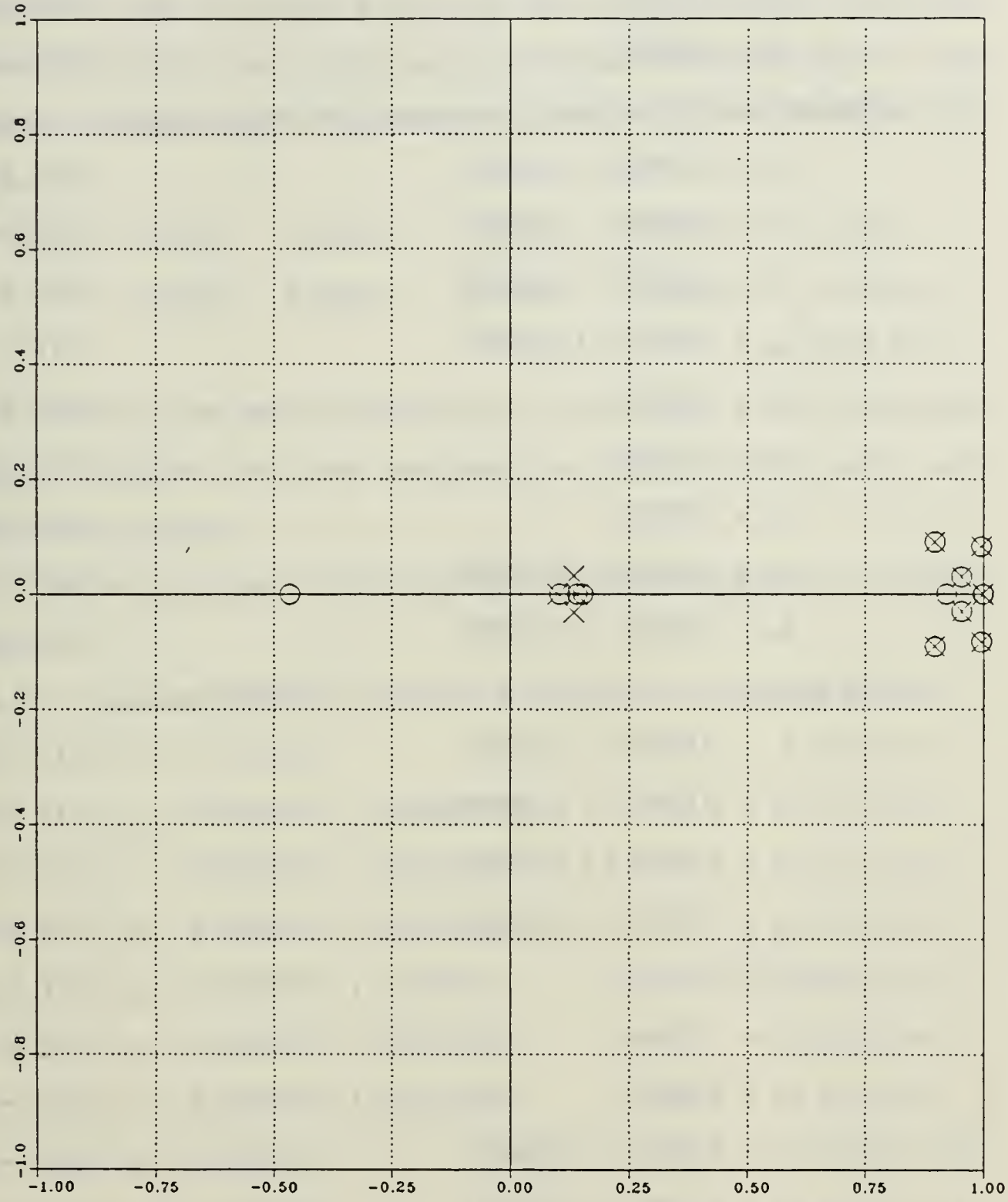

Figure 3.20 Pitch Tail Incidence; Uncoupled Pitch Channel; Discrete State Feedback and Estimator Autopilots; Pole-Zero Map.

$$z_6 = 0.9956 - j\,0.08307 \quad \text{(III.C.2-16)}$$

$$z_7 = 0.8468 \quad \text{(III.C.2-17)}$$

$$z_8 = 1.0000 \quad \text{(III.C.2-18)}$$

$$z_9 = 0.9982 \quad \text{(III.C.2-19)}$$

The zeros of the estimator's pitch angular rate are found to be at:

$$z_1 = 0.9956 + j\,0.08307 \quad \text{(III.C.2-20)}$$

$$z_2 = 0.9956 - j\,0.08307 \quad \text{(III.C.2-21)}$$

$$z_3 = 0.8970 + j\,0.09081 \quad \text{(III.C.2-22)}$$

$$z_4 = 0.8970 - j\,0.09081 \quad \text{(III.C.2-23)}$$

$$z_5 = 1.0000 \quad \text{(III.C.2-24)}$$

$$z_6 = 0.1056 \quad \text{(III.C.2-25)}$$

$$z_7 = 0.9982 \quad \text{(III.C.2-26)}$$

$$z_8 = 0.9536 + j\,0.02998 \quad \text{(III.C.2-27)}$$

$$z_9 = 0.9536 - j\,0.02998 \quad \text{(III.C.2-28)}$$

The zeros of the estimator's pitch tail incidence are found to be at:

$$z_1 = 0.9958 + j\,0.08305 \quad \text{(III.C.2-29)}$$

$$z_2 = 0.9958 - j\,0.08305 \quad \text{(III.C.2-30)}$$

$$z_3 = 0.9536 + j\,0.02997 \quad \text{(III.C.2-31)}$$

$$z_4 = 0.9536 - j\,0.02997 \quad \text{(III.C.2-32)}$$

$$z_5 = 0.1413 \quad \text{(III.C.2-33)}$$

$$z_6 = 1.0000 \quad \text{(III.C.2-34)}$$

$$z_7 = 0.9982 \quad \text{(III.C.2-35)}$$

$$z_8 = 0.8970 + j\,0.09081 \quad \text{(III.C.2-36)}$$

$$z_9 = 0.8970 - j\,0.09081 \quad \text{(III.C.2-37)}$$

3. Simplified Estimator Designed Autopilot

For the same reason, as in the case of simplified state-feedback autopilot, in order to eliminate returning loops in the design of simplified estimator autopilot, zero gains were introduced where the gains of the estimator (equation III.C.1-13) were very small. Then the resulted gain vector is:

$$L^T = [\ -1.8784 \quad 0.0200 \quad -0.0972 \quad 0.0219 \quad 0.0000$$
$$0.0000 \quad 0.3860 \quad 0.0720 \quad 0.0000 \quad -0.3370\ ] \qquad \text{(III.C.3-1)}$$

Following the same procedure, as in the case of the Estimator Designed Autopilot, the time responses and Pole-Zero Map plots were obtained and analyzed.

The pole locations of the simplified estimator autopilot are found to be at:

$$z_1 = 0.140707 \qquad \text{(III.C.3-2)}$$
$$z_2 = 0.101090 \qquad \text{(III.C.3-3)}$$
$$z_3 = 0.896885 + j\ 0.0938778 \qquad \text{(III.C.3-4)}$$
$$z_4 = 0.896885 - j\ 0.0938778 \qquad \text{(III.C.3-5)}$$
$$z_5 = 0.953882 + j\ 0.0288601 \qquad \text{(III.C.3-6)}$$
$$z_6 = 0.953882 - j\ 0.0288601 \qquad \text{(III.C.3-7)}$$
$$z_7 = 0.995605 + j\ 0.0830655 \qquad \text{(III.C.3-8)}$$
$$z_8 = 0.995605 - j\ 0.0830655 \qquad \text{(III.C.3-9)}$$
$$z_9 = 0.998202 \qquad \text{(III.C.3-10)}$$
$$z_{10} = 0.999985 \qquad \text{(III.C.3-11)}$$

A comparison of the above pole locations with those of the estimator designed autopilot (equations III.C.2-1 through III.C.2-10) shows no significant differences.

Figures 3.21 through 3.23 show the simplified closed loop estimator time responses of pitch normal acceleration (n_z), pitch angular rate (q), and pitch tail incidence (δ_p). An input step function representing "1 gee" was used. A comparison of the above responses with the corresponding time responses of the estimator designed autopilot (Figures 3.15 through 3.17) shows no significant differences.

Figures 3.24 through 3.26 show the Pole-Zero Map plots of n_z, q and δ_p for the simplified estimator designed autopilot. All the poles, given by equations III.C.3-2 through III.C.3-11,are inside the unit circle and the system is stable. There are no significant differences in the zero's locations from those of the estimator autopilot (equations III.C.2-11 through III.C.2-37).

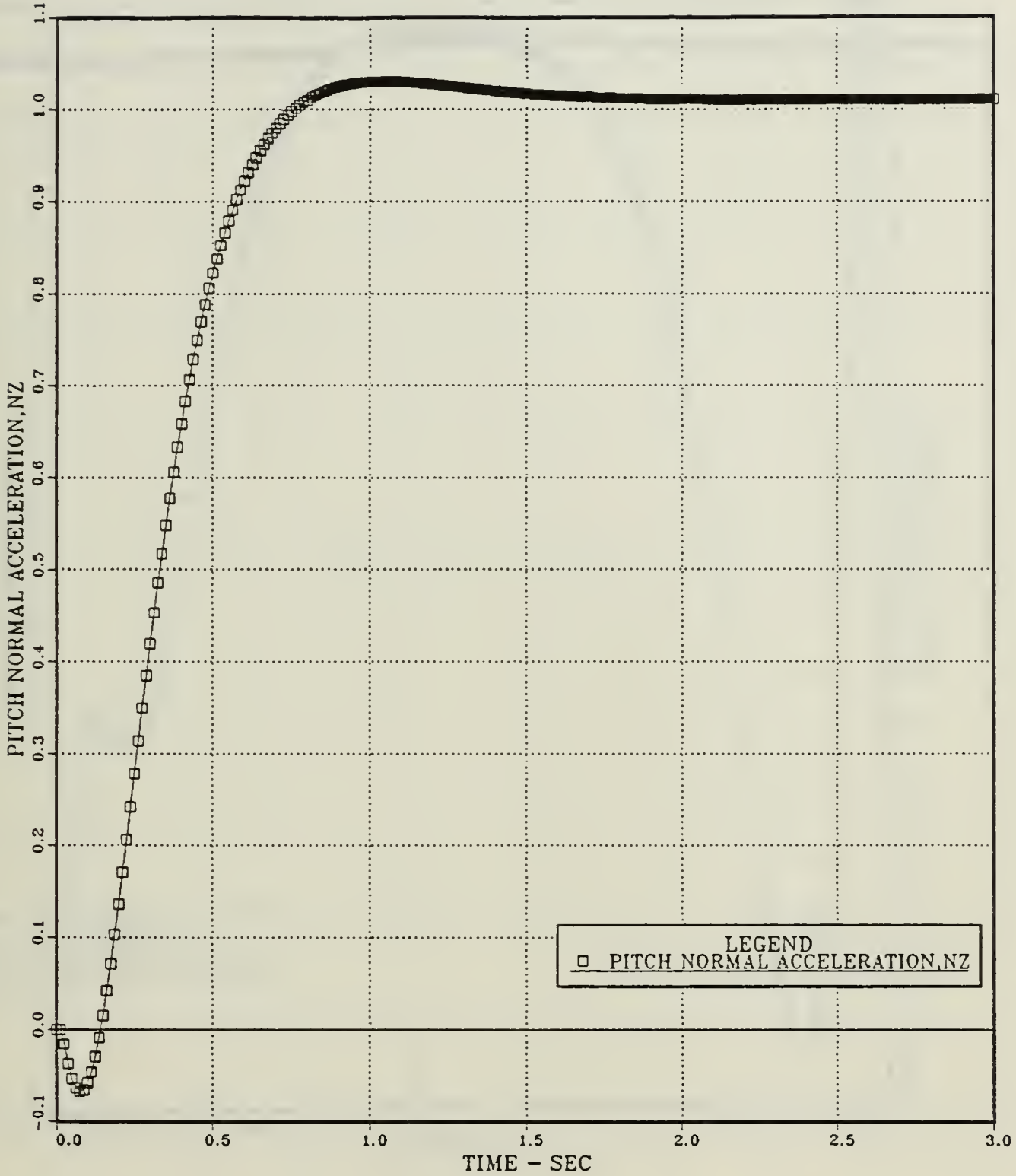

Figure 3.21 Pitch Normal Acceleration vs Time; Uncoupled Pitch Channel; Discrete Simplified Estimator Autopilots.

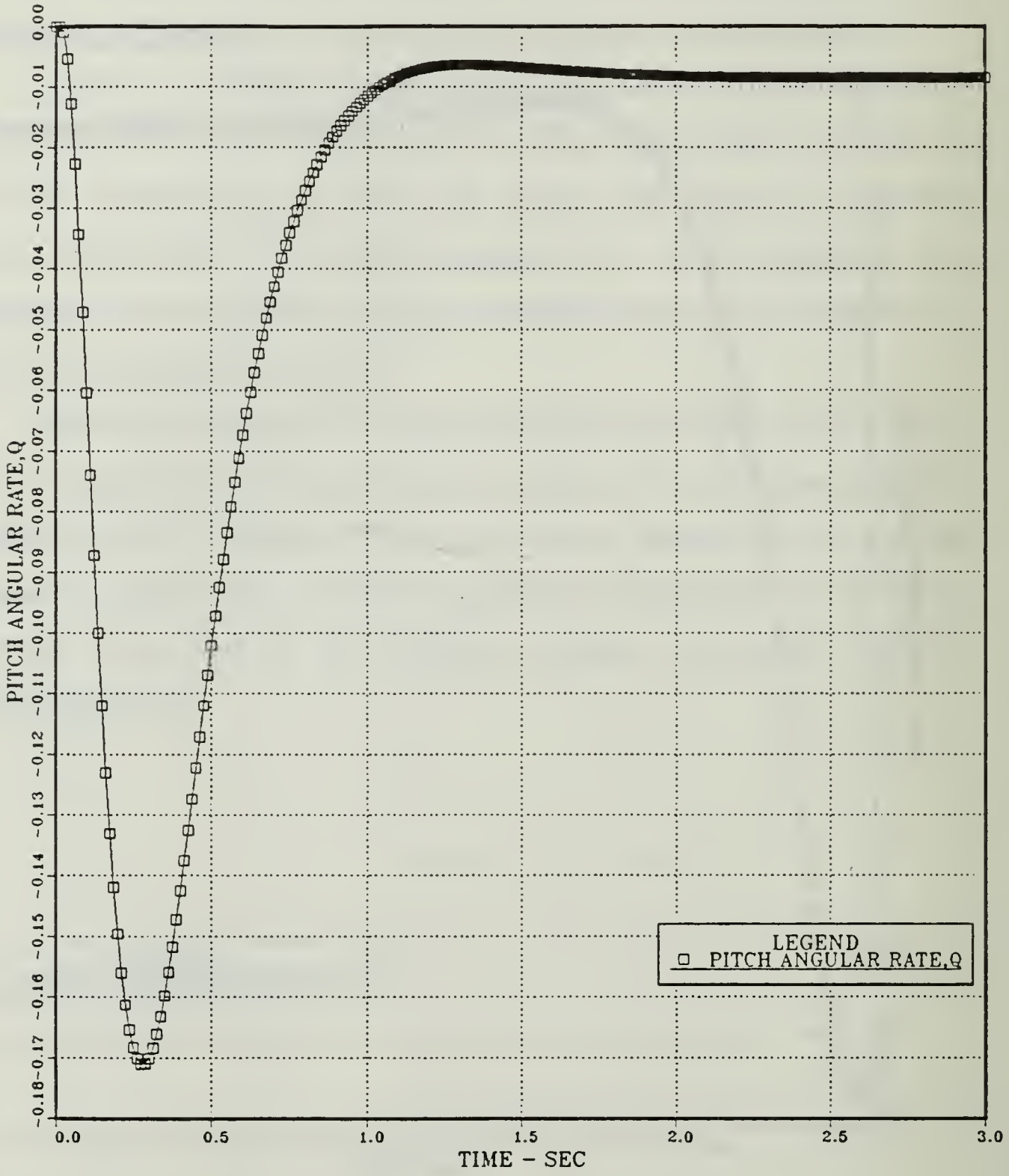

Figure 3.22 Pitch Angular Rate vs Time; Uncoupled Pitch Channel; Discrete Simplified Estimator Autopilot.

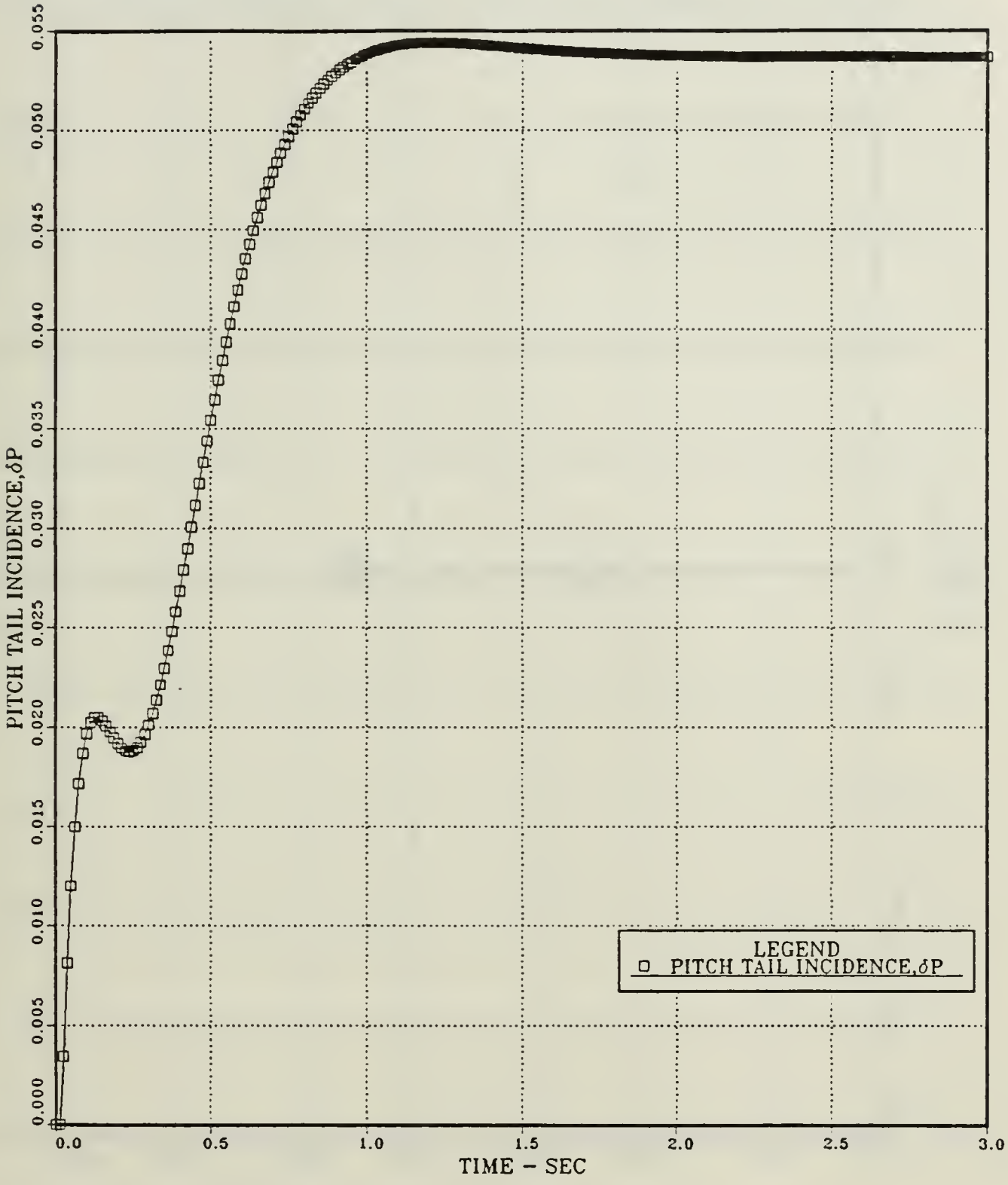

Figure 3.23 Pitch Tail Incidence vs Time; Uncoupled Pitch Channel; Discrete Simplified Estimator Autopilot.

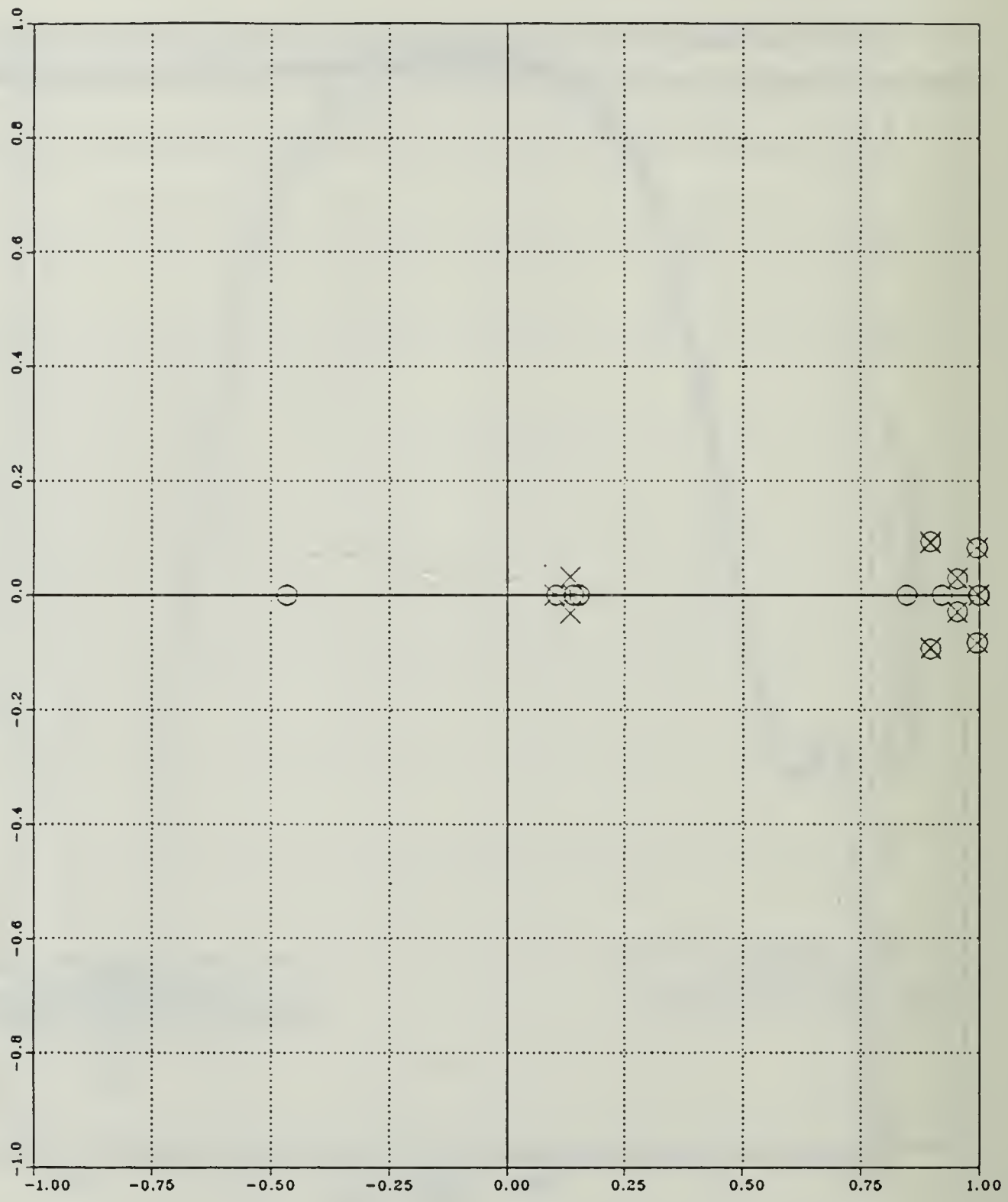

Figure 3.24 Pitch Normal Acceleration ; Uncoupled Pitch Channel;
Discrete Simplified Estimator Autopilot; Pole-Zero Map.

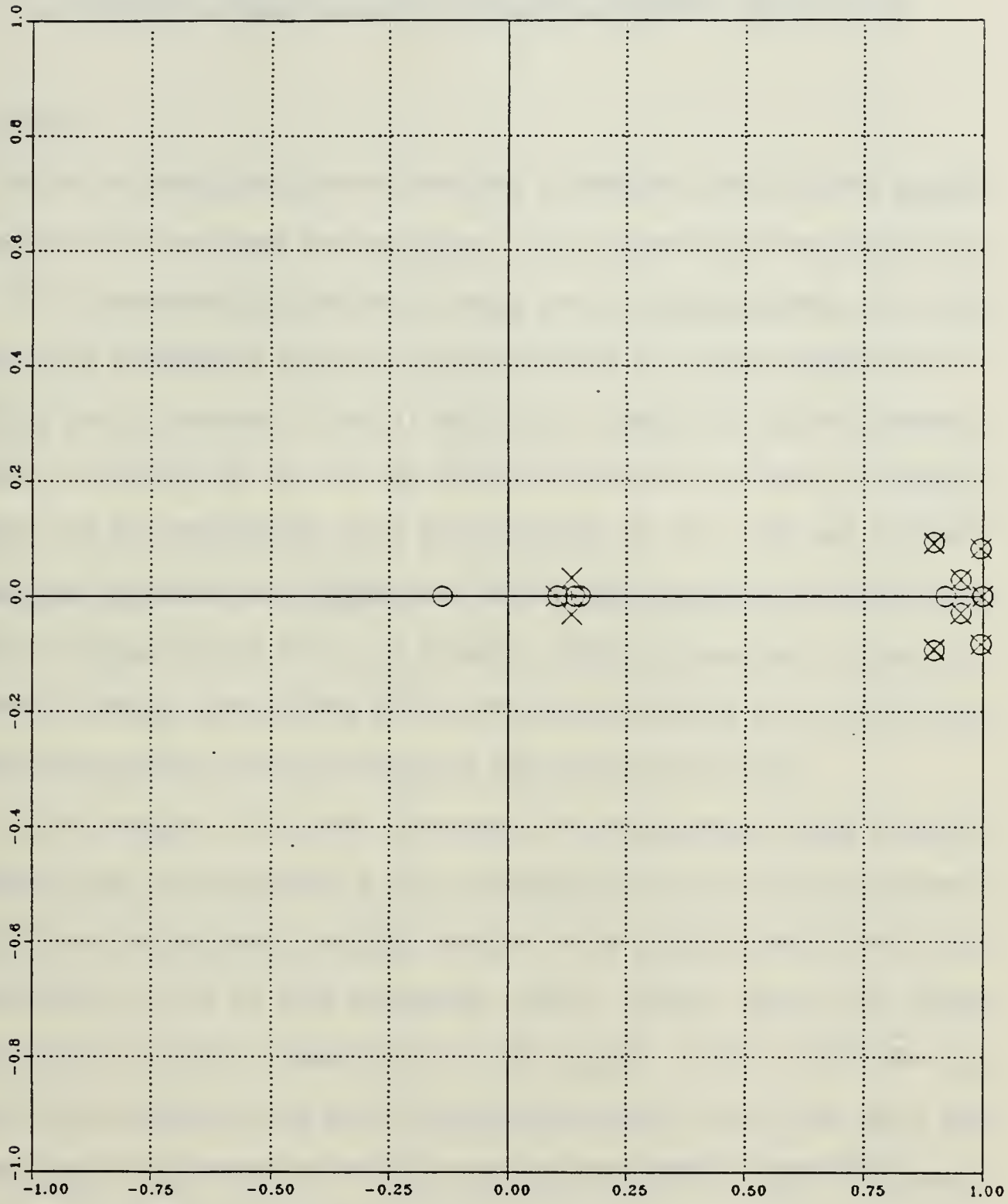

Figure 3.25 Pitch Angular Rate; Uncoupled Pitch Channel;
Discrete Simplified Estimator Autopilot; Pole-Zero Map.

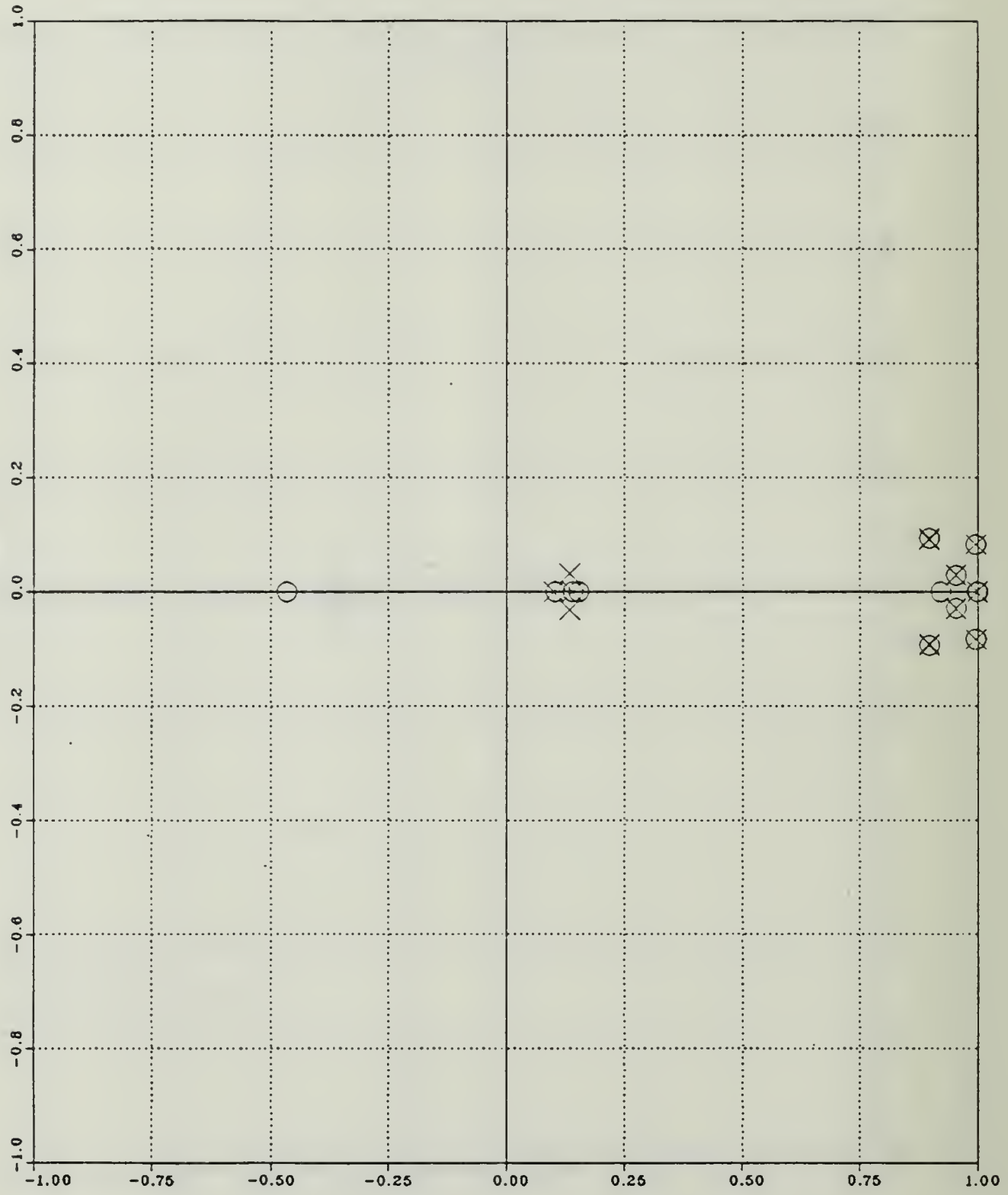

Figure 3.26 Pitch Tail Incidence; Uncoupled Pitch Channel;
Discrete Simplified Estimator Autopilot; Pole-Zero Map.

IV. DISCRETE COUPLED PITCH AND ROLL CHANNEL AUTOPILOTS

A. GENERAL

The control design procedures described in chapter II and III were applied to systems with one input and one output. The transfer-function approach in [Ref. 3] is fundamentally limited to single input/output systems while the state-space methods of chapter III were limited to single input/output to simplify the procedures. In fact, if one tries to apply the "pole-placement" approach of chapter III to a multivariable (more than one input or output) system, all the procedures work but the gains, **K** or **L**, are not uniquely determined by the resulting equations. Until a design approach is available which intelligently uses this extra freedom, the pole-placement concept for estimator designs for systems with more than one output or for controller designs for systems with more than one input has limited value.

In this chapter the pole placement and robustness design program (POPLAR), [Ref. 8] was used as a tool in the design of multivariable systems. This program is designed to employ singular value analysis and the use of an optimization to aid in pole placement control system design for linear multivariable systems. Robustness of the system is also considered by establishing singular value levels which correspond to multiloop gain and phase margins determined from the universal gain phase diagram developed by Newsom and Mukhapadhyay at NASA Langley.

B. DESIGN APPROACH AND ANALYSIS OF THE DISCRETE STATE FEEDBACK AUTOPILOT

The first step in any multivariable design should be an attempt to find an approximate model consisting of two or more single input/output model or else decouple the control law matrix **K** and the estimator law matrix **L**. This step will give better physical insight into the important feedback variables and may lead to a plant description which is substantially simpler for design purposes and yet yields no significant degradation from an analysis based on the full multivariable system.

Combining the pitch and roll channel autopilot, the roll channel taken from [Ref. 7], a seventeenth (17^{th}) order system is obtained and is shown in Appendix E.

Utilizing Transfer Function Analysis from TRANFUNC option of ORACLS and using the combined pitch and roll matrices **A**, **B** and **K** the discrete closed loop system was obtained and analyzed according to time responses and Pole-Zero Map plots.

C. PERFORMANCE OF SYSTEM

The discrete state-feedback eigenvalues, det[z**I**−**A**+**BK**]=0, of the coupled system, obtained from Transfer Function Analysis option of ORACLS, are:

$$z_1 = 0.134462 + j\,0.0320974 \qquad \text{(IV.C-1)}$$

$$z_2 = 0.134462 - j\,0.0320974 \qquad \text{(IV.C-2)}$$

$$z_3 = 0.896990 + j\,0.0906457 \qquad \text{(IV.C-3)}$$

$$z_4 = 0.896990 - j\,0.0906457 \qquad \text{(IV.C-4)}$$

$$z_5 = 0.953624 + j\,0.0299994 \qquad \text{(IV.C-5)}$$

$z_6 = 0.953624 - j\ 0.0299994$ (IV.C-6)

$z_7 = 0.998202$ (IV.C-7)

$z_8 = 1.000000$ (IV.C-8)

$z_9 = 0.995608 + j\ 0.0830713$ (IV.C-9)

$z_{10} = 0.995608 - j\ 0.0830713$ (IV.C-10)

$z_{11} = 0.0993086$ (IV.C-11)

$z_{12} = 0.836553 + j\ 0.306107$ (IV.C-12)

$z_{13} = 0.836553 - j\ 0.306107$ (IV.C-13)

$z_{14} = 0.967788 + j\ 0.0334452$ (IV.C-14)

$z_{15} = 0.967788 - j\ 0.0334452$ (IV.C-15)

$z_{16} = 0.895730$ (IV.C-16)

$z_{17} = 0.938133$ (IV.C-17)

Since all the poles are inside the unit circle the coupled system is stable.

Figures 4.1 through 4.3 show the closed loop time responses of pitch normal acceleration (n_z), pitch angular rate (q) and pitch tail incidence (δ_p). An input step function representing "1 gee" was used. All the responses are identical to those obtained for the uncoupled pitch channel and therethore they meet the desired requirements.

Figures 4.4 through 4.6 show the Pole-Zero Map of n_z, q and δ_p respectively. The poles of the system are given by equations IV.C-1 through IV.C-17 and they are the same as the uncoupled closed loop poles (equations III.B.2-11 through III.B.2-20). There are no real zeros in the state feedback coupled system.

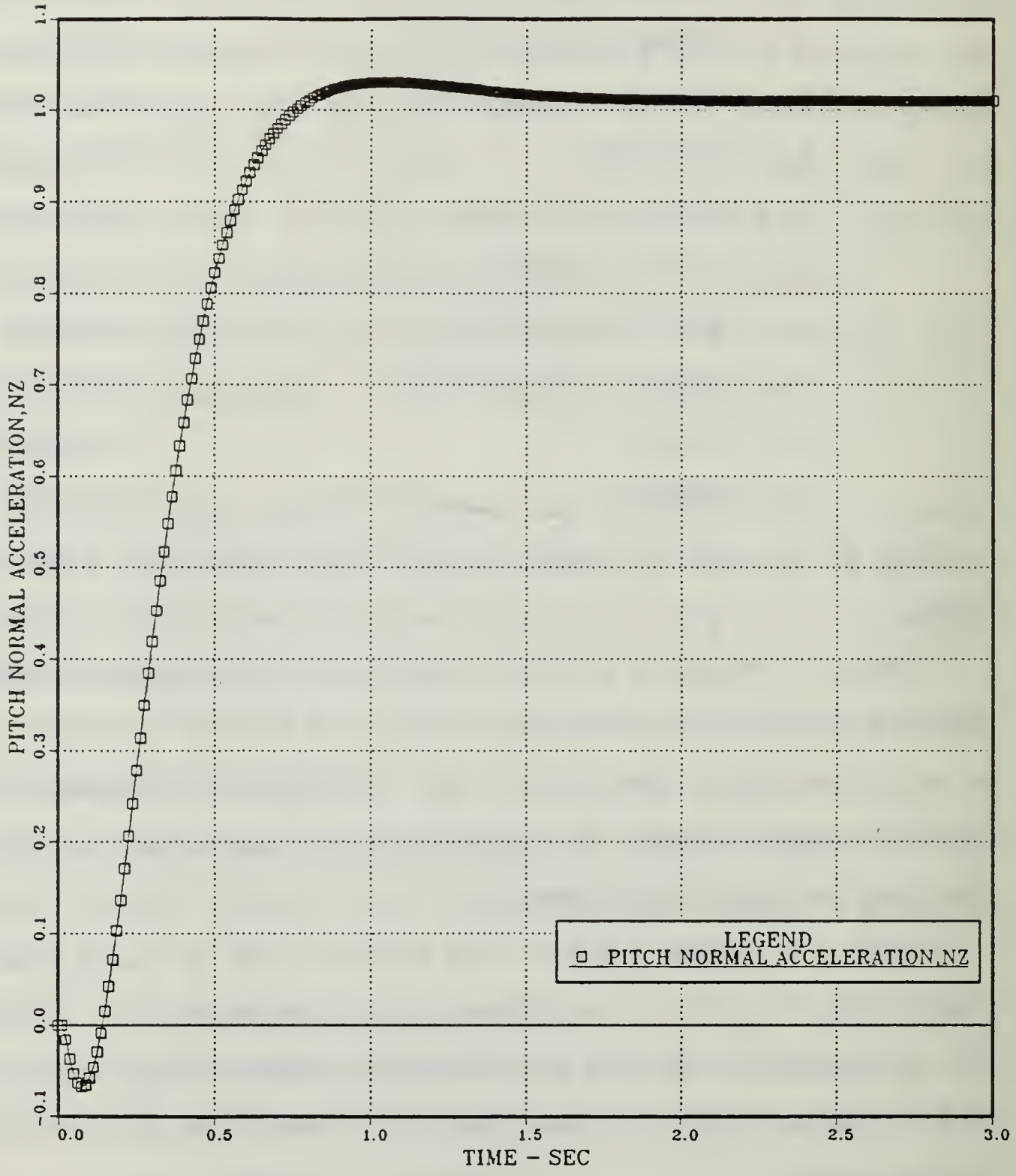

Figure 4.1 Pitch Normal Acceleration vs Time; Coupled Pitch and Roll Channels; Discrete State-Feedback Autopilot.

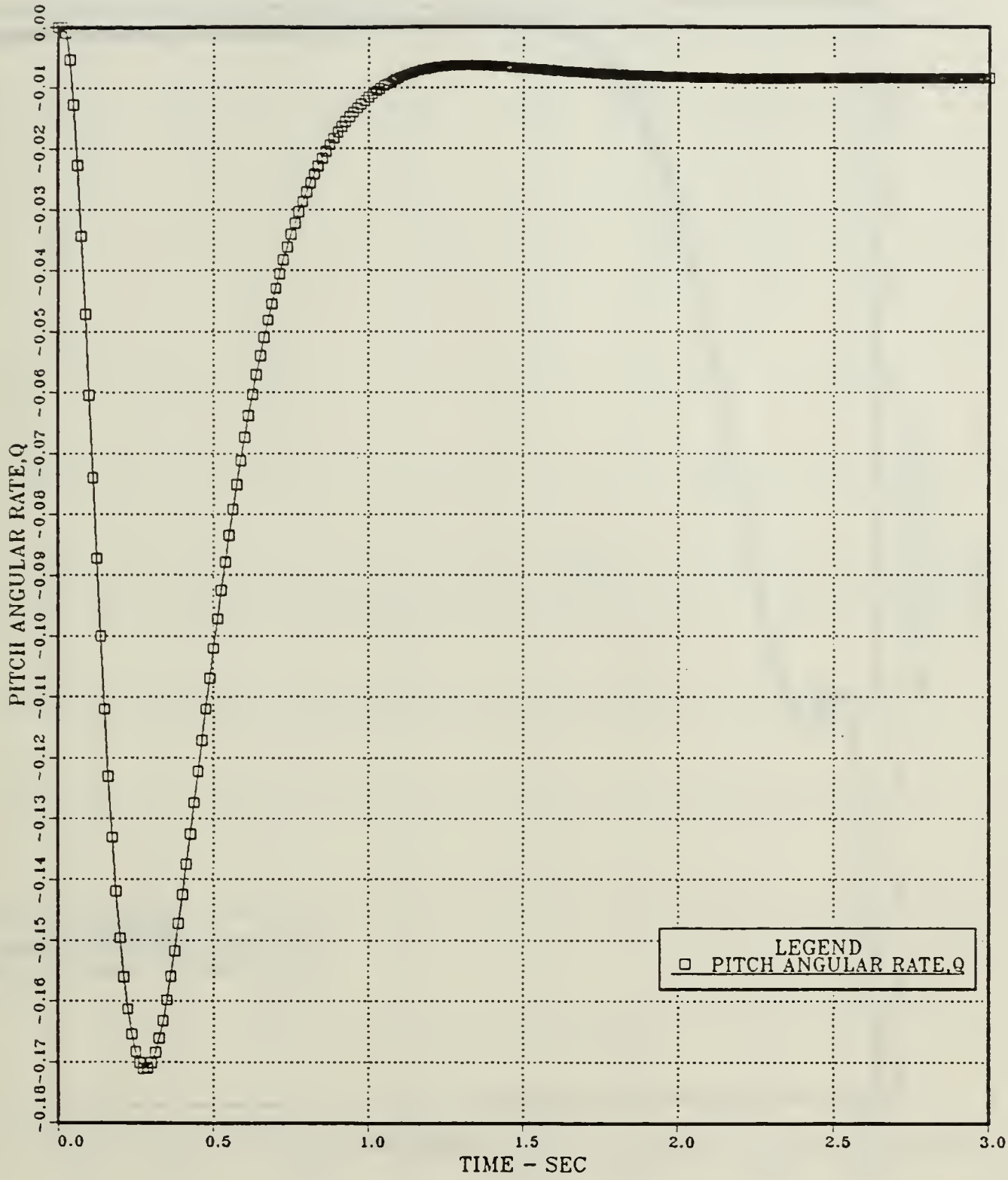

Figure 4.2 Pitch Angular Rate vs Time; Coupled Pitch and Roll Channels; Discrete State-Feedback Autopilot.

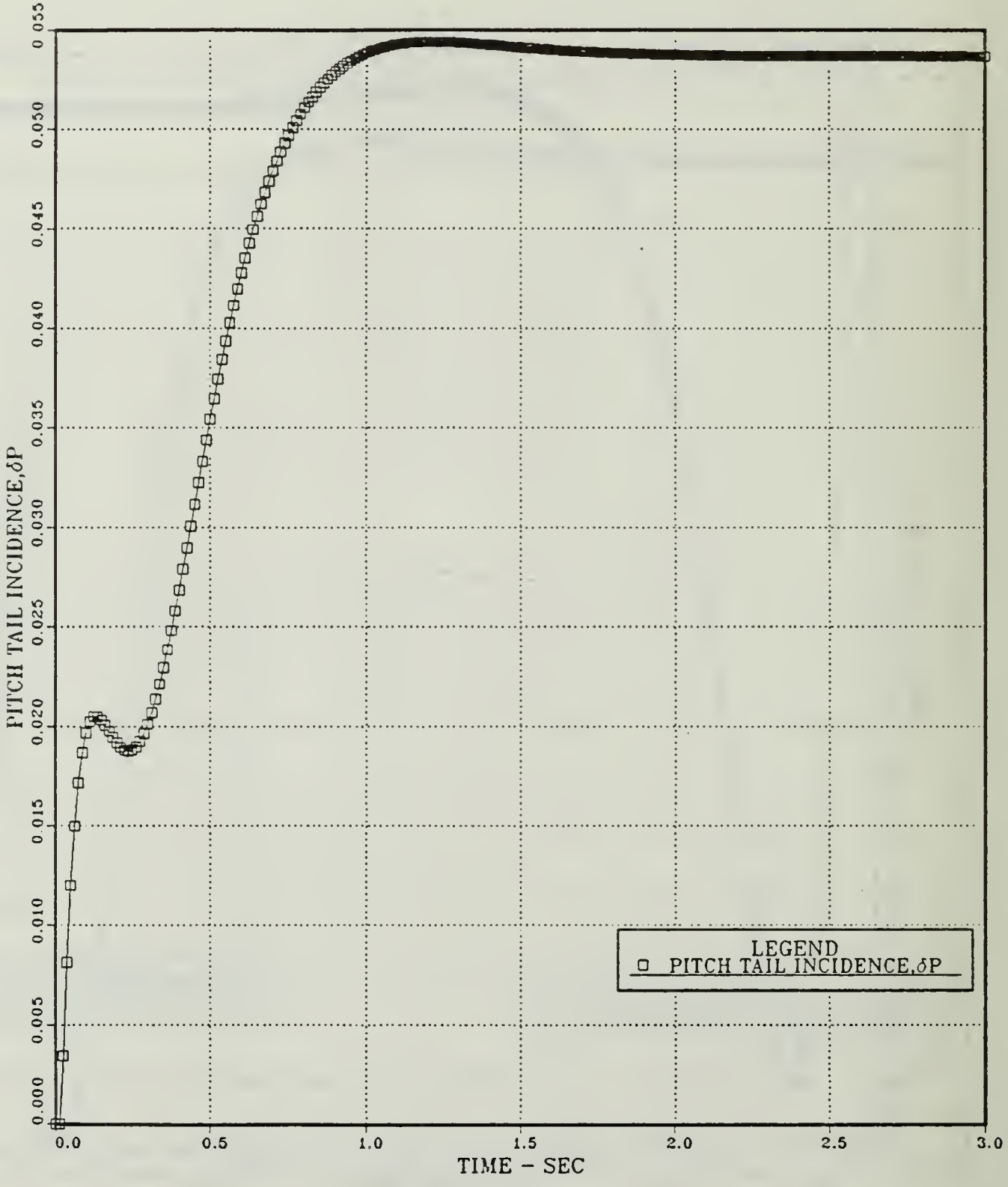

Figure 4.3 Pitch Tail Incidence vs Time; Coupled Pitch and Roll Channels; Discrete State-Feedback Autopilot.

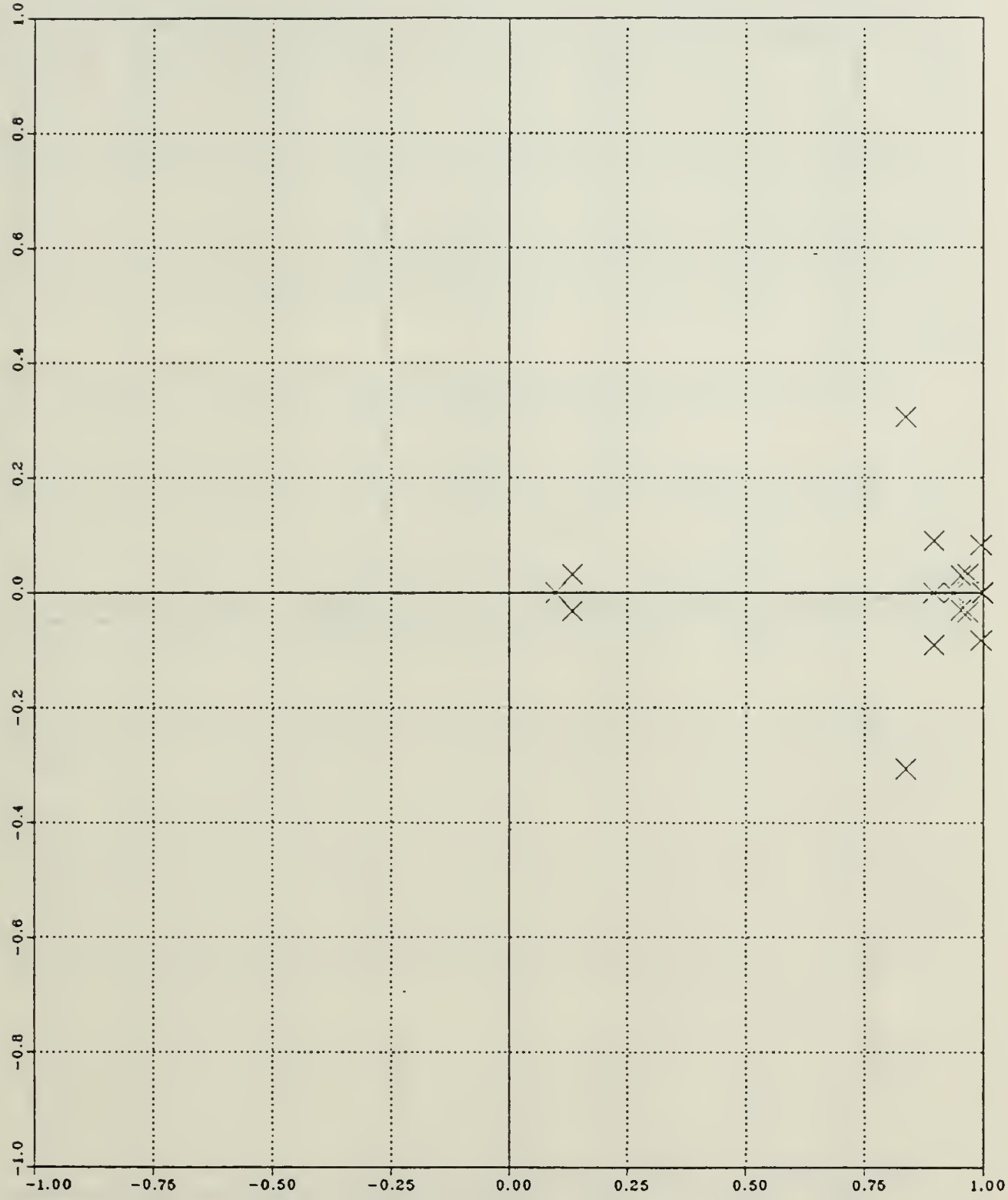

Figure 4.4 Pitch Normal Acceleration ; Coupled Pitch and Roll Channels; Discrete State-Feedback Autopilot; Pole-Zero Map.

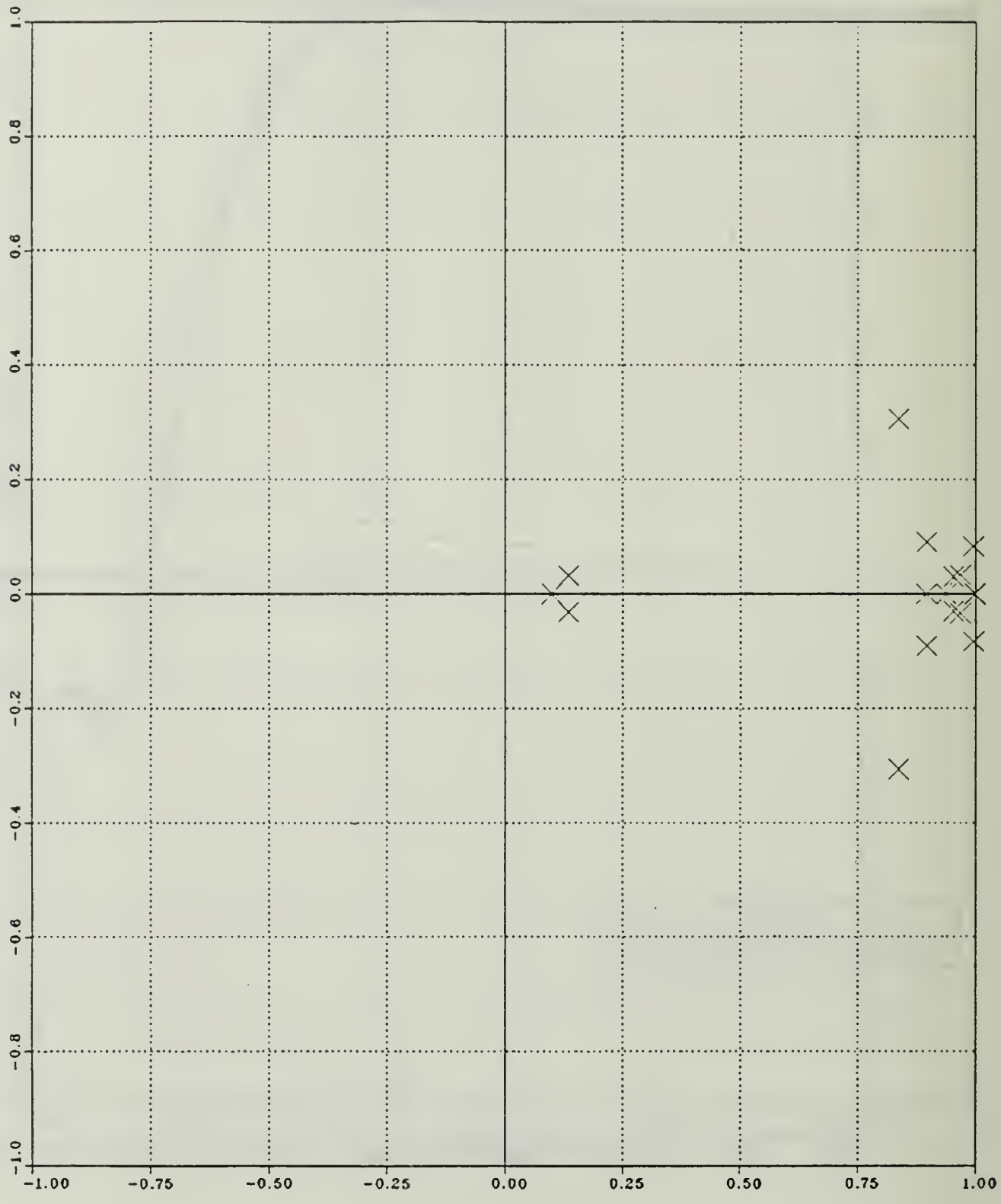

Figure 4.5 Pitch Angular Rate; Coupled Pitch and Roll Channels; Discrete State-Feedback Autopilot; Pole-Zero Map.

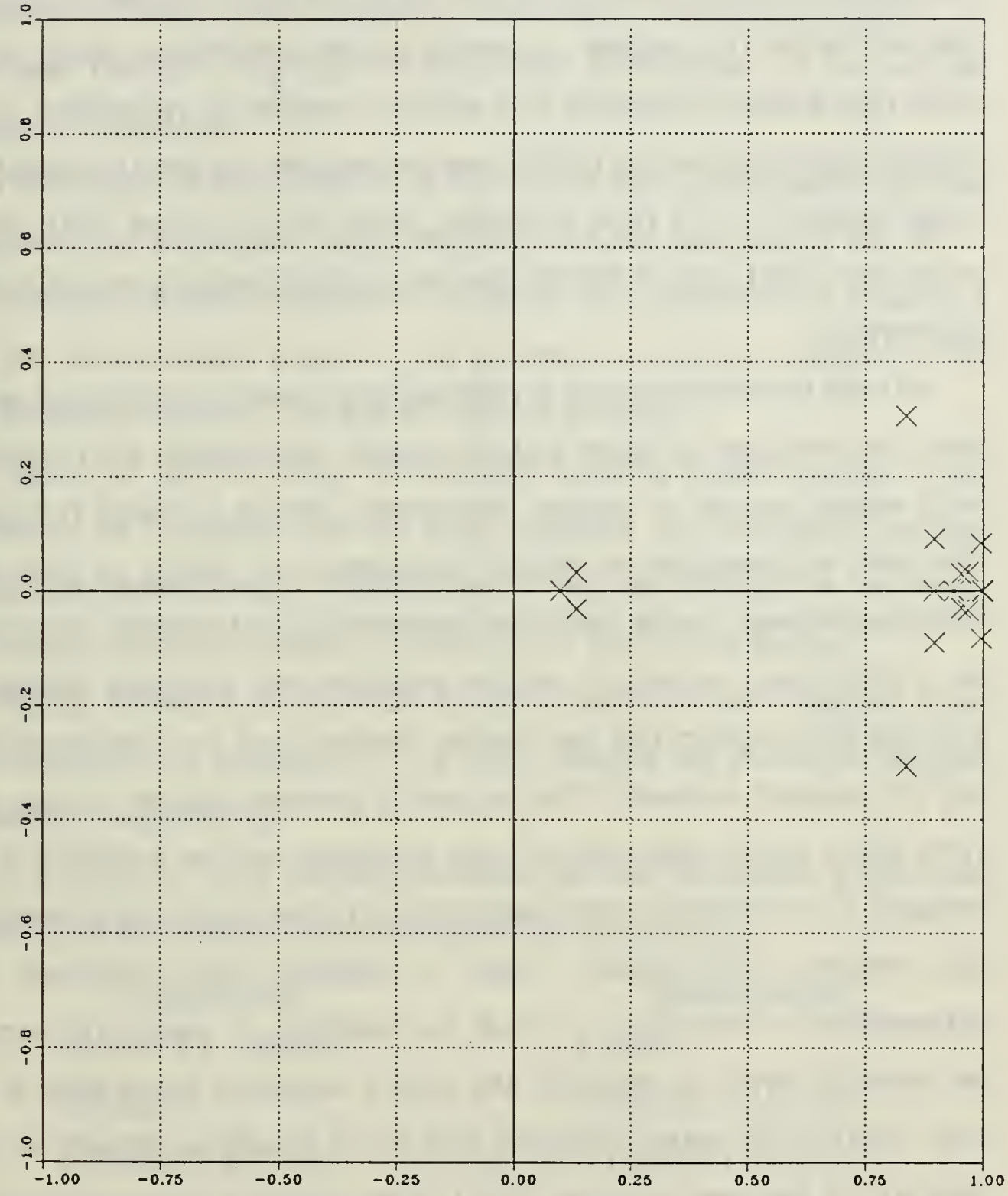

Figure 4.6 Pitch Tail Incidence; Coupled Pitch and Roll Channels; Discrete State-Feedback Autopilot; Pole-Zero Map.

D. ROBUSTNESS OF SYSTEM

With the rising interest in multivariable control theory brought on by increasingly complex systems the need has arisen to develop design methods that will allow the designer to specify system performance while at the same time ensuring relatively high stability margins or robustness. In the single-input-single-output (SISO) case the designer has had the tools to do these tradeoffs in the form of Nyquist, Bode and root-locus plots. In the multi-input-multi-output (MIMO) case the classical methods are not totally appropriate.

With the increased interest in MIMO systems numerous methods of design have been employed to obtain suitable system performance and robustness with varying degrees of success. One primary method of design is to keep the plant as decoupled as possible throughout the design so that each individual element may be controlled independently and designed essentially as a single loop system. In another procedure the multiloop system is modified into a system that has diagonal elements that are much larger than any off-diagonal elements. This diagonally dominant system is then in a form where conventional Nyquist type techniques can be employed in the analysis. A third common MIMO design method is that of the Linear Quadratic (LQ) method. This method uses a quadratic cost functional and optimamization principles to allow the designer to design for various performance levels by adjusting the matrix weighting terms used in the cost function. The major difficulty with all of the above methods is that they are not necessarily robust. This is especially true for cross-coupling terms between loops.

A simple interpretation of robustness is the ability of a system to tolerate design pertubations. These pertubations could be in the form of actuator failures, plant parameter uncertainty, unmodeled dynamic or nonlinear terms, or any one of many other pertubations to the nominal design of the system.

The analysis of the robustness of the system was obtained using the Pole Placement and Robustness Design Program (POPLAR) developed in [Ref. 8].

Utilizing the above program and using the data file shown in Appendix F for the state feedback autopilot, and the data file shown in Appendix G for the estimator autopilot, the system found to be robust.

Figures 4.7 and 4.8 show the Minimum Additive Output Singular Value (SVADMO) vs frequency for the state feedback and estimator designed autopilots respectively. It is noted that for very low frequencies the values of SVADMO are above 0.80680 and 0.83976 for each of the designs.

Figures 4.9 and 4.10 show the Minimum Additive Input Singular Value (MIN.ADD.IN.SV) vs frequency for the state feedback and estimator designed autopilots respectively.

In the case of state feedback autopilot the ordered complex eigenvalues (input), and the ordered computed eigenvalues (output) are:

Ordered input	Ordered output
-0.01000 + j 1.00000	0.09931
0.09928	0.13446 - j 0.03210
0.13199 - j 0.03194	0.13446 + j 0.03210
0.13199 + j 0.03194	0.83653 - j 0.30610
0.83522 - j 0.30974	0.83653 + j 0.30610

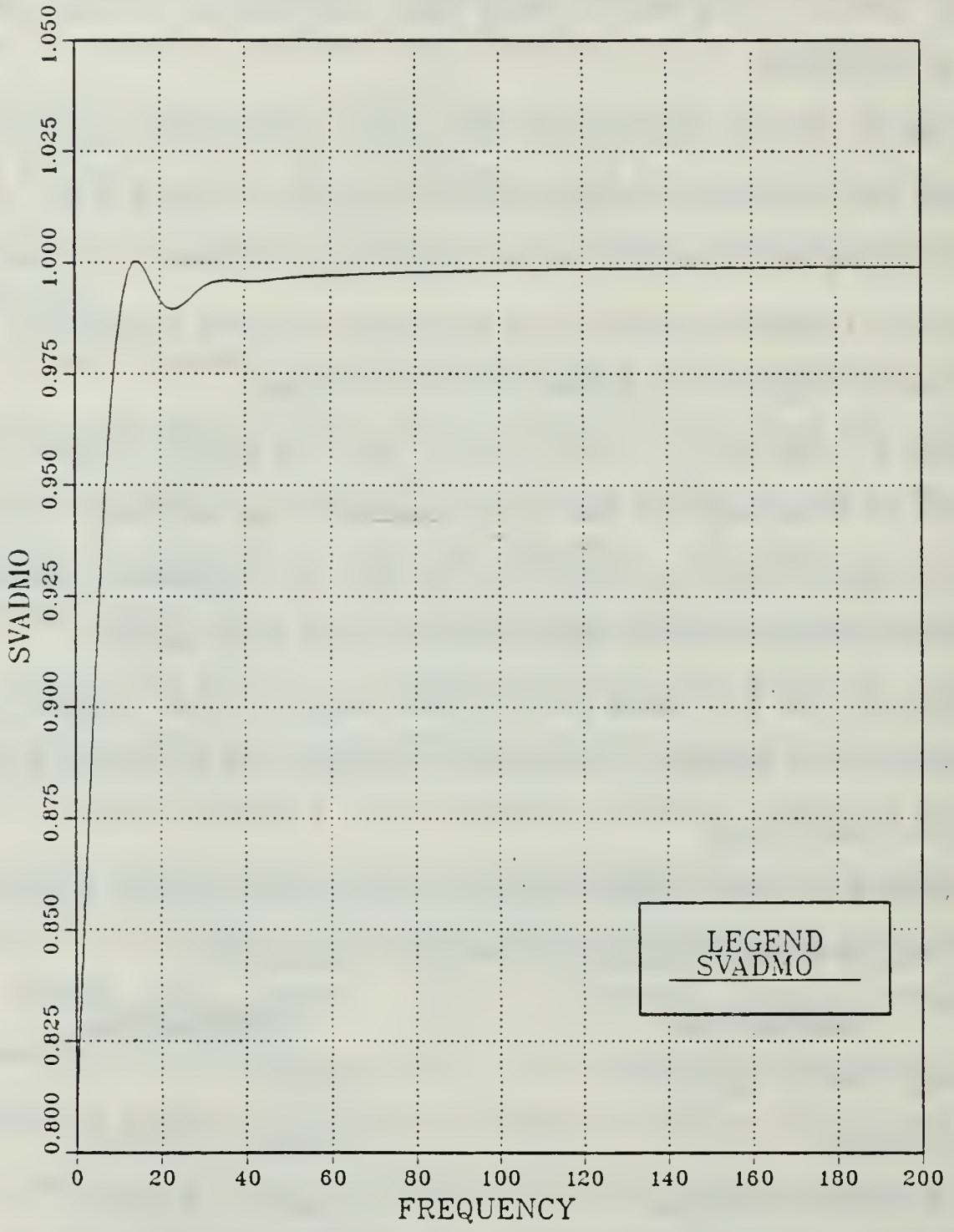

Figure 4.7 SVADMO vs Frequency; Coupled Pitch and Roll Channels; Discrete State-Feedback Autopilot.

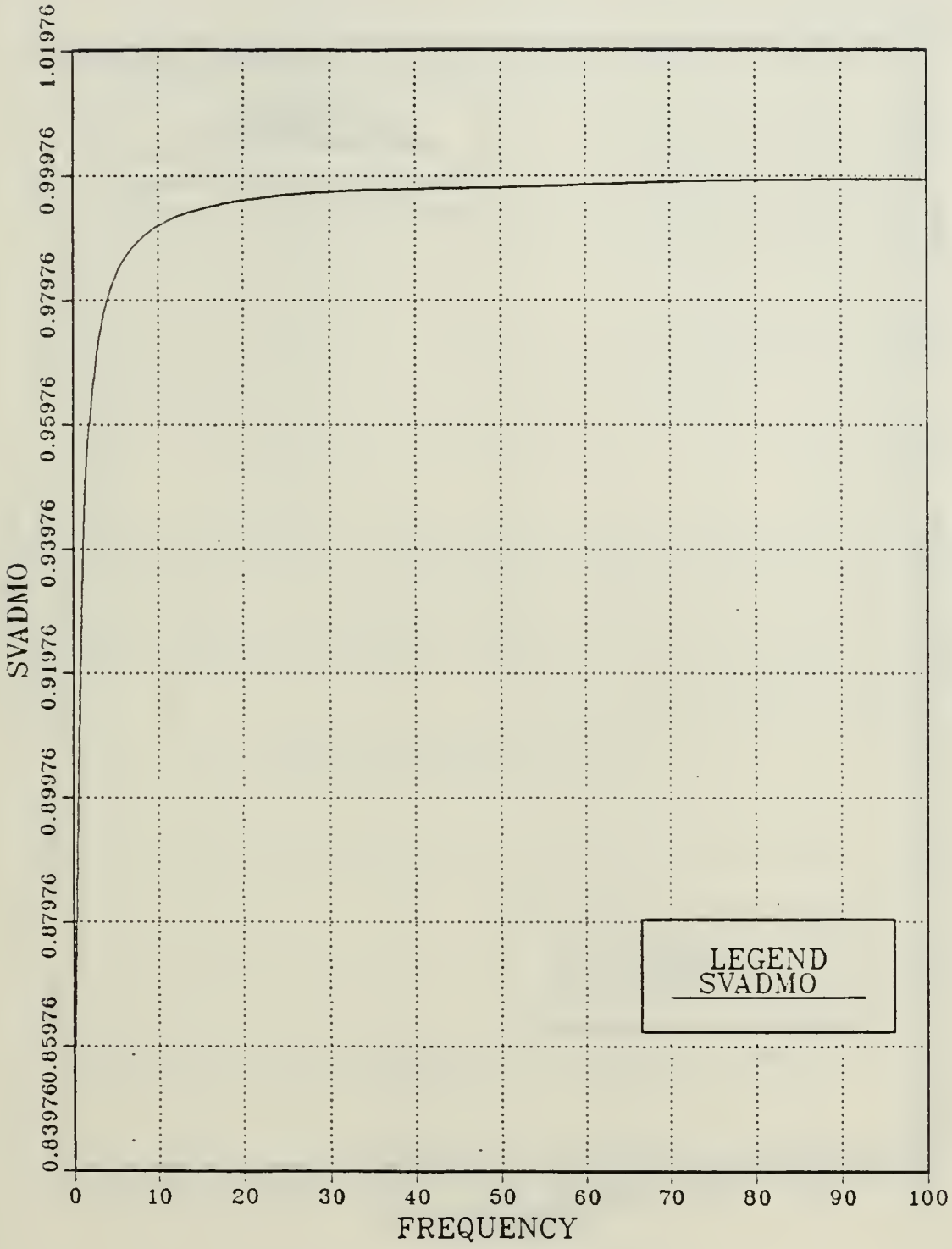

Figure 4.8 SVADMO vs Frequency; Coupled Pitch and Roll Channels; Discrete Estimator Autopilot.

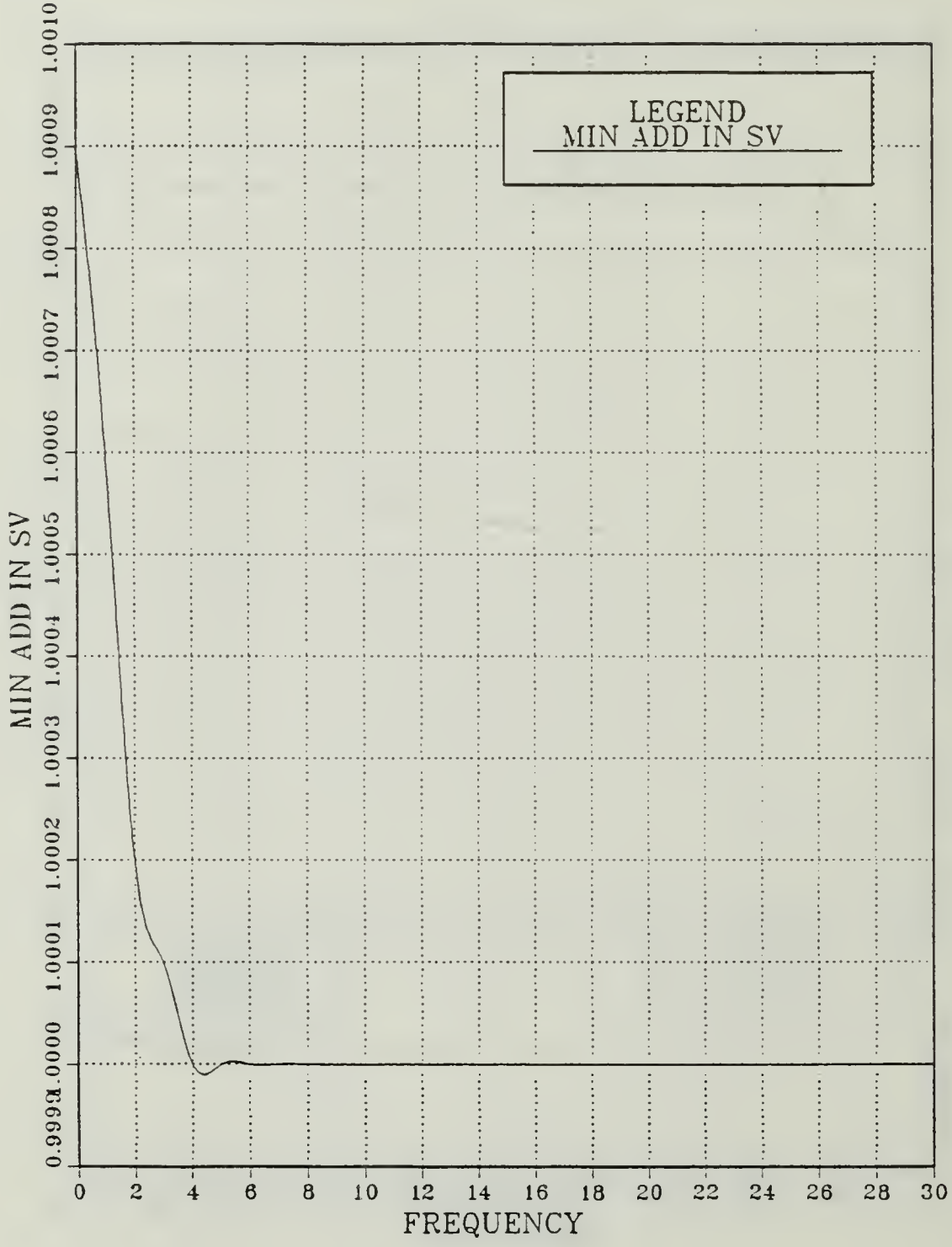

Figure 4.9 MIN.ADD.IN.SV vs Frequency; Coupled Pitch and Roll Channels; Discrete State-Feedback Autopilot.

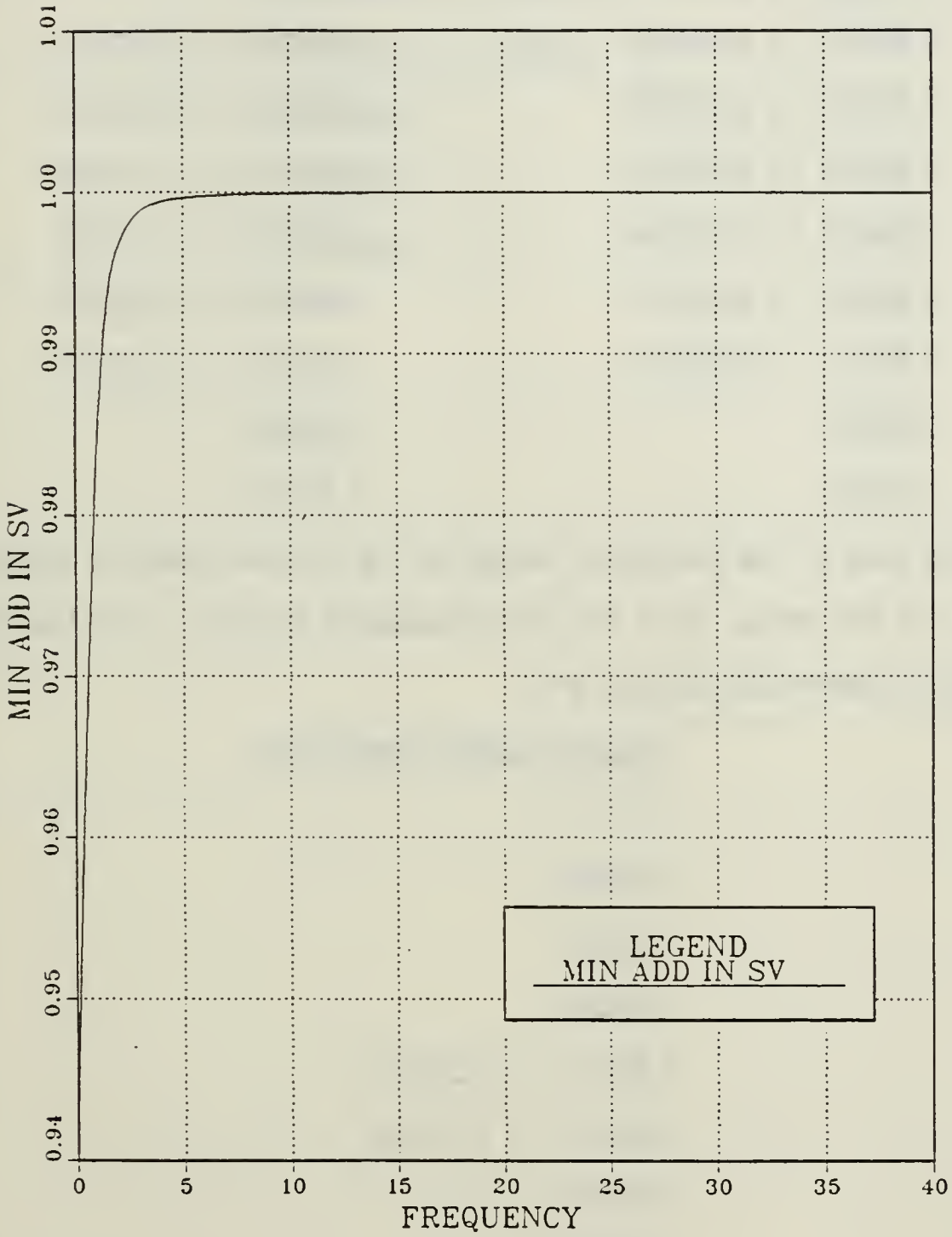

Figure 4.10 MIN.ADD.IN.SV vs Frequency; Coupled Pitch and Roll Channels; Discrete Estimator Autopilot.

0.83522 + j 0.30974	0.89571
0.89380	0.89698 - j 0.09064
0.89699 - j 0.09067	0.89698 + j 0.09064
0.89699 + j 0.09067	0.93813
0.95363 - j 0.02998	0.95360 - j 0.03001
0.95363 + j 0.02998	0.95360 + j 0.03001
0.96909 - j 0.03286	0.96776 - j 0.03345
0.96909 + j 0.03286	0.96776 + j 0.03345
0.99561 - j 0.08307	0.99559 - j 0.08307
0.99561 + j 0.08307	0.99559 + j 0.08307
0.99820	0.99820
1.00000	1.00000

In the case of the estimator autopilot the ordered complex eigenvalues (input) are the same, as in the state feedback autopilot, and the ordered computed eigenvalues (output) are:

Ordered output eigenvalues
0.07717
0.09855
0.25923
0.69508
0.83707 + j 0.30140
0.83707 - j 0.30140
0.89849
0.90064
0.93996

0.96207

0.96562 + j 0.03401

0.96562 - j 0.03401

0.99559 + j 0.08307

0.99559 - j 0.08307

0.99820

1.00000

1.06596

V. CONCLUSIONS AND RECOMMENDATIONS

A. CONCLUSIONS

The goal of this thesis was to design and analyze the discrete longitudinal autopilots for BTT and STT missiles.

The following are the principal conclusions based on this work.

1. The continuous and discrete longitudinal autopilots were proved to have identical performances.

2. The State-Feedback and Estimator autopilots were introduced as additional dynamic designs in order to implement control into the original system. Both performances were found to meet the desired requirements.

3. The Simplified State-Feedback and Estimator autopilots reduced the complexity of the system, by eliminating returning gain loops, and without any significant effects on the system's performance.

4. The performance of the Coupled Pitch and Roll channel autopilots was found to be satisfactory and also proved to be robust.

B. RECOMMENDATIONS

In order to make the whole design even simpler more returning gains loops, of the Simplified State-Feedback and Estimator autopilots, must be eliminated. A further investigation then must be conducted in order to examine whether the performance of the resulting design remain unchange.

APPENDIX A

GEOMETRIC AND MASS PROPERTIES OF MISSILE CONFIGURATION

Weight (lbs)	2525
Maximum Diameter (in)	24
Length (in)	168
I_{xx} (Slug Ft^2)	40
I_{yy} (Slug Ft^2)	804
I_{zz} (Slug Ft^2)	810
Center of Gravity Distance from Nose (in)	100.8
Reference Length (Ft)	2
Reference Area (Ft^2)	π

```
OPTMAT DATA FILE INPUT TO DRCONV PROGRAM:.....ORACLES PROGRAMS

     F     MATRIX       10 ROWS       10 COLUMNS
-1.5000000E+02   0.0000000E+00   0.0000000E+00   0.0000000E+00   0.0000000E+00   0.0000000E+00   0.0000000E+00
   0.0000000E+00   0.0000000E+00   1.5000000E+02
 1.3531000E+00   0.0000000E+00   1.0000000E+00   0.0000000E+00   0.0000000E+00   0.0000000E+00   0.0000000E+00
   0.0000000E+00   0.0000000E+00   0.0000000E+00
-6.5720000E+00   0.0000000E+00  -5.0000000E+00   0.0000000E+00   0.0000000E+00   0.0000000E+00   0.0000000E+00
   0.0000000E+00   0.0000000E+00   0.0000000E+00
 0.0000000E+00   0.0000000E+00   0.0000000E+00   1.0000000E+00   0.0000000E+00   0.0000000E+00   0.0000000E+00
  -5.9263700E+01   0.0000000E+00   0.0000000E+00
 0.0000000E+00   0.0000000E+00   0.0000000E+00  -4.4355700E+01  -1.4913600E-01   0.0000000E+00   0.0000000E+00
   1.7887000E+00   0.0000000E+00   0.0000000E+00
 0.0000000E+00   0.0000000E+00   0.0000000E+00   0.0000000E+00   0.0000000E+00   0.0000000E+00   1.0000000E+00
  -7.0192000E-01   0.0000000E+00   0.0000000E+00
 0.0000000E+00   0.0000000E+00   0.0000000E+00   0.0000000E+00   0.0000000E+00  -4.4355700E+01  -1.4919600E-01
  -1.5433600E+03   0.0000000E+00   0.0000000E+00
 0.0000000E+00   0.0000000E+00   0.0000000E+00   0.0000000E+00   0.0000000E+00   0.0000000E+00   0.0000000E+00
  -1.8840000E+02   1.8840000E+02   0.0000000E+00
-4.6083900E-01  -2.2308000E+00  -3.4058000E-01   2.2308000E+00   3.4058000E-01   0.0000000E+00   0.0000000E+00
  -2.0194000E+01  -1.4300000E-01   0.0000000E+00
 0.0000000E+00   0.0000000E+00   0.0000000E+00   0.0000000E+00   0.0000000E+00   0.0000000E+00  -1.0000000E+00
   8.8712400E+02  -8.8642200E+02   0.0000000E+00

     G     MATRIX       10 ROWS       1 COLUMNS
 0.0000000E+00
-1.3531000E+00
 6.5720000E+00
 0.0000000E+00
 0.0000000E+00
 0.0000000E+00
 0.0000000E+00
 0.0000000E+00
 4.6083900E-01
 0.0000000E+00

DRCONV: ANALOG - DIGITAL CONVERSION.....DISCRETE MATRICES...
        THE SAMPLE TIME INTERVAL FOR THIS RUN =    0.01250

     A     MATRIX       10 ROWS       10 COLUMNS
 1.5795758E-01   3.6369326E-02   5.5849592E-03  -3.5415286E-02  -5.6850634E-03   1.4376935E-03  -6.3550195E-03
   3.1215038E+00  -2.7434696E+00   8.4950341E-01
 7.3702121E-03   1.0001847E+00   1.2145713E-02  -1.3110829E-04  -2.8707903E-05   6.4803277E-06  -4.3148367E-05
   2.3554415E-02  -2.1657925E-02   9.0789743E-03
-3.5755072E-02  -8.9683556E-04   9.3927554E-01   8.7928240E-04   1.3937753E-04  -3.1463045E-05   2.0946996E-04
  -1.1434246E-01   1.0513494E-01  -4.4066551E-02
 6.3641914E-04   4.8072347E-03   7.3730452E-04   9.9184592E-01   1.1724094E-02   1.0387178E-07  -1.0276906E-06
  -2.5772733E-01  -4.3730676E-01   3.6239694E-04
-1.2632605E-04  -8.8102183E-04  -1.3533452E-04  -5.5242591E-01   9.9481481E-01  -1.1935039E-08   1.3487757E-07
   1.1052479E-01   1.0873558E-01  -5.5530062E-05
 5.0058503E-05   3.4906702E-04   5.3521335E-05  -3.4235257E-04  -5.4232194E-05   9.9653887E-01   1.2473878E-02
  -4.3837960E-02  -4.3103149E-02   2.2390223E-05
 1.1198072E-02   8.4589715E-02   1.2932564E-02  -8.2578336E-02  -1.3194430E-02  -5.5329815E-01   9.9465984E-01
  -4.5313172E+00  -7.6933073E+00   6.3774424E-03
-1.8197865E-03  -1.6475935E-02  -2.5342871E-03   1.5914437E-02   2.5927489E-03  -7.6937268E-07   6.1129260E-06
   1.9653250E-02   8.2551826E-01  -1.6117691E-03
-2.4201119E-03  -2.6250703E-02  -4.0458111E-03   2.5378784E-02   4.1674975E-03  -2.2085512E-06   1.4659039E-05
  -1.0104558E-01   8.5213330E-01  -3.0606437E-03
 8.5120361E-03   7.7170206E-02   1.1870299E-02  -7.4535066E-02  -1.2144550E-02   3.4647518E-03  -1.2532640E-02
   4.6563462E+00  -3.8409597E+00   1.0075610E+00

     B     MATRIX       10 ROWS       1 COLUMNS
-7.5609829E-03
-1.6449186E-02
 7.9821623E-02
-9.9881603E-04
 1.8285612E-04
-7.2448726E-05
-1.7575515E-02
 3.4315556E-03
 5.4807555E-03
-1.6073019E-02

MESSAGE SUMMARY: MESSAGE NUMBER - COUNT
```

PROGRAM LOGIC FOR COMPUTING CONTROL LAW K VIA ACKERMANN'S FORMULA

1. Read in **A**, **B**, T, and N_s, the number of states.
2. Comment: first we will read in the desired pole location in the plane,convert them to z-plane polynomial coefficients, and construct $\alpha(\mathbf{A})$.
3. **I** ← identity matrix, $N_s \times N_s$
4. **ALPHA** ← **I**
5. k ← 1
6. If $k > N_s$, go to step 18.
7. Read in pole location k as a+jb.
8. If b=0, go to step 14.
9. $A_1 \leftarrow -2\exp(aT)\cos(bT)$
10. $A_2 \leftarrow \exp(2aT)$
11. **ALPHA** ← **ALPHA** x (**A** x **A** + A_1**A** +A_2**I**)
12. k ← k + 2
13. Go to step 6.
14. $A_1 \leftarrow \exp(aT)$
15. **ALPHA** ← **ALPHA** x (**A** - A_1 x **I**)
16. k ← k + 1
17. Go to step 6.
18. Comment: now we construct the controllability matrix.
19. **C** ← **I**

20. **E** ← **B**

21. k ← 1

22. If k > N_s, go to step 28.

23. Comment: replace column k of **C** by **E**.

24. **C**[; k] ← **E**

25. k ← k + 1

26. **E** ← **A** x **E**

27. Go to step 22.

28. Comment: now solve for the control law, first form e^T_n as the last row of **I**

29. **E** ← **I**[N_s ;]

30. Solve **DC** = **E** for **D**.

31. **K** = **D** x **ALPHA**

32. END

APPENDIX D

COMPUTER PROGRAM FOR APPLICATION OF ACKERMANN'S FORMULA

```
FILE: ACKERMAN FATFIV   A1

$JOB                                                                    ACK00010
      INTEGER     NS,K,IA,IER,I,J,NI                                    ACK00020
      REAL        PH(20,20),GA(20,20),AI(20,20),ALPHA(20,20),WK(40)     ACK00030
      REAL     A2  ,B(20,20),C(20,20),S(20),BF(20,20),UK(20,20)         ACK00040
      REAL  A,B,T,  R,ATEMP(20,20)                                      ACK00050
      REAL     A1   ,TO(20,20),TI(20,20),TS(20,20),C(20,20),TM(20,20)   ACK00060
C                                                                       ACK00070
C    INPUT OF NS= NUMBER OF STATES                                      ACK00080
C           T= SAMPLE TIME                                              ACK00090
      PRINT ,   ' ENTER NUMBER OF STATES.'                              ACK00100
      READ, NS                                                          ACK00110
      PRINT, ' ENTER SAMPLE TIME '                                      ACK00120
      READ, T                                                           ACK00130
C    INPUT OF PHI=A MATRIX                                              ACK00140
      DO 100  I=1,NS                                                    ACK00150
      DO 101  J=1,NS                                                    ACK00160
      WRITE(6,103) I,J                                                  ACK00170
  103 FORMAT(4X,'ENTER PH(',I2,',',I2,')')                              ACK00180
      READ,PH(I,J)                                                      ACK00190
  101 CONTINUE                                                          ACK00200
  100 CONTINUE                                                          ACK00210
C    INPUT OF GA=B MATRIX                                               ACK00220
      DO 200   I=1,NS                                                   ACK00230
        J=1                                                             ACK00240
      WRITE(6,105) I,J                                                  ACK00250
  105 FORMAT(4X,'ENTER GA(',I2,',',I2,')')                              ACK00260
      READ,GA(I,J)                                                      ACK00270
  200 CONTINUE                                                          ACK00280
C    BUILDING THE IDENTITY MATRIX                                       ACK00290
C    ALPHA=C=I                                                          ACK00300
      DO 1 I=1,NS                                                       ACK00310
      DO 5 J=1,NS                                                       ACK00320
      IF (I.EQ.J) GO TO 300                                             ACK00330
      AI(I,J)=0.                                                        ACK00340
      ALPHA(I,J)=0.                                                     ACK00350
      C(I,J)=0.                                                         ACK00360
      GO TO 5                                                           ACK00370
  300 AI(I,J)=1.                                                        ACK00380
      ALPHA(I,J)=1.                                                     ACK00390
      C(I,J)=1.                                                         ACK00400
    5 CONTINUE                                                          ACK00410
    1 CONTINUE                                                          ACK00420
      K=1                                                               ACK00430
   16 IF (K.GT.NS) GO TO 18                                             ACK00440
C                                                                       ACK00450
C     INPUT OF DESIRED POLES LOCATION                                   ACK00460
C                                                                       ACK00470
      WRITE (6,43)                                                      ACK00480
   43 FORMAT(' ENTER REAL PART OF DESIRED POLE LOCATION.')              ACK00490
      READ,A                                                            ACK00500
      WRITE(6,44)                                                       ACK00510
   44 FORMAT(' ENTER IMAGINARY PART OF DESIRED POLE LOCATION.')         ACK00520
      READ,B                                                            ACK00530
C   BUILDING ALPHA(PHI)                                                 ACK00540
      IF (B .EQ.0) GO TO 14                                             ACK00550
      A1=-2.*EXP(A*T)*COS(B*T)                                          ACK00560
      A2=EXP(2.*A*T)                                                    ACK00570
C    EVALUATE PHI*PHI                                                   ACK00580
      CALL VMULFF (PH,PH,NS,NS,NS,20,20,TM,20,IER)                      ACK00590
C                                                                       ACK00600
      DO 2 I=1,NS                                                       ACK00610
      DO 6 J=1,NS                                                       ACK00620
        TO(I,J)=PH(I,J)*A1                                              ACK00630
        TI(I,J)=AI(I,J)*A2                                              ACK00640
        TS(I,J)=TM(I,J)+TO(I,J)+TI(I,J)                                 ACK00650
    6 CONTINUE                                                          ACK00660
    2 CONTINUE                                                          ACK00670
      CALL VMULFF (ALPHA,TS,NS,NS,NS,20,20,ATEMP,20,IER)                ACK00680
      DO 600 I=1,NS                                                     ACK00690
      DO 601 J=1,NS                                                     ACK00700
  601 ALPHA(I,J)=ATEMP(I,J)                                             ACK00710
  600 CONTINUE                                                          ACK00720
```

```
      K= K+2                                                          ACK00730
      GO TO 16                                                        ACK00740
   14 A1=EXP(A*T)                                                     ACK00750
      DO 3 I=1,NS                                                     ACK00760
      DO 7 J=1,NS                                                     ACK00770
      TO(I,J)=A1(I,J)*A1                                              ACK00780
    7 TI(I,J)=PH(I,J)-TO(I,J)                                         ACK00790
    3 CONTINUE                                                        ACK00800
      CALL VMULFF(ALPHA,TI,NS,NS,NS,20,20,ATEMP,20,IER)               ACK00810
      DO 700 I=1,NS                                                   ACK00820
      DO 701 J=1,NS                                                   ACK00830
  701 ALPHA(I,J)=ATEMP(I,J)                                           ACK00840
  700 CONTINUE                                                        ACK00850
      K=K+1                                                           ACK00860
      GO TO 16                                                        ACK00870
   18 DO 9 I=1,NS                                                     ACK00880
      J=1                                                             ACK00890
    9 E(I,J)=GA(I,J)                                                  ACK00900
      K=1                                                             ACK00910
   22 IF (K.GT.NS) GO TO 28                                           ACK00920
      DO 10 I=1,NS                                                    ACK00930
      C(I,K)=E(I,1)                                                   ACK00940
   10 CONTINUE                                                        ACK00950
      K=K+1                                                           ACK00960
      CALL VMULFF (PH,E,NS,NS,1 ,20,20,E,20,IER)                      ACK00970
      GO TO 22                                                        ACK00980
   28 DO 11 J=1,NS                                                    ACK00990
   11 E( 1,J)=A1(NS,J)                                                ACK01000
      R=0.                                                            ACK01010
      CALL LGINF (C,20,NS,NS,R,D,20,S,WK,IER)                         ACK01020
C                                                                     ACK01030
      CALL VMULFF (E,D,1 ,NS,NS,20,20,BF,20,IER)                      ACK01040
      CALL VMULFF (BF,ALPHA,1 ,NS,NS,20,20,UK,20,IER)                 ACK01050
C                                                                     ACK01060
      PRINT, '      CONTROL GAIN  VECTOR  '                           ACK01070
      WRITE (6,45)  (UK(1,J),J=1,NS)                                  ACK01080
   45 FORMAT(8F15.4)                                                  ACK01090
      RETURN                                                          ACK01100
      END                                                             ACK01110
$ENTRY                                                                ACK01120
```

APPENDIX E

ANALOG TO DIGITAL CONVERSION OF COUPLED PITCH AND ROLL CHANNEL AUTOPILOTS

OPTIMAL DATA FILE INPUT TO ORACONV PROGRAMS.....ORACLES PROGRAMS
F MATRIX 17 ROWS 17 COLUMNS
G MATRIX 17 ROWS 2 COLUMNS
CRCONV: ANALOG - DIGITAL CONVERSION.....DISCRETE MATRICES...
THE SAMPLE TIME INTERVAL FOR THIS RUN =

```
     A     MATRIX        17 ROWS          17 COLUMNS
 1.5795575E-01   3.6369332E-02   5.5845592E-03  -3.5415286E-02  -5.0350633E-03   1.4378695E-03  -6.9550195E-04
   3.1215033E-00  -2.7434696E+00   8.4953341E-01   0.0000000E+00   0.0000000E+00   0.0000000E+00   0.0000000E+00
   0.0000000E+00   0.0000000E+00   0.0000000E+00
 7.3702121E-03   1.0001847E+00   1.2145713E-02  -1.3110329E-04  -2.3737703E-05   6.4803277E-06  -4.3143367E-05
   2.3554415E-02  -2.1657925E-02   9.0789743E-03   0.0000000E+00   0.0000000E+00   0.0000000E+00   0.0000000E+00
   0.0000000E+00   0.0000000E+00   0.0000000E+00
-3.5755072E-02  -8.9633355E-04   9.3227554E-01   8.7328241E-04   1.3737755E-04  -3.1463345E-05   2.0946996E-04
  -1.1434246E-01   1.0513494E-01  -4.4866551E-02   0.0000000E+00   0.0000000E+00   0.0000000E+00   0.0000000E+00
   0.0000000E+00   0.0000000E+00   0.0000000E+00
 6.3641914E-04   4.8072547E-03   7.3780452E-04   9.9134592E-01   1.1724094E-02   1.0389178E-07  -1.0276906E-06
  -2.5772735E-01  -4.3730676E-01   3.6239694E-04   0.0000000E+00   0.0000000E+00   0.0000000E+00   0.0000000E+00
   0.0000000E+00   0.0000000E+00   0.0000000E+00
-1.2632605E-04  -8.8102185E-04  -1.3508452E-04  -5.5242591E-01   9.9431481E-01  -1.1935039E-08   1.3487756E-07
   1.1052479E-01   1.0873558E-01  -5.6530062E-05   0.0000000E+00   0.0000000E+00   0.0000000E+00   0.0000000E+00
   0.0000000E+00   0.0000000E+00   0.0000000E+00
 5.0058503E-05   3.4706702E-04   5.3521335E-05  -3.4235257E-04  -5.4232194E-05   9.9653837E-01   1.2473879E-02
  -4.3837950E-02  -4.3103149E-02   2.2390223E-05   0.0000000E+00   0.0000000E+00   0.0000000E+00   0.0000000E+00
   0.0000000E+00   0.0000000E+00   0.0000000E+00
 1.1198372E-02   8.4509715E-06   1.2932664E-02  -3.2578336E-02  -1.3194430E-02  -5.5328815E-01   9.9465984E-01
  -4.5313172E+00  -7.6733073E+00   6.3774425E-03   0.0000000E+00   0.0000000E+00   0.0000000E+00   0.0000000E+00
   0.0000000E+00   0.0000000E+00   0.0000000E+00
-1.8197865E-03  -1.6475936E-02  -2.5342871E-03   1.5914437E-02   2.5927489E-03  -7.6937268E-07   6.1129260E-06
   1.9658256E-02   8.2551826E-01  -1.6117691E-03   0.0000000E+00   0.0000000E+00   0.0000000E+00   0.0000000E+00
   0.0000000E+00   0.0000000E+00   0.0000000E+00
-2.4201118E-03  -2.6250703E-02  -4.0468111E-03   2.5078784E-02   4.1674975E-03  -2.2085612E-06   1.4659039E-05
  -1.0104558E-01   8.5213330E-01  -3.8636457E-03   0.0000000E+00   0.0000000E+00   0.0000000E+00   0.0000000E+00
   0.0000000E+00   0.0000000E+00   0.0000000E+00
 8.5120362E-03   7.7170206E-02   1.1870299E-02  -7.4535066E-02  -1.2144650E-02   3.4647518E-03  -1.2502640E-02
   4.6563462E+00  -3.8405597E+00   1.0075610E+00   0.0000000E+00   0.0000000E+00   0.0000000E+00   0.0000000E+00
   0.0000000E+00   0.0000000E+00   0.0000000E+00
 0.0000000E+00   0.0000000E+00   0.0000000E+00   0.0000000E+00   0.0000000E+00   0.0000000E+00   0.0000000E+00
   0.0000000E+00   0.0000000E+00   0.0000000E+00   9.9773873E-01  -2.7013690E-03   1.0245876E-03   2.2685736E-01
  -2.2392478E-01   3.2485155E+00   3.5730433E-02
 0.0000000E+00   0.0000000E+00   0.0000000E+00   0.0000000E+00   0.0000000E+00   0.0000000E+00   0.0000000E+00
   0.0000000E+00   0.0000000E+00   0.0000000E+00   1.2492612E-02   9.9999121E-01   3.3686339E-06   7.9213881E-04
  -7.8251019E-04   1.6122065E-02   3.2146565E-04
 0.0000000E+00   0.0000000E+00   0.0000000E+00   0.0000000E+00   0.0000000E+00   0.0000000E+00   0.0000000E+00
   0.0000000E+00   0.0000000E+00   0.0000000E+00  -1.3299604E-03  -2.0935729E-01   9.0483727E-01  -3.6881965E-05
   3.6451129E-05  -9.6597313E-04  -2.6308370E-05
 0.0000000E+00   0.0000000E+00   0.0000000E+00   0.0000000E+00   0.0000000E+00   0.0000000E+00   0.0000000E+00
   0.0000000E+00   0.0000000E+00   0.0000000E+00  -9.0797723E-03  -1.1024037E-02   3.9997292E-03   9.2763032E-01
   1.1630732E-02  -1.7007972E-01  -2.3023512E-03
 0.0000000E+00   0.0000000E+00   0.0000000E+00   0.0000000E+00   0.0000000E+00   0.0000000E+00   0.0000000E+00
   0.0000000E+00   0.0000000E+00   0.0000000E+00  -1.7340942E-04  -2.0717899E-04   7.8564538E-05   1.7374049E-02
   9.1059431E-01   2.4503591E-01   2.7257510E-03
 0.0000000E+00   0.0000000E+00   0.0000000E+00   0.0000000E+00   0.0000000E+00   0.0000000E+00   0.0000000E+00
   0.0000000E+00   0.0000000E+00   0.0000000E+00  -1.9081030E-03  -2.3081830E-03   8.4609805E-04   1.5283715E-01
  -1.5037418E-01   7.4697747E-01  -1.1429485E-03
 0.0000000E+00   0.0000000E+00   0.0000000E+00   0.0000000E+00   0.0000000E+00   0.0000000E+00   0.0000000E+00
   0.0000000E+00   0.0000000E+00   0.0000000E+00  -6.2875713E-02  -7.5602497E-02   2.8176191E-02   5.6122435E+00
  -5.5314055E+00   4.3323648E+01   5.1040685E-02

     B     MATRIX        17 ROWS          2 COLUMNS
-7.5609829E-03   0.0000000E+00
-1.6449186E-02   0.0000000E+00
 7.9821623E-02   0.0000000E+00
-9.9881503E-04   0.0000000E+00
 1.8285612E-04   0.0000000E+00
-7.2448726E-05   0.0000000E+00
-1.7575515E-02   0.0000000E+00
 3.4315550E-03   0.0000000E+00
 5.4807555E-03   0.0000000E+00
-1.6073019E-02   0.0000000E+00
 0.0000000E+00   2.7613690E-03
 C.0000000E+00   8.7926971E-06
 0.0000000E+00   2.0935729E-01
 0.0000000E+00   1.1024087E-02
 0.0000000E+00   2.0717899E-04
 0.0000000E+00   2.3081830E-03
 C.0000000E+00   7.5602497E-02

MESSAGE SUMMARY: MESSAGE NUMBER - COUNT

                 187        6
```

APPENDIX F

ROBUSTNESS DATA FILE FOR THE DISCRETE STATE FEEDBACK DESIGNED AUTOPILOT

FILE: FEEDBACK DATA A1

```
 1000     0
     200.0          0.0          1.0
        1             0            0
      0.4          0.4          0.0     0
    0     0     0     5     3     3 1000     0
1717170217170217171717
   1.5795758E-01    3.6369326E-02    5.5848592E-03   -3.5415286E-2   -5.6850634E-3
   1.4376905E-03   -6.3550195E-3     3.1215038OE+0   -2.7434696E+0    8.4960341E-01
                0                0                0               0                0
                0                0
   7.3702121E-03    1.0001847E-00    1.2145713E-02   -1.8110829E-4   -2.8707903E-5
   6.4803277E-06   -4.3148367E-5     2.3554415E-02   -2.1657925E-2    9.0787743E-03
                0                0                0               0                0
                0                0
  -3.5755072E-2    -8.9683556E-4    9.3927554E-01    8.7928240E-04    1.3937755E-04
  -3.1463045E-5     2.0940996E-04   -1.1434246E-1     1.0513494E-01   -4.4066551E-2
                0                0                0               0                0
                0                0
   6.3641914E-04    4.8072347E-03    7.3780452E-04    9.9184592E-01    1.1724094E-02
   1.0389178OE-7    -1.0276906E-6   -2.5772733E-1    -4.3730676E-1    3.6239694E-04
                0                0                0               0                0
                0                0
  -1.2632605E-4     -8.3102133E-4    -1.3508452E-4    -5.5242591E-1    9.9461481E-01
  -1.1935039E-8     1.3467757E-07    1.1052479E-01    1.0373553E-01   -5.6530062E-5
                0                0                0               0                0
                0                0
   5.0058503E-05    3.4906762E-04    5.3521335E-05   -3.4235257E-4    -5.4232194E-5
   9.9653887E-01    1.2473873E-02   -4.3637960E-2    -4.3103149E-2    2.2390223OE-5
                0                0                0               0                0
                0                0
   1.1198072E-02    8.4589715E-02    1.2982664E-02   -8.2578336E-2    -1.3194430E-2
  -5.5328815E-1     9.9465984E-01   -4.5313172E-0    -7.6933073E-0    6.3774424E-03
                0                0                0               0                0
                0                0
  -1.8197865E-3    -1.6475936E-2    -2.5342871E-3    1.5914437E-02    2.5927489E-03
  -7.6937268E-7     6.1129260E-06    1.9658256E-02    8.2551326E-01   -1.6117691E-3
                0                0                0               0                0
                0                0
  -2.4201118E-3    -2.6250703E-2    -4.0468111E-3    2.5078784E-02    4.1674975E-03
  -2.2085612E-6     1.4659039E-05   -1.0104558E-1     8.5213330E-01   -3.0665437E-3
                0                0                0               0                0
                0                0
   8.5120361E-03    7.7170206E-02    1.1870299E-02   -7.4535066E-2    -1.2144650E-2
   3.4647518E-03   -1.2502640E-2     4.6503462E-06   -3.8409597E-0     1.0075610E-00
                0                0                0               0                0
                0                0
                0                0                0               0                0
                0                0                0               0                0
   9.9773878E-01   -2.7013690E-3     1.0245896E-03    2.2685736E-01   -2.2392478E-1
   3.2285155E-00    3.6730433E-02
                0                0                0               0                0
                0                0                0               0                0
   1.2492612E-02    9.9999121E-01    3.3686339E-06    7.9213881E-04   -7.8251019E-4
   1.6120605E-02    3.2146565E-04
                0                0                0               0                0
                0                0                0               0                0
  -1.3299604E-3    -2.0935729E-1     9.0483727E-01   -3.6881965E-5    3.6451128E-05
  -9.6597318E-4    -2.6908370E-5
                0                0                0               0                0
                0                0                0               0                0
  -9.0797723E-3    -1.1024087E-2     3.9997292E-03    9.2763032E-01    1.1630732E-02
  -1.7007972E-1    -2.0028512E-3
                0                0                0               0                0
                0                0                0               0                0
  -1.7340942E-4    -2.0717899E-4     7.8564538E-05    1.7374049E-02    9.1059431E-01
   2.4505510E-01    2.7257510E-03
                0                0                0               0                0
                0                0                0               0                0
  -1.9081030E-3    -2.3061830E-3     8.4009805E-04    1.5280715E-01   -1.5037418E-1
   7.4692747E-01   -1.1429485E-3
                0                0                0               0                0
                0                0                0               0                0
```

FILE: FEEDBACK DATA A1

-6.2875718E-2	-7.5002497E-2	2.8170191E-02	5.6122435E-00	-5.5314055E-0
4.3323648E+01	5.1040685E-02			
-7.5609829E-3	0			
-1.6449186E-2	0			
7.9821623E-02	0			
-9.9881608E-4	0			
1.8285612E-04	0			
-7.2448726E-5	0			
-1.7575515E-2	0			
3.4315556E-03	0			
5.4807555E-03	0			
-1.6073019E-2	0			
0	2.7013690E-03			
0	8.7920971E-06			
0	2.0935729E-01			
0	1.1024087E-02			
0	2.0717899E-04			
0	2.3081830E-03			
0	7.5002497E-02			
1.0000000E-00	0	0	0	0
0	0	0	0	0
0	0	0	0	0
0	0			
0	1.0000000E-00	0	0	0
0	0	0	0	0
0	0	0	0	0
0	0			
0	0	1.0000000E-00	0	0
0	0	0	0	0
0	0	0	0	0
0	0			
0	0	0	1.0000000E-00	0
0	0	0	0	0
0	0	0	0	0
0	0			
0	0	0	0	1.0000000E-00
0	0	0	0	0
0	0	0	0	0
0	0			
1.0000000E-00	0	0	0	0
0	0	0	0	0
0	0	0	0	0
0	0			
0	1.0000000E-00	0	0	0
0	0	0	0	0
0	0	0	0	0
0	0			
0	0	1.0000000E-00	0	0
0	0	0	0	0
0	0	0	0	0
0	0			
0	0	0	1.0000000E-00	0
0	0	0	0	0
0	0	0	0	0
0	0			
0	0	0	0	1.0000000E-00
0	0	0	0	0
0	0	0	0	0
0	0			
1.0000000E-00	0	0	0	0
0	0	0	0	0
0	0	0	0	0
0	0			
0	1.0000000E-00	0	0	0
0	0	0	0	0
0	0	0	0	0
0	0			
0	0	1.0000000E-00	0	0
0	0	0	0	0
0	0	0	0	0

FILE: FEEDBACK DATA A1

```
                0                    0                    0                    0                    0
                0                    0                    0   1.0000000E-00                    0
                0                    0                    0                    0                    0
                0                    0                    0                    0                    0
                0                    0                    0                    0   1.0000000E-00
                0                    0                    0                    0                    0
                0                    0                    0                    0                    0
                0                    0                    0                    0                    0
  1.0000000E-00                      0                    0                    0                    0
                0                    0                    0                    0                    0
                0                    0                    0                    0                    0
                0                    0                    0                    0                    0
                0   1.0000000E-00
 -0.0188000E-00  -0.0279000E-00  -0.0042000E-00   0.0290000E+00   0.0041000E+00
  0.0000000E+00   0.0001000E+00   1.7732000E+00  -2.0162000E+00   0.0131000E+00
  0.0000000E+00   0.0000000E+00   0.0000000E+00   0.0000000E+00   0.0000000E+00
  0.0000000E+00     0.0000000E+0
  0.0000000E+00   0.0000000E+00     0.0000000E+0     0.0000000E+0   0.0000000E+0
  0.0000000E-00   0.0000000E+00     0.0000000E+0     0.0000000E+0   0.0000000E+0
  0.0000000E+00   0.0000000E-00   0.0000000E+00     0.0178000E-0  -0.0179000E-0
 -1.4990000E-00   0.0023000E-00
0 0 0 0 0 0 0 0 0 0 0 0 0 0 0 0 0 0
0 0 0 0 0 0 0 0 0 0 0 0 0 0 0 0 0 0
   -10000      10000
 0.13199300  0.0319377C
 0.13199300 -0.0319377C
 0.89698700  0.0906708C
 0.89698700 -0.0906708C
 0.95362500  0.0299850C
 0.95362500 -0.0299850C
 0.99820200  0.0000000C
 1.00000000  0.0000000C
 0.99560800  0.0830713C
 0.99560800 -0.0830713C
 0.0992805C  0.0000000C
 0.83521600  0.3097360C
 0.83521600 -0.3097360C
 0.96908700  0.0328588C
 0.96908700 -0.0328588C
 0.89379700  0.0000000C
 0.93707500  0.0000000C
```

APPENDIX G

ROBUSTNESS DATA FILE FOR THE DISCRETE ESTIMATOR DESIGNED AUTOPILOT

```
FILE: ESTIMATO DATA      A1

 1000     0
      100.0          0.0          1.0
             1            0            0
           0.4          0.4          0.0     0
     0     0     0      5     3      3 1000     0
17171702171702171717
    1.5795758E-01    3.6369326E-02    5.5348592E-03   -3.5415286E-2   -5.6850634E-3
    1.4376905E-03   -6.3550195E-3    5.1215038OE+0   -2.7434696E+0    8.4960341E-01
                0                0                0               0               0
                0                0
    7.3702121E-03    1.0001847E-00    1.2145713E-02   -1.8110829E-4   -2.3707903E-5
    6.4803277E-06   -4.3148367E-5    2.3554415E-02   -2.1657925E-2    9.0789743E-03
                0                0                0               0               0
                0                0
   -3.5755072E-2    -8.9683556E-4    9.3927554E-01    8.7923240E-04    1.3937755E-04
   -3.1463045E-5    2.0946996E-04   -1.1434246E-1    1.0513494E-01   -4.4065551E-2
                0                0                0               0               0
                0                0
    6.3641914E-04    4.8072347E-03    7.3780452E-04    9.9184592E-01    1.1724094E-02
    1.0389178OE-7   -1.0276906E-6   -2.5772733E-1   -4.3730676E-1    3.6239694E-04
                0                0                0               0               0
                0                0
   -1.2632605E-4    -8.8102163E-4    -1.3508452E-4   -5.5242591E-1    9.9481481E-01
   -1.1935039E-8    1.3487757E-07    1.1052479E-01    1.0873558E-01   -5.6530062E-5
                0                0                0               0               0
                0                0
    5.0058503E-05    3.4906702E-04    5.3521335E-05   -3.4235257E-4   -5.4232194E-5
    9.9653887E-01    1.2473678E-02   -4.3837960E-2   -4.3103149E-2    2.2390223OE-5
                0                0                0               0               0
                0                0
    1.1198072E-02    8.4589715E-02    1.2932664E-02   -3.2578336E-2   -1.3194430E-2
   -5.5328815E-1    9.9465984E-01   -4.5313172E-0   -7.6933073E-0    6.3774424E-03
                0                0                0               0               0
                0                0
   -1.8197865E-3    -1.6475936E-2    -2.5342871E-3    1.5914437E-02    2.5927489E-03
   -7.6937268E-7    6.1129260E-06    1.9658256E-02    8.2551326E-01   -1.6117691E-3
                0                0                0               0               0
                0                0
   -2.4201118E-3    -2.6250703E-2    -4.0468111E-3    2.5073784E-02    4.1674975E-03
   -2.2085612E-6    1.4059039E-05   -1.0104558E-1    8.5213330E-01   -3.0605437E-3
                0                0                0               0               0
                0                0
    8.5120361E-03    7.7170206E-02    1.1870299E-02   -7.4535066E-2   -1.2144650E-2
    3.4647518E-03   -1.2502640E-2    4.6563462E-00   -3.5409597E-0    1.0075610E-00
                0                0                0               0               0
                0                0
                0                0                0               0               0
                0                0                0               0               0
    9.9773878E-01   -2.7013690E-3    1.0245896E-03    2.2685736E-01   -2.2392478E-1
    3.2285155E-00    3.6730433E-02
                0                0                0               0               0
                0                0                0               0               0
    1.2492612E-02    9.9999121E-01    3.3686339E-06    7.9213881E-04   -7.8251019E-4
    1.6120605E-02    3.2140565E-04
                0                0                0               0               0
                0                0                0               0               0
   -1.3299604E-3    -2.0935729E-1    9.0483727E-01   -3.6881965E-5    3.6451128E-05
   -9.6597318E-4    -2.6908370E-5
                0                0                0               0               0
                0                0                0               0               0
   -9.0797723E-3    -1.1024087E-2    3.9997292E-03    9.2763032E-01    1.1630732E-02
   -1.7007972E-1    -2.0028512E-3
                0                0                0               0               0
                0                0                0               0               0
   -1.7340942E-4    -2.0717899E-4    7.8564538E-05    1.7374049E-02    9.1059431E-01
    2.4505510E-01    2.7257510E-03
                0                0                0               0               0
                0                0                0               0               0
   -1.9081030E-3    -2.3081830E-3    8.4609805E-04    1.5280715E-01   -1.5037418E-1
    7.4692747E-01   -1.1429485E-3
                0                0                0               0               0
                0                0                0               0               0
```

FILE: ESTIMATD DATA A1

-6.2875718E-2	-7.5602497E-2	2.8176191E-02	5.6122435E-00	-5.5314055E-0
4.3323648E+01	5.1040685E-02			
-7.5609329E-3	0			
-1.6449186E-2	0			
7.9821623E-02	0			
-9.9881608E-4	0			
1.8235612E-04	0			
-7.2448725E-5	0			
-1.7575515E-2	0			
3.4315526E-03	0			
5.4807555E-03	0			
-1.6073019E-2	0			
0	2.7013690E-03			
0	8.7926971E-06			
0	2.0935729E-01			
0	1.1024087E-02			
0	2.0717899E-04			
0	2.3081830E-03			
0	7.5602497E-02			
1.0000000E-00	0	0	0	0
0	0	0	0	0
0	0	0	0	0
0	0			
0	1.0000000E-00	0	0	0
0	0	0	0	0
0	0	0	0	0
0	0			
0	0	1.0000000E-00	0	0
0	0	0	0	0
0	0	0	0	0
0	0			
0	0	0	1.0000000E-00	0
0	0	0	0	0
0	0	0	0	0
0	0			
0	0	0	0	1.0000000E-00
0	0	0	0	0
0	0	0	0	0
0	0			
1.0000000E-00	0	0	0	0
0	0	0	0	0
0	0	0	0	0
0	0			
0	1.0000000E-00	0	0	0
0	0	0	0	0
0	0	0	0	0
0	0			
0	0	1.0000000E-00	0	0
0	0	0	0	0
0	0	0	0	0
0	0			
0	0	0	1.0000000E-00	0
0	0	0	0	0
0	0	0	0	0
0	0			
0	0	0	0	1.0000000E-00
0	0	0	0	0
0	0	0	0	0
0	0			
1.0000000E-00	0	0	0	0
0	0	0	0	0
0	0	0	0	0
0	0			
0	1.0000000E-00	0	0	0
0	0	0	0	0
0	0	0	0	0
0	0			
0	0	1.0000000E-00	0	0
0	0	0	0	0
0	0	0	0	0
0	0			
0	0	0	0	0

FILE: ESTIMATC DATA 41

```
                    0                    0                    0    1.0000000E-00                    0
                    0                    0                    0                    0                    0
                    0                    0                    0                    0                    0
                    0                    0                    0                    0    1.0000000E-00
                    0                    0                    0                    0                    0
                    0                    0                    0                    0                    0
                    0                    0                    0                    0                    0
  1.0000000E-00     0                    0                    0                    0                    0
                    0                    0                    0                    0                    0
                    0                    0                    0                    0                    0
                    0   1.0000000E-00
 -1.8784000E-00     0.0200000E-00   -0.0972000E-00    0.0219000E+00    0.0041000E+00
 -0.0016000E+00     0.3860000E+00    0.0720000E+00    0.0007000E+00   -0.3370000E+00
  0.0000000E+00     0.0000000E+00    0.0000000E+00    0.0000000E+00    0.0000000E+00
  0.0000000E+00       0.0000000E+0
  0.0000000E+00     0.0000000E+00    0.0000000E+00      0.0000000E+0     0.0000000E+00
  0.0000000E-00     0.0000000E+00     0.0000000E+0      0.0000000E+0      0.0000000E+0
  0.0040000E+00     0.0000000E+00    0.0000000E+00    -0.0002000E-0      0.0003000E-0
  0.0000000E+00    -0.0492000E-00
0 0 0 0 0 0 0 0 0 0 0 0 0 0 0 0 0 0
0 0 0 0 0 0 0 0 0 0 0 0 0 0 0 0 0 0
   -10000      10000
 0.13199300   0.03193770
 0.13199300  -0.03193770
 0.89698700   0.09067080
 0.89698700  -0.09067080
 0.95362500   0.02998500
 0.95362500  -0.02998500
 0.99820200   0.00000000
 1.00000000   0.00000000
 0.99560800   0.08307130
 0.99560800  -0.08307130
 0.09928050   0.00000000
 0.83521600   0.30973600
 0.83521600  -0.30973600
 0.96908700   0.03285880
 0.96908700  -0.03285880
 0.89379700   0.00000000
 0.93707500   0.00000000
```

LIST OF REFERENCES

1. Reichert, R.T., Homing Performance Comparison of Selected Airframe Configurations Using Skid-to-Turn and Bank-to-Turn Steering Policies ,NASA CR-3420, May 1981.

2. Riebel, F.W., Bank-to-Turn Control Techology Survey for Homing Missiles , NASA CR-3325 , September 1980.

3. Arrow, A., An Analysis of Aerodynamic Requirements for Coordinated Bank-to-Turn Autopilots, NASA CR-3644, November 1982.

4 Graves, E.B., Aerodynamic Characteristics of a Monoplanar Missile Concept with Bodies of Circular and Elliptical Cross Sections, NASA TM-74079, December 1977.

5. Ogata, K., Modern Control Engineering, Prentice-Hall Inc., 1970.

6. Franklin, G.F. and Powell, J.D., Digital Control of Dynamic Systems, Addison-Wesley Publishing Company, 1981.

7. Karadimas, C., Design and Analysis of Discrete Lateral Autopilots for BTT Missiles, M.S. Thesis, Naval Postgraduate School, Monterey, California, December 1985.

8. Gordon, V.C., Utilization of Numerical Optimization Techniques in the Design of Robust Multi-Input Multi-Output Control Systems, Ph.D. Thesis, Naval Postgraduate School, Monterey, California, September 1984.

INITIAL DISTRIBUTION LIST

		No. Copies
1.	Defense Technical Information Center Cameron Station Alexandria, Virginia 22304-6145	2
2.	Library, Code 0142 Naval Postgraduate School Monterey, California 93943-5100	2
3.	Department Chairman, Code 67 Department of Aeronautics Naval Postgraduate School Monterey, California 93943	1
4.	Professor D.J. Collins, Code 67Co Department of Aeronautics Naval Postgraduate School Monterey, California 93943	2
5	Professor H.A. Titus, Code 67Ts Department of Electrical and Computer Engineering Naval Postgraduate School Monterey, California 93943	2
6.	Hellenic General Naval Staff 2nd Branch, Education Department Stratopedon Papagou Athens, GREECE	4
7.	LT Karaiskos, Ioannis H.N Pelopos 1, Koridallos 18121 Piraeus, GREECE	4
8.	LT Karadimas, Christos H.N Kolokotroni 156 Piraeus GREECE	1

9. LT Karadimitris, Antonios H.N 1
201 Glenwood Circle #35A
Monterey, California 93943

10. LCDR Protonotarios, Nicolaos H.N 1
841 Belden #1
Monterey, California 93940

216575

Thesis
K142575 Karaiskos
c.1 The effects of digital control on longitudinal autopilots for bank-to-turn and skid-turn missiles.

216575

Thesis
K142575 Karaiskos
c.1 The effects of digital control on longitudinal autopilots for bank-to-turn and skid-turn missiles.

AMERICAN BINDERIES 2

thesK142575
The effects of digital control on longit
3 2768 000 65189 7
DUDLEY KNOX LIBRARY